TÉCNICO LISBOA

Modelling of aqueous electrolyte solutions with the SAFT $\gamma-$Mie framework

Ana Patrícia Cardoso Cotrim

Thesis to obtain the Master of Science Degree in

Chemical Engineering

Advisor(s)/Supervisor(s): Dr. Thomas Lafitte
Dr. Pedro Jorge Rodrigues Morgado

Examination Committee

Chairperson: Prof./Dr. Carlos Henriques
Advisor: Prof./Dr. Pedro Morgado
Members of the Committee: Prof./Dr. Eduardo Filipe

November 2018

Acknowledgements

This thesis is not the result of merely a single person's effort. In the first place, I would like to extend my sincere gratitude to Professor Costas Pantelides for the opportunity to work at Process Systems Enterprise. A special acknowledgement goes to Professor Eduardo Filipe, for all his invaluable support and, again, for the opportunity to make this internship possible. I would especially like to thank my supervisor, Dr. Pedro Morgado, for all his help at every stage.

To all the gSAFT team, who were always willing to help whenever necessary. To my supervisor, Dr. Thomas Laffite, it was a pleasure to work with you and learn from you. Furthermore, I cannot find the words to express my gratitude to Dr. Simon Dufal and Dr. Vasileios Papaioannou who followed this project from the beginning, advising and supporting me during all this experience. Without them, this thesis would have been much more difficult to accomplish.

To my friends and my housemates: Alexandre, Diogo and Mauro, who were my family here. The experiences and moments we shared will always be remembered with affection. To Renato, Artur, Tom and André for hosting us in our first days in London, and to all the other Portuguese people present in London: Mariana, Francisco, João, Beatriz and João Barras. We were extremely fortunate to have such nice people here with us.

To my family and to José, for always believing in me as well as advising and supporting me in every moment of my life. I will be forever in great debt to you and I will always remember your endless love and encouragement.

Abstract

This thesis is based on a study of the thermodynamic properties of electrolyte solutions. The purpose of this work is to understand which combination of experimental data should be used to develop the SAFT γ-Mie model parameters for electrolytes. In order to carry out this study, the approach that is used is based on studying first four different salts ($NaCl$, $NaBr$, KCl and KBr) and then applying what is believed to be the best estimation strategy to other salts such as NaI, KI, $RbCl$, $RbBr$, $CsCl$, $CsBr$, $NaNO_3$, KNO_3, NH_4Cl and NH_4Br.

The obtained results are based on the computation of a broad set of properties such as solubilities, liquid phase densities, liquid phase heat capacities and heats of dilution. One of the important conclusions taken from this work is the importance of including calorific properties (heat capacities and heats of dilution) when developing model parameters for electrolytes.

Keywords: SAFT, gSAFT, Modelling, Electrolyte Solutions, Salt Based Solutions, Solubility, Liquid Phase Density, Liquid phase Heat Capacities, Dilution Enthalpy, Mean Activity Coefficients, Osmotic Coefficients

Resumo

Esta tese baseia-se num estudo das propriedades termodinâmicas de soluções de eletrólitos. O objetivo deste trabalho é perceber qual a combinação de dados experimentais que deve ser utilizada para desenvolver os parâmetros do modelo de SAFT γ-Mie para eletrólitos. De modo a prosseguir com este estudo a estratégia que é usada é baseada em estudar primeiro quatro sais distintos ($NaCl$, $NaBr$, KCl and KBr) e depois em aplicar aquela que se crê ser a melhor estratégia de estimativas a outros sais, tais como NaI, KI, $RbCl$, $RbBr$, $CsCl$, $CsBr$, $NaNO_3$, KNO_3, NH_4Cl and NH_4Br.

Os resultados obtidos são baseados na computação de um conjunto amplo de propriedades tais como solubilidades, densidades da fase líquida, capacidades caloríficas e entalpias de dissolução. Uma das conclusões importantes que se reteve deste trabalho é a importância de se incluirem propriedades caloríficas (capacidades caloríficas e entalpias de diluição) aquando o desenvolvimento de parâmetros do modelo para eletrólitos.

Keywords: SAFT, gSAFT, Modelação, Soluções de eletrólitos, Soluções de sais, Solubilidade, Densidade da fase líquida, Capacidades caloríficas da fase líquida, Entalpia de diluição, Coeficientes de Atividade, Coeficientes Osmóticos.

Contents

List of Tables

List of Figures

Nomenclature

Acronyms

EoS	Equation of State
GC	Group Contribution
MCA	Macroscopic Compressibility Approximation
MSA	Mean Spherical Approximation
NC	Number of Compounds
NP	Number of Phases
NR	Number of Reactions
PSE	Process Systems Enterprise
RDF	Radial Distribution Function
SAFT	Statistical Associating Fluid Theory
TPT1	First order thermodynamic perturbation theory

Greek Letters

$\Delta H_i^{F,ig}$	Enthalpy of formation of component i ideal gas
$\Delta H_{d,i}$	Dilution enthalpy of compound i
$\Delta S_i^{F,ig}$	Entropy of formation of component i ideal gas
Δ	Packing fraction of the ions as a function of their diameter
Δ_i^3	de Broglie volume
ϵ_0	Vacuum permittivity ($8.854 * 10^-12 C^2 Jm^-1$)
ϵ_{kl}	Depth of the potential well
Γ	Screening length of electrostatic forces
λ_{kl}^a	Attractive exponent in SAFT γ-Mie
λ_{kl}^r	Repulsive exponent in SAFT γ-Mie
$\mu_i^{[k]}$	Chemical Potential of compound i in phase k
μ_i^{Born}	Chemical potential of an ion i in solution

μ_i^{ig}	Chemical Potential of the Ideal Gas
ν_k^*	Number of identical segments that form group k
ν_{ij}	Stoichiometric coefficient of compound i in reaction j
$\nu_{k,i}$	Number of occurrences of group k
Ω	Coupling parameter to the packing factor of the ions
Φ_{kl}^{LJ}	Lennard-Jones Potential
Φ_{kl}^{Mie}	Mie Potential
ρ_i	Density of compound i
σ_{kl}	Segment Diameter

Symbols

$A^{Association}$	Association term of Helmholtz free energy
A^{Born}	Born term of Helmholtz free energy
A^{Chain}	Chain term of Helmholtz free energy
A^{HS}	Hard sphere Helmholtz free energy
a^{HS}	Dimensionless contribution to the hard sphere free energy per segment
A^{Ideal}	Ideal term of Helmholtz free energy
A^{ion}	Ion term of Helmholtz free energy
A^{Mono}	Monomer term of Helmholtz free energy
$C_{p,i}^{ig}$	Heat Capacity of compound i in the ideal gas state
$C_{p,i}^{s}$	Heat Capacity of compound i in the solid state
D	Relative permittivity of an uniform dielectric medium
e	Elementary charge ($1.602 \times 10^{-19} C$)
G	Gibbs free energy
k_b	Boltzmann constant
$m_{seg,i}$	Number of segments per chain
N	Total number of molecules
N_i	Number of molecules of component i
$n_{i,k}$	Amount of compound i in phase k
P	Pressure
P_n	Coupling parameter to the charge of the ions
P_{ref}	Reference Pressure

Q_i	Effective charge of the ions
q_i	charge of compound i
r_{ij}	Centre-centre distance between charges i and j
s_i	Solubility of salt i
S_k	Shape factor
T	Absolute Temperature
T	Temperature
T_{ref}	Reference Temperature
U^{MSA}	MSA contribution to the internal energy U
V	Volume of the system
x_i	Mole fraction of compound i in a mixture
$X_{a,i}$	Fraction of molecules not bonded at a given site type a on species i
$x_{s,k}$	Fraction of segments of a group of type k in a mixture
z_i	Bearing charge

Chapter 1

Introduction

Physical property data is the raw material of chemical process design, and consequently, thermodynamic models are constantly being developed and improved in order to meet the need of accurate properties predictions. Since process simulation has become such an important tool for the development, design and optimization of several chemical processes, it has become clear that thermodynamic properties are key inputs for the development of diverse process models. Taking into account what was previously mentioned, it becomes well known that thermodynamic methodologies are applied extensively in broad sectors of the chemical industry regarding the prediction of diverse properties of highly complex fluids and mixtures.[1, 2]

To date, most of the applications of different Equations of State have been applied in organic systems. However, inorganic systems, particularly electrolyte systems, are also of interest in an ever-expanding number of applications. Electrolyte solutions find numerous applications in physical sciences including chemistry, material science, medicine, biochemistry as well as in many engineering fields.[3] In all these applications thermodynamics plays a crucial role over a wide range of temperatures, pressures and concentrations. Considering what was previously stated, accurate knowledge of salt containing solutions may be crucial in the design and understanding of a process and, for this reason, an ability to model electrolytes is of great importance. Nonetheless, modelling electrolyte solutions presents a considerable challenge as both short range repulsive and attractive contributions, and long range polar and Coulombic interactions need to be taken into account.[4] In this context, much of the difficulty can be ascribed to the range of the electrostatic forces, and the corresponding paucity of analytical theories that can be used to describe the relevant many-body effects.[5]

Group Contribution (GC) approaches are a specific class of predictive methodologies which have been developed based on the assumption that the molecule properties can be calculated as an appropriate sum of contributions that are attributed to different functional groups. In this methodology molecules are divided into chemical functional groups, instead of being described in a molecule representation.[2]

In a simple way, an Equation of State (EoS) can be defined as an equation capable of giving the residual Helmholtz free energy of a system (given by the difference of the total Helmholtz free energy of the system and the Helmholtz energy of an ideal gas). Once the residual Helmholtz free energy has been obtained it is possible to obtain all the properties of the system using derivatives in temperature, volume and composition. The Statistical Associating Fluid Theory (SAFT) is a general framework for the development of equations of state based on the statistical thermodynamics of associating chain molecules. This EoS allows for the calculation of phase equilibrium data and bulk properties of a given mixture assuming that molecules are modelled as chains of bonded spherical segments interacting via a dispersive potential with short-range sites placed on the segments.[2]

The mathematical complexity associated with the SAFT EoS is probably one of the main reasons

why it has not been widely applied yet in process modelling softwares. However, the gSAFT software developed by the Process Systems Enterprise (PSE) company has overcome this adversity and allows its users to compute different parameters, and use SAFT as a basis for process modelling, and obtain the requested properties for different types of mixtures.

Motivation and Purpose

Considering the rising interest in the prediction of properties for electrolyte solutions, some recent works on this topic have been published and new models capable of predicting properties are being tested and developed. The main purpose of this work is to achieve a model capable of predicting solubilities and energetic features of electrolyte solutions by using the SAFT γ-Mie EoS. Along with solubility it is intended to get a model robust enough to predict heat capacities and heats of dilution while ensuring reliable results for mean activity coefficients and osmotic coefficients. The goal is to obtain a model for diverse salts, such as $NaCl$, $NaBr$, KCl, KBr, NaI, KI, $RbCl$, $RbBr$, $CsCl$, $CsBr$, NH_4Cl and NH_4Br using the SAFT γ-Mie framework.

Chapter 2

State of the Art

2.1 Thermodynamic modelling of electrolyte-containing systems

Different types of EoS have been developed for different applications over the years. Whereas both liquid and vapour phases can be described by the same fluid EoS, solids need to be treated with different methods. Most practical engineering models for the liquid phase are based on equations directly for the activity coefficients that are often extensions of well-established models for electrolyte solutions (like NRTL and UNIQUAC) by adding a suitable electrolyte term.[3] Apart from the aforementioned models, over the past 30 years, great advances have been made in the development of thermodynamic models for hydrogen bonding mixtures through SAFT. This has given rise to a long list of SAFT-based models (such as PC-SAFT and Cubic Plus Association), which calculate contributions to the total residual Helmholtz energy of a fluid through a perturbation theory, which is based on a mathematical model for specific interactions in the fluid.[6] In this work the SAFT γ-Mie framework will be used to study electrolyte solutions.

2.1.1 Primitive and non-primitive models

There are two main types of models used to describe electrolyte solutions: primitive and non-primitive models.

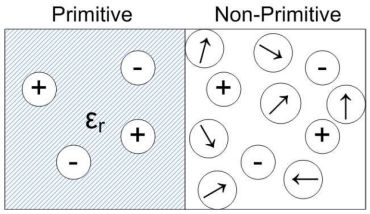

Figure 2.1: Schematic representation of the primitive and non-primitive model[6]

Primitive Models

Primitive models are characterised by a description of the solvent as a continuous dielectric medium (characterised by a dielectric constant) to represent the average dipolar contribution. This dielectric constant is a measure of the screening power of the solvent, *i.e.* its capacity to separate the ions by decreasing the magnitude of ion-ion interactions.[7]

Most of the thermodynamic modelling of electrolyte solutions is carried out with primitive models. However, these models are still limited by the approximation of the solvent as a continuous dielectric.

Two main routes[7] have been employed over the years to study primitive models of electrolyte solutions. The first one is due to Debye and Hückel and the second, more recent, is the Mean Spherical Approximation (MSA), in which the ions are treated as charged hard spheres.

Non-primitive Models

Non-primitive models use the coupling of all the electrostatic interactions (ion-ion, ion-dipole, dipole-dipole) and do not need to include models for the static permittivity. Nevertheless, accurate contributions are not easy to obtain, and thus primitive models are preferred despite the less realistic representation of the system.

In this work the primitive model was used with the MSA approach.

2.2 Published works

The application of SAFT to electrolyte solutions started 20 years ago, and since then several articles and papers have been published. Some of the latest works are presented below.

In 2013, the Department of Chemical Engineering of the Imperial College of London proposed the modelling of the thermodynamic and solvation properties of electrolyte solutions with the statistical associating fluid theory for potentials of variable range (SAFT-VR).[4] In this work they adjusted several parameters, such as the ion-ion σ and the ion-solvent and ion-ion ϵ in order to obtain models capable of predicting vapour pressures, liquid phase densities and mean activity coefficients for diverse salts. They also studied the free energy of solvation.

Later, in 2015, the same research group developed intermolecular potential models for electrolyte solutions using an electrolyte SAFT-VR Mie EoS.[5] Here, they used the assumption of complete salt dissociation and they only adjusted the $\epsilon_{water-ion}$, using literature data for the remaining necessary parameters. With these adjustments they have managed to get models capable of predicting vapour pressures, liquid densities and osmotic coefficients as well as guaranteeing that the values of the mean activity coefficients were also reliable.

The latest work was published this year by the Texas $A\&M$ University at Qatar.[8] They also present a model that can predict mean activity coefficients, osmotic coefficients, vapour pressures and liquid phase densities. In order to obtain these results, two parameters are adjusted: the ion-water cross dispersion energy parameter and the ion segment diameter, which are optimized against experimental data for electrolyte solution densities and mean activity coefficients. In this work a temperature-dependent expression is presented for cross interaction parameters.[8]

All the studies published so far are related to vapour pressures, mean activity coefficients, liquid phase densities and osmotic coefficients. However, other properties such as solubilities and energetic properties (*e.g.* enthalpy of dilution) are also crucially important for process models, but have not been studied yet with SAFT approaches. The goal of this work is to assess the capacity of SAFT γ-Mie to capture this broader set of properties.

Chapter 3

Thermodynamic fundamentals for solubility calculation

Phase equilibrium occurs when two or more phases are presented in equilibrium. The conditions which enforce phase equilibrium of electrolyte solutions are similar to those of non-electrolyte systems, with additional constraints related to the charge balances and the necessary charge neutrality of a given phase. In order to have a thermodynamic equilibrium there is the need to verify chemical, thermal and mechanical equilibrium all at the same time. The chemical equilibrium is expressed through the equality of chemical potentials, μ_i, of each component i of the system, defined as:

$$\mu_i = \left(\frac{dU}{dn_i}\right)_{S,V,n_{j\neq}n_i} = \left(\frac{dH}{dn_i}\right)_{S,P,n_{j\neq}n_i} = \left(\frac{dG}{dn_i}\right)_{P,T,n_{j\neq}n_i} = \left(\frac{dA}{dn_i}\right)_{T,V,n_{j\neq}n_i} \tag{3.1}$$

in all of the phases. Regarding the thermal and mechanical equilibrium conditions, these must be satisfied for pressures and temperatures in all phases:

$$T^{\alpha} = T^{\beta} = ... = T^{N_P} \tag{3.2}$$

$$p^{\alpha} = p^{\beta} = ... = p^{N_P} \tag{3.3}$$

In phase and reaction equilibrium the main goal is to minimize the Gibbs free energy of a given system. This energy is related to the chemical potential of each phase and can be calculated and described by Equation 3.4.

$$G = \sum_{k=1}^{NP}\sum_{i=1}^{NC} n_{ik}(\mu_i^{[k]} + F\psi_k q_i) \tag{3.4}$$

where NC stands for the number of compounds, NP for the number of phases, n_{ik} for the amount of compound i in each phase k at a given temperature and pressure, q_i for the charge of a given compound and $\mu_i^{[k]}$ for the chemical potential of compound i in phase k. This last parameter is generally a function of temperature, pressure and the molar amount of compounds in phase k. (n_k)

Once one can get the Gibbs free energy equation minimized it is possible to obtain:

- Reaction equilibrium equation

$$\sum_{i=1}^{NC} \nu_{ij}\mu_i^{[NP]} = 0, \qquad \forall_j = 1, ..., NR \tag{3.5}$$

where ν_{ij} represents the stoichiometric coefficient of compound i in reaction j, and NR represents the number of equations.

- Phase equilibrium equation

$$\mu_i^{[k]}(T,P,n_k) - \mu_i^{[NP]}(T,P,n_k) + F(\psi_k - \psi_{NP})q_i = 0, \qquad \forall_i \forall_k = 1,...,NP-1 \tag{3.6}$$

- Electroneutrality equation

$$\sum_{i=1}^{NC} q_i n_{i,k} = 0, \qquad \forall_i \forall_k = 1,...,NP-1 \tag{3.7}$$

3.1 Liquid Phase Chemical Potential

The only thermodynamic property required for solubility calculations is the chemical potential of each compound present in the system.[9] Regarding the liquid phase potential we know that:

$$\mu_i^l(T,P,n) = \mu_i^{ig}(T,P,n) + \mu_i^{res}(T,P,n) \tag{3.8}$$

where

$$\mu_i^{ig}(T,P,n) = \Delta H_i^{F,ig} + \Delta S_i^{F,ig} + \left[\int_{T_{ref}}^{T} C_{p,i}^{ig}(T')\, dT' - T \int_{T_{ref}}^{T} \frac{C_{p,i}^{ig}}{T'}\, dT' \right] + RTln\left(\frac{P}{P_{ref}}\right) + RTln(x_i) \tag{3.9}$$

and $\mu_i^{res}(T,P,n)$ is calculated through the SAFT EoS. The chemical potential μ_i^l can also be expressed in terms of reference states other than the ideal gas such as, the pure liquid state or the infinite dilution state.

There are different strategies to get the residual chemical potential, as represented in Figure 3.1.

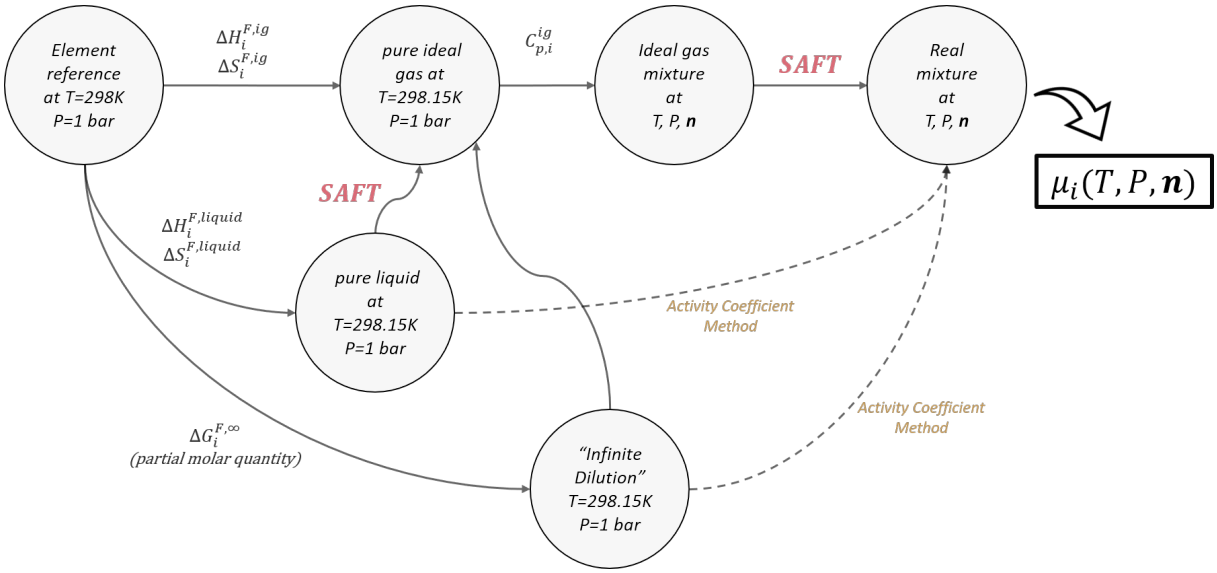

Figure 3.1: Summary of the various possible thermodynamic paths for the computation of chemical potential of compound i in liquid phases $\mu_i^l(T,P,n)$ from the various standard state formation properties, ideal gas, pure liquid, and "infinite dilution". The thermodynamic integration path depends on whether an equation of state (EoS) or activity coefficient model (ACM) is used to model the mixture non-idealities.[9]

The purpose of this work is the study of electrolyte solutions. Taking this into account, one needs to decide which one of the three strategies should be chosen and employed to compute the liquid phase chemical potential.

Taking a look at the Figure presented aboved, the first option demands the use of the pure ideal gas data. As the chemical potential of an ideal gas is a function of the enthalpy and entropy of formation of a given compound in the ideal gas state, this approach cannot be used. This happens because this data is unknown for ions. Regarding the pure liquid strategy, this cannot be used either. The reason why this path is not viable is because this approach considers one mol of liquid at 298.15K and 1 bar, and this cannot be applied for ions. The only missing strategy is the infinite dilution one. Indeed, this is the right path to choose, where the ideal chemical potential is a function of ΔH_{aq}^F and ΔS_{aq}^F. This data can all be found in [10].

3.2 Solid Phase Chemical Potential

SAFT is a fluid theory, so it does not recognize or consider solid phases. In particular, both equations of state and activity coefficient models are restricted to phases exhibiting only liquid-like structures, and cannot describe the behaviour of phases where the underlying microscopic structure follows a well-defined geometric pattern such as crystalline or solid phases. There are different ways to calculate the chemical potential of a solid phase[9]. The one used in this current work is the one described in Equation 3.10.

$$\mu_i^s(T) = \Delta H_i^{F,s\ ref} - T\Delta S_i^{F,s\ ref} + \int_{T_{ref}}^{T} C_{p,i}^s(T')dT' - T\int_{T_{ref}}^{T} \frac{C_{p,i}^s(T')}{T'}dT' \tag{3.10}$$

where the required experimental data is the enthalpy of formation, the entropy of formation in the reference conditions (for the solid) and the solid heat capacity.

Chapter 4

SAFT γ - Mie Equation of State

4.1 Evolution of Equations of State

Since the formulation of the ideal gas law and the Van der Waals conception for real gases, many other equations of state have been developed in order to obtain rigorous predictions for phase equilibria, single phase properties and activity coefficients. Many followed the Van der Waals framework and those developed thermodynamic models known as cubic equations of state. However, this type of equations has some limitations and does not predict properly the properties of associating and non-spherical molecules. The main reason for this deficiency is that the cubic equations of state do not take into account the shape of the molecules and assume that all the molecules can be represented as spheres, especially when dealing with large molecules. Moreover, they are a good approximation for simple molecules that interact through London dispersion, but, with more complex molecules and interactions the model breaks down. Apart from that, it is also known that they do not provide accurate results when trying to obtain second derivative properties.

The main difference between the previous models and Statistical Associating Fluid Theory (SAFT) is that this last equation is underpinned by a physically realistic representation of the molecule that includes not only their shape but also their sizes and interactions between molecules (Including hydrogen bonding). The SAFT Equation of State (EoS) is a perturbation theory and has its roots in the First order thermodynamic perturbation theory (TPT1) of Wertheim for associating and chain fluids. It provides a framework that allows the calculation of different properties of a system based on the knowledge of a monomeric reference fluid. This means that to obtain a given property, this EoS evaluates the property for the reference fluid and then ”estimates” perturbations.

In SAFT, molecules are modelled as chains of bonded spherical segments interacting via an attractive potential with short-range sites placed on the segments.[2]. Each group is then characterized by different parameters as will be explained in the following topic.

There are different versions of SAFT and their main difference is in the choice of their intermolecular potential for the sphere-sphere interactions. These interactions can be, for example, Lennard-Jones, Square-Well and Mie Potential. The SAFT γ - Mie framework was the approach used in this work, and so, its terms will be explained below.

4.2 Molecular model and intermolecular potential

The interactions between molecules need to be modelled as accurately as possible and different contributions based on the electrostatics, such as dispersion interactions and those arising from the

different multipole moments, need to be taken into account to describe the behaviour of molecules.[7] As long as we have matter, we have two main types of forces: attractive and repulsive. Many potential models have been developed, by combining different repulsive and attractive parts, with some common features: most repulsive terms tend to infinity at short separations, preventing a complete overlap of two molecules, and the attractive terms tend to zero at infinity, so that the energy is not infinite.[7]

As was previously stated, SAFT γ - Mie is a variant of the general SAFT framework. This formulation is based on a generalised Lennard-Jones potential, or so called Mie-Potential, and takes into account a group contribution approach. With this, molecules are described in terms of the functional groups, whereby the functional groups are assumed to behave independently of the molecule structure on which they are found.[9]

Overall, Group Contribution (GC) approaches consider that molecules are divided into different functional groups. This theory is underlined by the fact that all the molecular properties can be calculated as a sum of the different contributions of the different functional groups, and that these group properties remain the same even if they appear in a different host molecule. There are a set of parameters that characterize these functional groups, namely the shape factor, S_k that describes the group non-sphericity, and some parameters related with the intermolecular potentials.

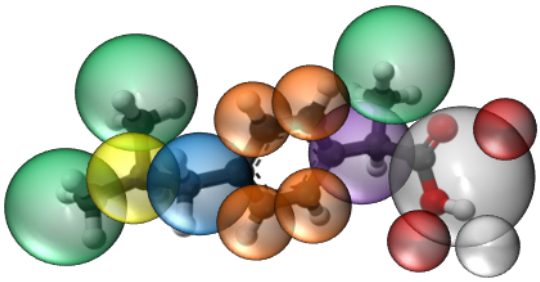

Figure 4.1: SAFT γ - Mie group contribution representation[11]

The Lennard-Jones potential describes the interaction of two neutral particles in terms of energy. These particles are subject to two opposing forces: attractive and repulsive. Although this model has sometimes been found too poor to describe the repulsive potential, it is widely used as a building block of many force fields due to its computational expediency. The equation that describes this model is given in 4.1

$$\Phi_{kl}^{LJ}(r_{kl}) = C_{kl}\epsilon_{kl}\Big[\Big(\frac{\sigma_{kl}}{r}\Big)^{12} - \Big(\frac{\sigma_{kl}}{r}\Big)^{6}\Big] \tag{4.1}$$

where σ_{kl} is the segment diameter (at which the potential is zero) and ϵ_{kl} is the depth of the potential well and it is a measure of the attraction that two particles have for each other. The term with the power of 12 represents the repulsive forces, whereas the term with the power of 6 represents the attractive forces.

A more versatile option is the Mie intermolecular potential, Φ^{Mie}, with adjustable attractive and repulsive exponents. The advantage of the Mie potential lies in its soft-core variable range. The Mie potential can be described as:

$$\Phi_{kl}^{Mie}(r_{kl}) = C_{kl}\epsilon_{kl}\Big[\Big(\frac{\sigma_{kl}}{r}\Big)^{\lambda_{kl}^{r}} - \Big(\frac{\sigma_{kl}}{r}\Big)^{\lambda_{kl}^{a}}\Big] \tag{4.2}$$

with:

$$C = \frac{\lambda_{kl}^r}{\lambda_{kl}^r - \lambda_{kl}^a} \left(\frac{\lambda_{kl}^r}{\lambda_{kl}^a} \right)^{\frac{\lambda_{kl}^a}{\lambda_{kl}^r - \lambda_{kl}^a}} \tag{4.3}$$

where λ_{kl}^r and λ_{kl}^a are the repulsive and attractive exponents of the unlike interactions. The pre-factor C_{kl} is a function of the exponents of the potential and ensures that the minimum interaction is given by $-\epsilon_{kl}$. A graphical representation of the Mie Potential is given in figure 4.2:

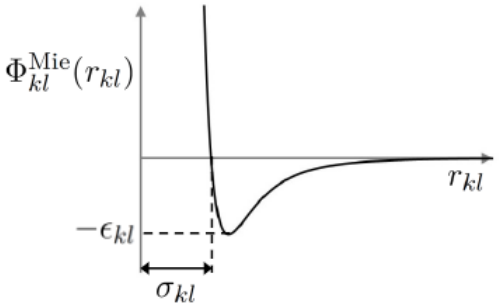

Figure 4.2: Mie potential representation in function of the distance between two particles

In case of the existence of different groups in the same mixture we also need to consider the cross interactions, like the cross ϵ_{kl}. In general, when dealing with mixtures with different groups, the existent interactions are divided into two groups: self-interactions (for groups of the same type) and cross-interactions (for groups of different types).

4.3 SAFT γ - Mie: free energy contributions

The total Helmholtz free energy A of a mixture of heteronuclear associating molecules from different Mie segments can be written as a sum of different contributions. The original SAFT equation just takes into account the first four terms of equation 4.4 . However, when dealing with electrolyte mixtures two more terms need to be added, namely the ion term (that considers the ion-ion interactions) and the Born term (related to the process of charging the ionic species). As a result, a "new" formulation of the SAFT EoS is presented below.

$$\frac{A}{Nk_bT} = \frac{A^{ideal}}{Nk_bT} + \frac{A^{mono}}{Nk_bT} + \frac{A^{chain}}{Nk_bT} + \frac{A^{assoc.}}{Nk_bT} + \frac{A^{Born}}{Nk_bT} + \frac{A^{Ion}}{Nk_bT} \tag{4.4}$$

where A^{ideal} stands for the free energy of an ideal gas, $A^{mono.}$ is the term accounting for interactions between monomer segments, A^{chain} is the contribution to the free energy for the formation of molecules, $A^{assoc.}$ is the term accounting for the association interactions, A^{Born} is the Helmholtz free energy associated with the process of charging the ions incorporated in the solvent, A^{Ion} is the Helmholtz free energy related with electrostatic interactions between charged species, N is the total number of molecules, k_B is the Boltzmann constant and T is the absolute temperature.

As was stated above, the monomer fluid consists of spherical hard segments to which dispersion forces are added and chains can be formed through covalent bonds. A perturbation scheme is presented in 4.3.

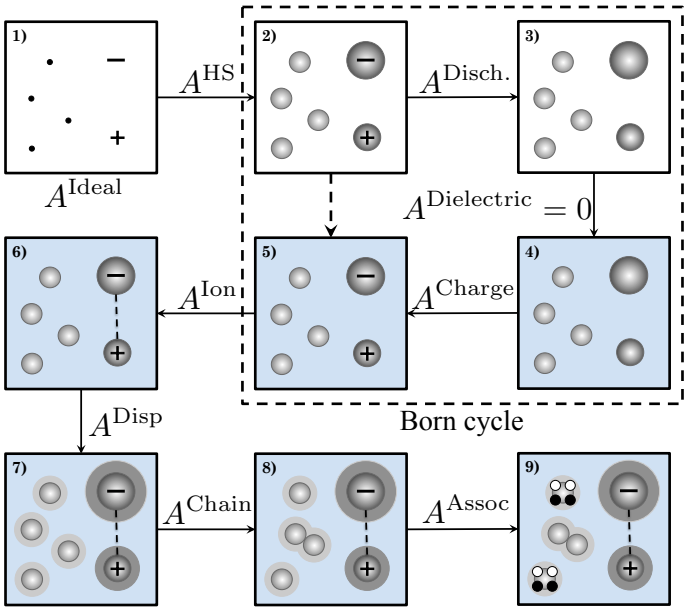

Figure 4.3: Schematic representation of the different free energy contributions. The darker background represents the dielectric medium.[4]

In Figure 4.3, one can see that in the first frame we have a mixture of neutral and charged particles that do not interact in vacuum. From frame (1) to frame (2) a hard sphere fluid with non interacting charges in vacuum is presented. Here, the change in the Helmholtz free energy is given as A^{HS}. In the second step ions are discharged leading to frame (3), a mixture of hard-spheres in vacuum, where the energy that corresponds to the free energy change is presented as $A^{discharge}$. In frame (4) a continuous dielectric medium, D, is introduced, and then, the ions are recharged. In this step, the charged ions continue not interacting and the free energy change is given by A^{charge}. Once charged, the ions start to have charge-charge Coulomb interactions and the corresponding system is a mixture of charged hard-spheres in a dielectric medium. The last frames, (7),(8) and (9) represent the remaining contributions of the standard SAFT EoS, namely the dispersion interactions, the formation of chains and the inclusion of association.

It is important to understand that the developed work for this thesis was merely the modelling and the parameter estimation of some aqueous electrolyte solutions. A summary of the main equations can be found in the next subsections in order to provide some theorethical background to the reader. The full derivation of those equations can be found in the original SAFT papers.[5][4][12][13]

4.3.1 Ideal term

The ideal Helmholtz free energy term of a mixture is given by equation (4.5).

$$\frac{A^{Ideal}}{Nk_bT} = \left(\sum_{i=1}^{N_C} x_i ln(\rho_i \Lambda_i^3)\right) - 1 \tag{4.5}$$

where x_i stands for the mole fraction of a given component i in the mixture, $\rho_i = \frac{N_i}{V}$ is the number density of component i, N_i is the number of molecules of component i and V the volume of the system.

The ideal fee energy incorporates the effects of the translational, rotational, and vibrational contributions to the kinetic energy implicitly through the thermal de Broglie volume, Λ_i^3.

4.3.2 Monomer term

The monomer term accounts for the interactions between each segment, or monomer (whether it is an atom, a molecule or a GC) and for that reason requires that an intermolecular potential is defined. In the SAFT γ - Mie framework, the monomer contribution of the Helmholtz free energy is obtained as a third-order perturbation expansion. [12]

$$\frac{A^{Mono}}{Nk_bT} = \frac{A^{HS}}{Nk_bT} + \frac{A_1}{Nk_bT} + \frac{A_2}{Nk_bT} + \frac{A_3}{Nk_bT} \tag{4.6}$$

where A^{HS} stands for the hard sphere Helmholtz free energy of the mixture and is given by:

$$\frac{A^{HS}}{Nk_Bt} = \left(\sum_{i=1}^{N_C} x_i \sum_{k=1}^{N_G} \nu_{k,i} \nu_k^* S_k \right) a^{HS} \tag{4.7}$$

where N_C is the number of components, N_G is the number of group types, $\nu_{k,i}$ is the number of occurrences of group k, ν_k^* is the number of identical segments that form group k and a^{HS} is the dimensionless contribution to the hard-sphere free energy per segment. This last parameter can be obtained using the expression of Boublík and Mansoori. [12]

A_1,A_2 and A_3 correspond to the attractive perturbation terms. The first order term A_1 of the perturbation expansion correlates to the mean attractive energy per molecule and, as for the hard-sphere term, it is obtained as a summation of the contributions to the mean-attractive energy per segment a_1:

$$\frac{A_1}{Nk_BT} = \frac{1}{k_BT} \left(\sum_{i=1}^{N_C} x_i \sum_{k=1}^{N_G} \nu_{k,i} \nu_k^* S_k \right) a_1 \tag{4.8}$$

where

$$a_1 = \sum_{k=1}^{N_G} \sum_{l=1}^{N_G} x_{s,k} x_{s,l} a_{1,kl} \tag{4.9}$$

with $x_{s,k}$ standing for the fraction of segments of a group of type k in the mixture, and $a_{1,kl}$ for pairwise interactions between groups k and l over all types of functional groups present in the system.

The second order perturbation is calculated using the improved Macroscopic compressibility approximation (MCA) with the modification proposed by Paricaud. [5] This particular term accounts for the local fluctuation in the attractive interactions and is obtained as:

$$\frac{A_2}{Nk_BT} = \left(\frac{1}{k_BT} \right)^2 \left(\sum_{i=1}^{N_C} x_i \sum_{l=1}^{N_G} x_{s,k} x_{s,l} a_{2,kl} \right) \tag{4.10}$$

with,

$$a_2 = \sum_{k=1}^{N_G} \sum_{l=1}^{N_G} x_{s,k} x_{s,l} a_{2,kl} \tag{4.11}$$

Last but not least, an empirical expression is used for the third order perturbation term, A_3, with coefficients obtained to reproduce the critical point and fluid-phase equilibrium of Mie fluids.[5] This term is obtained for the contribution per segment a_3 as[12]:

$$\frac{A_3}{Nk_BT} = \left(\frac{1}{k_BT} \right)^3 \left(\sum_{i=1}^{N_C} x_i \sum_{l=1}^{N_G} \nu_{k,i} \nu_k^* S_k \right) a_3 \tag{4.12}$$

and,

$$a_3 = \sum_{k=1}^{N_G} \sum_{l=1}^{N_G} x_{s,k} x_{s,l} a_{3,kl} \tag{4.13}$$

4.3.3 Chain term

The SAFT approach accounts for chain length by taking the limit of complete bonding in Wertheim's TPT1. By including the chain term, the SAFT EoS considers the free energy contributions due to the formation of chains made of monomer segments. In the case of a mixture, the expression is given as [5]:

$$\frac{A^{chain}}{N k_B T} = -\sum_{i=1}^{N_c} x_i (m_{seg,i} - 1) ln g_{ii}^{Mie}(\sigma_i) \tag{4.14}$$

where $m_{seg,i}$ stands for the number of segments per chain and lng_{ii}^{Mie} takes into account the Radial Distribution Function (RDF) of the monomeric Mie fluid system at contact σ_i.

4.3.4 Association term

Associating fluids are able to form clusters of associated molecules. Therefore, the SAFT model for associating fluids not only accounts for monomers but also for associated clusters.

The association contribution has its roots in the Weirtheim's first order thermodynamic perturbation theory (TPT1) and it is motivated because some molecules tend to "stick together". As a consequence, the $A^{Association}$ term accounts for the free energy due to the association between molecules through the bonding sites and can be calculated by:

$$\frac{A^{Association}}{N k_B T} = \sum_{i=1}^{N_C} x_i \sum_{k=1}^{N_G} \nu_{k,i} \sum_{a=1}^{N_{ST,k}} n_{k,a} \left(ln X_{i,k,a} + \frac{1 - X_{i,k,a}}{2} \right) \tag{4.15}$$

This fraction is obtained through a set of equations called mass-action equations, which essentially result from a mass balance to association sites.

4.3.5 Born Contribution

The change in the free energy of a system, due to the insertion of all ions in the dielectric medium, is given by the free energy of solvation.[5] In other words, one can say that the Born solvation energy can be defined as the change in the free energy that results from the electrostatic interactions when ions are transferred from vacuum into a dielectric medium at infinite dilution.[4] Though simplistic, the theory used to describe the process of solvation is the Born approach. Despite its simplicity, this method captures the basic thermodynamic features and gives good estimates. Overall, in his original derivation a thermodynamic cycle is proposed in which the work of discharging the particle in vacuum and the work of recharging it in the medium are incorporated, while neglecting the work required to transfer the uncharged particle into the solvent.[4] The final result, at infinite dilution, leads to:

$$\mu_i^{Born} = -\frac{e^2}{4\pi\epsilon_0} \left(1 - \frac{1}{D} \right) \left(\frac{z_i^2}{\sigma_i^{Born}} \right) \tag{4.16}$$

where μ_i^{Born} is the chemical potential of a certain ion, i, in solution, e is the elementary charge ($1.602 \times 10^{-19} C$), ϵ_0 is the vacuum permittivity ($8.854 \times 10^{-12} C^2 J m^{-1}$), D is the relative permittivity of a

uniform dielectric medium, z_i is the bearing charge, and σ_i^{Born} is the diameter of a non-polarized sphere that represents the ion.

In equations based on primitive model expressions, the accuracy of the Couloumbic free energy contributions (A^{Ion} and A^{Born}) is crucially dependent on the usage of accurate values for the dielectric constant that is used in place of an explicit accounting of the solvent electric properties. There are a number of rigorous models to obtain the dielectric constant, however they are not easy to implement, and generally, they require new added adjustable parameters. Instead, the relative static permittivity D is calculated with a Harvey-Prausnitz model. This correlative model depends on the solvent composition, density, and temperature, and thereby exhibits an implicit dependence on the ion concentration. This model suggests that there is a relationship between the dielectric constant and the density of many polar media.[4],[5]

$$D = 1 + \rho_{solv} d \tag{4.17}$$

where d is a solvent-dependent parameter (calculated through the following equation) and ρ_{solv} is the density of the solvent.

$$d = d_V \left(\frac{d_T}{T} - 1 \right) \tag{4.18}$$

where d_V is a volume parameter and d_T a temperature parameter. Both of them are component specific parameters.

Considering a constant volume and temperature, and assuming the same change in free energy for the insertion of each of the ions, the Helmholtz free energy change is given by:

$$A^{Born} = -\frac{e^2}{4\pi\epsilon_0} \left(1 - \frac{1}{D} \right) \sum_{ion,i=1} \frac{N_i z_i^2}{\sigma_i^{Born}} \tag{4.19}$$

4.3.6 MSA Contribution

The ionic contribution to the Helmholtz free energy illustrates the replacement of the solvent by a dielectric medium in which Coulombic interactions are screened.[4] This means that ion-ion interactions are expressed with a Coulomb potential in a dielectric medium, i.e.

$$u^{ion}(r_{ij}) = \frac{e^2}{4\pi\epsilon_0 D} \frac{Z_i Z_j}{r_{ij}} \tag{4.20}$$

where r_{ij} represents the centre centre distance between charges i and j. There is more than one theory when considering electrolyte modelling: the primitive one and the non-primitive one. In the case of the primitive model either the Debye-Hückel theory or the Mean Spherical Approximation (MSA) is used and leads to accurate and similar results. Applying the MSA approach, the change in the Helmholtz free energy due to electrostatic interactions between charged species within the MSA formalism can be expressed as:

$$A^{ion} = U^{MSA} + \frac{\Gamma^3 k_B T V}{3\pi} \tag{4.21}$$

where U^{MSA} stands for the MSA contribution to the internal energy U, and Γ is the screening length of the electrostatic forces. The MSA internal energy can be obtained by:

$$U^{MSA} = -\frac{e^2 V}{4\pi\epsilon_0 D} \left[\frac{\Gamma}{V} \sum_{i=1}^{n_{ion}} \left(\frac{N_i Z_i^2}{1 + \Gamma\sigma_i} \right) + \frac{\pi}{2\Delta} \Omega P_n^2 \right] \tag{4.22}$$

with Δ representing the packing fraction of the ions as a function of their diameter, σ_i^3:

$$\Delta = 1 - \frac{\pi}{6V} \sum_{i=1}^{n_{ion}} N_i \sigma_i^3 \tag{4.23}$$

With regard to the P_n and Ω functions, they are coupling parameters, where P_n couples to the charge of the ions, whereas Ω relates to the packing fraction of the ions.[5] They can both be obtained by the following equations:

$$P_n = \frac{1}{\Omega V} \sum_{i=1}^{n_{ion}} \frac{N_i \sigma_i Z_i}{1 + \Gamma \sigma_i} \tag{4.24}$$

$$\Omega = 1 + \frac{\pi}{2\Delta V} \sum_{i=1}^{n_{ion}} \frac{N_i \sigma_i^3}{1 + \Gamma \sigma_i} \tag{4.25}$$

Ultimately, the screening length, given by Γ, is a function of the relative static permittivity and the effective charge $Q_i(\Gamma)$ of the ions:

$$\Gamma^2 = \frac{\pi e^2}{(4\pi\epsilon_0) D k_B T V} \sum_{i=1}^{n_{ion}} N_i Q_i^2 \tag{4.26}$$

where the effective charge is related to the electric charge of the individual species and the P_n coupling parameter:

$$Q_i = \frac{Z_i - \sigma_i^2 P_n(\frac{\pi}{2\Delta})}{1 + \Gamma \sigma_i} \tag{4.27}$$

To establish Γ it is necessary to run an iterative procedure, in which the initial guess is given by Γ_0. This initial guess is, on the other hand, obtained by the Debye-Hückel formulation, as seen in the following equation:

$$\Gamma_0 = \frac{\kappa}{2} = 0.5 \sqrt{\frac{e^2}{4 D \epsilon_0 V k_B T} \sum_{i=1}^{n_{ion}} N_i Z_i^2} \tag{4.28}$$

where κ is the inverse Debye-Hückel length.

Chapter 5

Development of model parameters and analyses of the systems of interest

5.1 Description of parameters

The SAFT γ- Mie framework is used to describe the behaviour of electrolyte solutions. Various electrolyte solutions are considered focusing on a broad set of experimental data. The goal of this work is to determine the best combination of thermodynamic properties to include in the parameter regression procedure to ensure that the resulting model parameters can capture all the desired results.

The EoS is formulated such that model parameters are ion based (as opposed to salt based), which allows for the properties of multiple salts to be calculated with fewer parameters.[8]

In this work ions are modelled as spheres consisting of a single segment $(m_{seg,i} = 1)$ of diameter σ_i and carrying a single point charge $(q_i = Z_i e)$. All the ions experience dispersion interactions, represented by Mie potentials, both with the other ions in solution and with the neutral species. Water is represented as a spherical molecule with four off-centre association sites.[5]

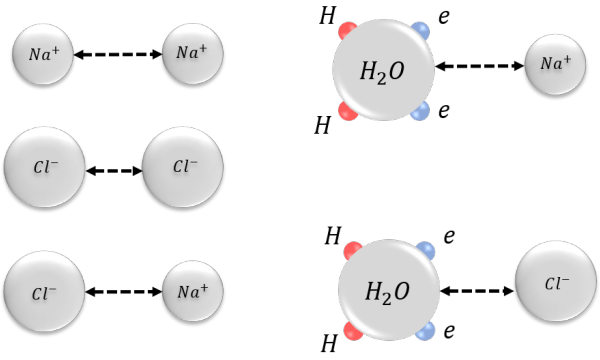

Figure 5.1: Schematic representation of the model used for the like and unlike interactions between ion-ion and ion-water. ($NaCl$ example) The associative sites are labelled as e and H, typically representing either a lone-pair of electrons on an electronegative atom or hydrogen atoms in the functional group.

The adjustable parameters for the like-interactions include the diameter σ_i and the interaction energy ϵ_{ii}, whereas the adjustable unlike interactions include the interaction energy between two different ions,

ϵ_{ij} and between an ion with the solvent, $\epsilon_{i-water}$. With regard to the repulsive and attractive exponents they were set with the value of 12 and 6, respectively, as described in the Lennard-Jones potential. This approach allows the reduction of the number of parameters to be estimated and, as will be seen, leads to good results.

In order to compensate for some of the shortcomings of the Born term, and hence capture the solvation effects more accurately, an extra adjustable parameter for ions called the ionic diameter increment $\Delta\sigma_i$ was found to be necessary in some previous works[8], which is related to the ion group diameter through:

$$\sigma_i^{Born} = \sigma_i + \Delta\sigma_i \tag{5.1}$$

Finally we have found that it is necessary to consider that cross interactions can be temperature dependent. As a consequence, another adjustable parameter was considered: epsilon expansion coefficient, B. If we take the $\epsilon_{i-water}$ as an example, we can see in equation 5.2 how it can be calculated.

$$\frac{\epsilon_{i-water}}{k} = \frac{\epsilon_{0,i-water}}{k} + \frac{B_{i-water}}{kT} \tag{5.2}$$

where $\epsilon_{0,i-water}$ accounts for the ion-water interaction parameter.

5.2 Experimental Data

Experimental data is not only necessary to the estimation of parameters for a thermodynamic model but also to validate the model. Before starting the parameter estimation several data had to be gathered and diverse literature was used. For this work experimental data on solubilities, liquid phase densities, mean activity coefficients, osmotic coefficients, heat capacities of the solid and liquid phases and heats of dilution was needed.

One important thing to understand is that some of these data, like the solid properties, had to be provided to the model. This was found to be necessary because SAFT is a fluid theory, and so, the theory cannot calculate these data by itself.

For the construction of the databank, it was necessary to have:

- Ions enthalpy and entropy of formation [10]
- Molecular weights of ions and salts [14]
- Solid enthalpy and entropy of formation [10]
- Solid heat capacities [14],[15]

On the other hand, it was also necessary to obtain some data to build the model and to fit the diverse parameters. Among that data we have:

- Salts solubilities in water [16],[17],[18],[19],[20]
- Solution liquid phase densities [21]
- Liquid phase heat capacities [22]
- Enthalpies of dilution [22]

Last but not least, there were properties that were not used in the modelling but were verified in order to see if the predicted results were in line with the expected.

- Mean Activity Coefficients [23]
- Osmotic Coefficients [23]

5.3 Systems of interest

One of the decisions that had to be made was which salts would be studied and considered to build the desired model. In the previous section, all the necessary experimental data was introduced to build the databank and to proceed with the parameter estimation. In order to find out in which salts the study would be based on, diverse literature was consulted in order to choose which salts could be considered.

In Table 5.1, all the results of the literature review are summed up. From all the ions combinations, the only resulting salts that could be considered in this study were the ones covered with a blue shading. For the ones covered with a red shading, either it was not possible to find the necessary data, like solubilities, formation enthalpies and entropies and solid phase heat capacities, or the available data was not consistent and reliable. Regarding the yellow shaded cells, the presented salts are always found in the hydrate form. Solid heat capacities and formation properties were not found for these compounds, and for that reason they could not be considered and studied. In order to overcome this problem, it was attempted to fit solid heat capacities for hydrates, however, the obtained results were not trustworthy. (See Appendix B)

Table 5.1: Literature review results. The blue shaded cells have to do with the salts that can be considered to build the model, the yellow shaded cells represent the salts that are only in the hydrate form in the studied conditions, and the red shaded cells represent the salts for which it wasn't found the necessary data.

	F^-	Cl^-	Br^-	I^-	NO_3^-	ClO_4^-	SO_4^{2-}
Li^+	LiF	$LiCl$	$LiBr$	LiI	$LiNO_3$	$LiClO_4$	Li_2SO_4
Na^+	NaF	$NaCl$	$NaBr$	NaI	$NaNO_3$	$NaClO_4$	Na_2SO_4
K^+	KF	KCl	KBr	KI	KNO_3	$KClO_4$	K_2SO_4
Rb^+	RbF	$RbCl$	$RbBr$	RbI	$RbNO_3$	$RbClO_4$	Rb_2SO_4
Cs^+	CsF	$CsCl$	$CsBr$	CsI	$CsNO_3$	$CsClO_4$	Cs_2SO_4
Mg^{2+}	MgF_2	$MgCl_2$	$MgBr_2$	MgI_2	$Mg(NO_3)_2$	$Mg(ClO_4)_2$	$MgSO_4$
Ca^{2+}	CaF_2	$CaCl_2$	$CaBr_2$	CaI_2	$Ca(NO_3)_2$	$Mg(ClO_4)_2$	$CaSO_4$
Sr^{2+}	SrF_2	$SrCl_2$	$SrBr_2$	SrI_2	$Sr(NO_3)_2$	$Sr(ClO_4)_2$	$SrSO_4$
Ba^{2+}	BaF_2	$BaCl_2$	$BaBr_2$	BaI_2	$Ba(NO_3)_2$	$Ba(ClO_4)_2$	$BaSO_4$
Mn^{2+}	MnF_2	$MnCl_2$	$MnBr_2$	MnI_2	$Mn(NO_3)_2$	$Mn(ClO_4)_2$	$MnSO_4$
NH_4^+	NH_4F	NH_4Cl	NH_4Br	NH_4I	NH_4NO_3	NH_4ClO_4	$(NH_4)_2SO_4$
Cd^{2+}	CdF_2	$CdCl_2$	$CdBr_2$	CdI_2	$Cd(NO_3)_2$	$Cd(ClO_4)_2$	$CdSO_4$

As a first approach, the ions that were parametrized were Na^+, K^+, Cl^- and Br^- and, for that reason, the data needed is referred to $NaCl$, KCl, $NaBr$ and KBr.

Still regarding the solubility data, it is important to underline that the range of temperatures used was between 25 and a 100 Celsius degrees.

The estimation of the group parameters is carried out using the gSAFT Material Modeller (gSAFTmm) by minimizing an objective function. The objective function applied is given by:

$$f_{obj} = \sum_{i=1}^{NP} \left(\frac{s_i^{cal} - s_i^{exp}}{s_i^{cal}} \right)^2 + \sum_{i=1}^{NP} \left(\frac{\rho_i^{cal} - \rho_i^{exp}}{\rho_i^{cal}} \right)^2 + \sum_{i=1}^{NP} \left(\frac{Cp_i^{cal} - Cp_i^{exp}}{Cp_i^{cal}} \right)^2 + \sum_{i=1}^{NP} \left(\frac{\Delta H_{d,i}^{cal} - \Delta H_{d,i}^{exp}}{\Delta H_{d,i}^{cal}} \right)^2 \tag{5.3}$$

where s_i stands for the solubility of a given salt, ρ_i for the density, Cp_i for the heat capacity and $\Delta H_{d,i}$ for the dilution enthalpy.

One interesting thing to say is that, when computing the different adjustable parameters, it is possible to give different weights to the different properties that are being used. This means that properties with lower weights will have a lower impact in the results of the final model.

Chapter 6

Parameter Estimation Strategy and Results

To introduce this chapter it is important to say that not all of the obtained results and plots are shown in each step of the parameter estimation strategy. Those information is only available in the mentioned Appendixes. The reason why it was chosen to present the results in this way is due to the fact that, as will be seen, we can only obtain all the desired results by combining data on every property (solubilities, liquid phase densities, liquid phase heat capacities and dilution enthalpies).

6.1 Estimation using solubility

During all the parameter estimation startegy it was considered that the solubility of inorganic compounds in water was crucial to be described.

In order to obtain these results, the parameters for all the ions were fitted at the same time and only the data on salts solubilities was used. The model proved to be able to accurately fit the results without it being necessary to include all the available experimental points.

Regarding the considered fitted parameters, in this particular case it was only needed to estimate the values of:

- σ_i
- ϵ_{ii}
- ϵ_{ij}
- $\epsilon_{i-water}$

All the regressed parameters can be seen in Appendix C.1, Tables C.1 and C.2 .

The obtained results are presented in Figure 6.1 and, as can be seen, SAFT γ-Mie could fit the results properly. One interesting result is the $NaBr$ solubility as a function of temperature. $NaBr$ for temperatures below 60 ℃ is in a hydrate form ($NaBr.2H_2O$).[19],[16] As was already stated, hydrate forms are difficult to study due to the lack of information on the solid form heat capacities as a function of temperature. However, taking into account only the hydrate data at 25 ℃ the problem is overcome (check Equation 3.10), and as can be seen, the model is able to predict the right solubility behaviour for the other temperatures as well.

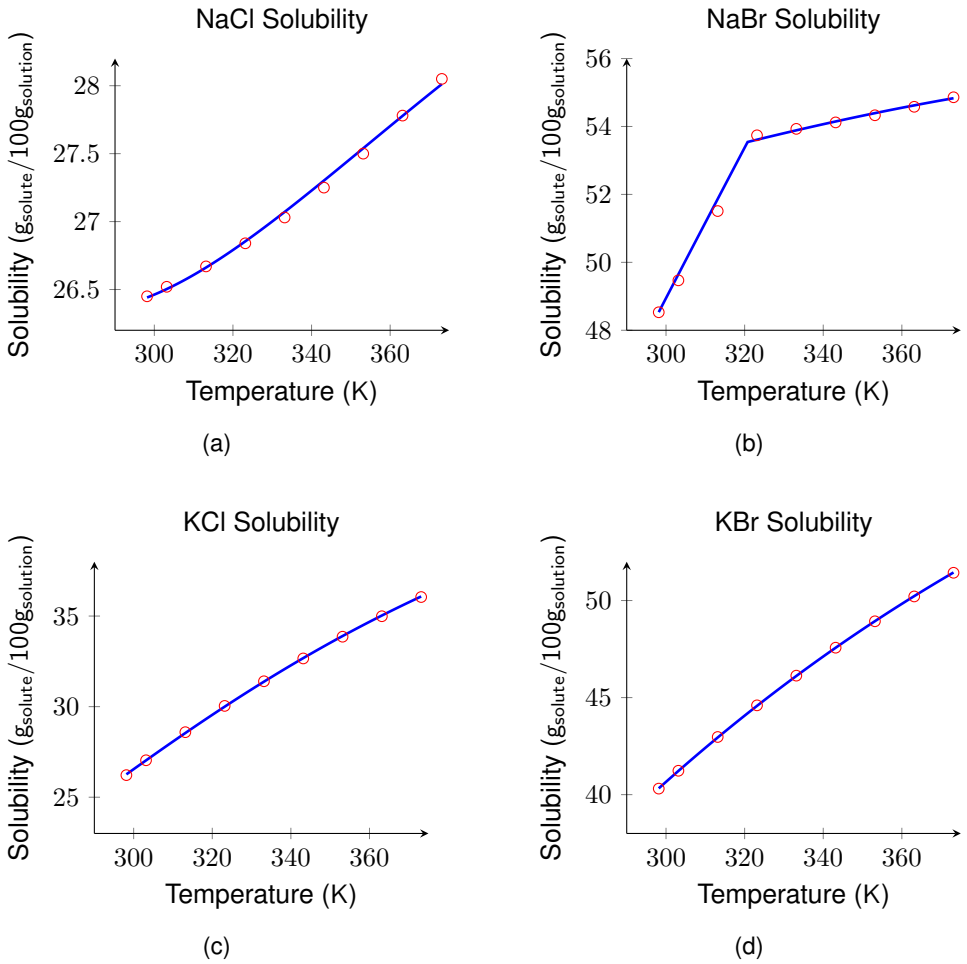

Figure 6.1: Solubility of a salt depending on the temperature, taking into account only experimental data on solubility. The different plots have both experimental (○) and SAFT predictions data (−).

Looking beyond these results, it was of interest to know if only by fitting the parameters to the solubility values, it would be possible to predict all the other properties. The obtained results were evaluated for mean activity coefficients, liquid phase densities, liquid phase heat capacities, osmotic pressures and enthalpies of dilution. Unfortunately none of these properties revealed good results when compared with all the experimental data. All the results can be analysed in the Appendix C.1.

6.2 Estimation using solubility and liquid phase density

The second startegy was to adjust the the liquid phase density. The amount of a species in a given volume depends on its size, and because of that, sigma values and densities are related with one another. In fact, when comparing the results of the previous approach with the final ones it is possible to see that the final sigma values (accounted by the Born sigma) are very different.

Approach 6.2.1

It was of interest to understand if it would be possible to fit the results to solubility and density when using a reduced set of adjustable parameters. Therefore, it was studied if it would be possible to reach accurate results when regressing the same parameters as before: σ_i, ϵ_{ii}, ϵ_{ij} and $\epsilon_{i-water}$. The results (presented in the Appendix C.2) proved that the objective function was not sufficiently low to reproduce

the experimental results in such a good way as before. The desire to improve these results resulted in a second attempt of parameters fitting.

In view of the above, in Figure 6.2 it is possible to analyse the change in the solubility results for the $NaCl$.

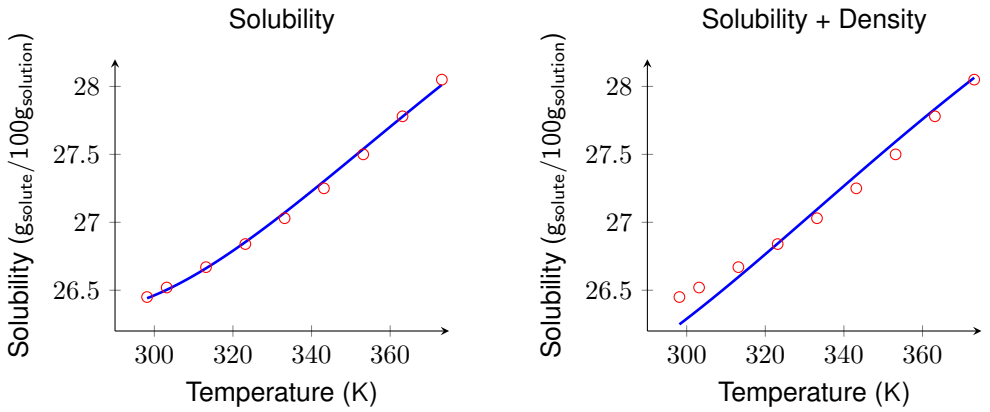

(a) (b)

Figure 6.2: Comparison of solubilities predictions for $NaCl$. (a) Model-Fitting to Solubility, (b) Model-Fitting to Solubility and Liquid Phase Density (Approach 1)

The quantitative results can be observed in the following table.

Table 6.1: Comparison of solubility results for $NaCl$ and corresponding %Δ.

		Solubility		Solubility + Density	
Temperature (K)	Experimental Solubilities $g_{solute}/100g_{solution}$	SAFT	%Δ	SAFT	%Δ
298.15	26.45	26.44	0.03	26.25	0.76
303.15	26.52	26.50	0.06	26.36	0.60
313.15	26.67	26.66	0.03	26.60	0.27
323.15	26.84	26.85	0.05	26.84	0.01
333.15	27.03	27.07	0.15	27.09	0.24
343.15	27.25	27.30	0.19	27.35	0.35
353.15	27.50	27.54	0.14	27.59	0.34
363.15	27.78	27.78	0.01	27.83	0.19
373.15	28.05	28.01	0.14	28.06	0.05

Approach 6.2.2

In order to keep good results for solubility, a new parameter was considered adjustable: $\Delta\sigma_i$. By adding this parameter, as was expected, the solubility values could be once again obtained with accuracy. This happens because the same propreties were being considered but a new parameter was added.

All the regressed parameters can be seen in the Appendix C.2, Tables C.3 and C.4 .

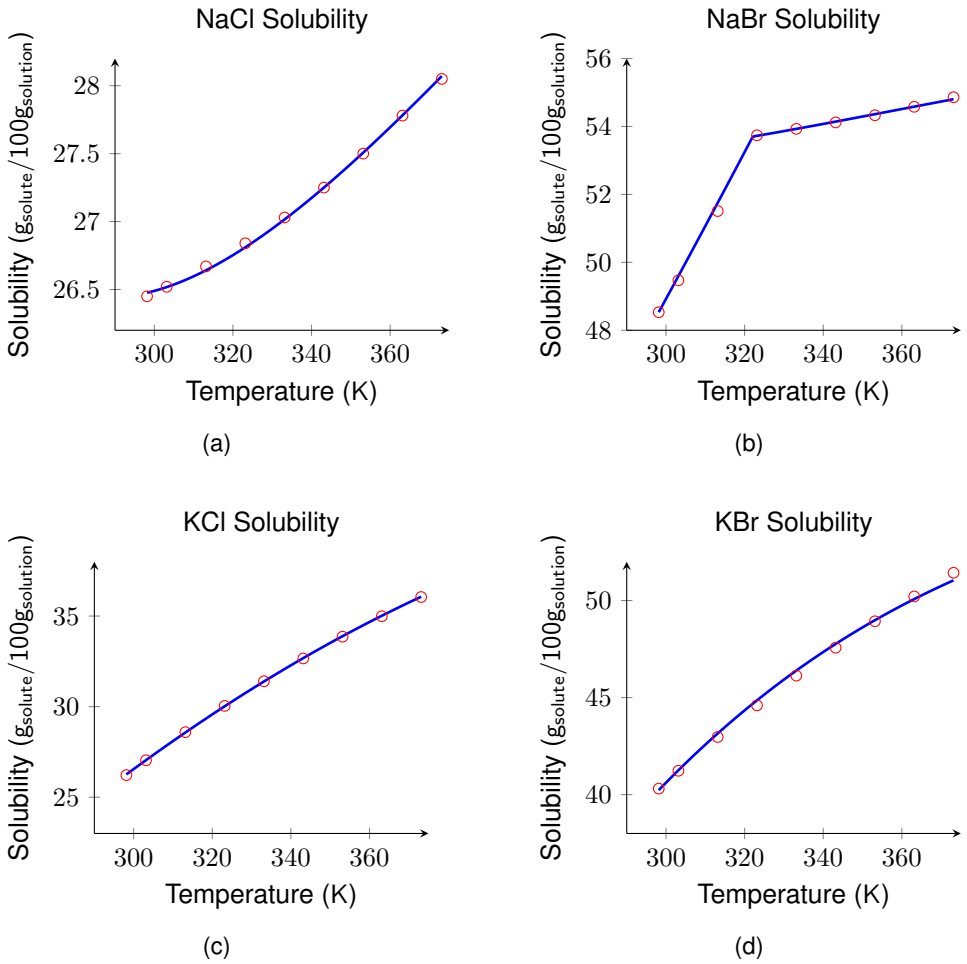

Figure 6.3: Solubility of a salt depending on the temperature, taking into account experimental data on solubility and liquid phase densities. The different plots have both experimental (○) and SAFT predictions data (−).

As the fitting is also being done to liquid phase densities, the results of the calculation appear to be accurate as well. (when compared to the experimental data) The obtained results can be seen in Figure 6.4.

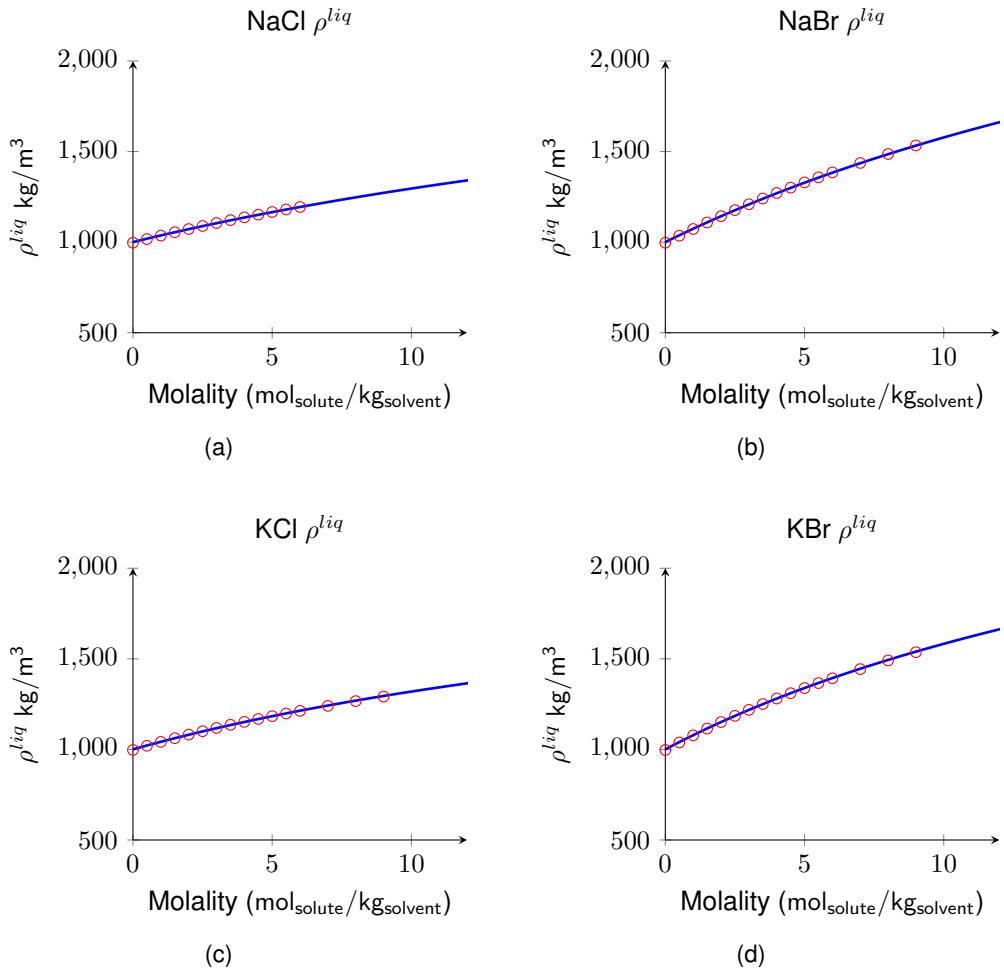

Figure 6.4: Liquid phase densities results, taking into account experimental data on solubility and liquid phase densities. The different plots have both experimental (○) and SAFT predictions data (−).

After adding the liquid phase densities, it is possible to see that the mean activity coefficient values predicted by the model are similar to the experimental values. The same happens for the osmotic coefficients, as can be seen in the Appendix C.2.

It was also verified if by adding the liquid phase densities, the other properties, apart from the mean activity coefficients and osmotic coefficients, would be obtained. The liquid phase heat capacities and enthalpies of dilution could not be obtained yet, as can be seen in the Appendix C.2.

6.3 Estimation using solubility, liquid phase density and heat capacity

Another aim of this work was to obtain a model that could predict liquid phase heat capacities of electrolyte solutions. Heat capacities are widely used in industry since they are needed to understand heat transfer phenomena. Their use in energy balances makes them an important tool for the understanding of stream heats and equipment sizing.

Being able to predict this property is undeniably important and, since simpler models cannot catch it, this data was used to fit new parameters. To guarantee that the accuracy of the previous approaches

is maintained, data on solubilities, liquid phase densities and liquid phase heat capacities was used simultaneously.

Approach 6.3.1

The first attempt consisted of using the same parameters as before, which means that they were considered: σ_i, ϵ_{ii}, ϵ_{ij}, $\epsilon_{i-water}$ and the $\Delta\sigma_i$.

By using the same amount of parameters it is not possible to obtain a model with the same accuracy as before. (See the Appendix C.3 and Figure 6.5).

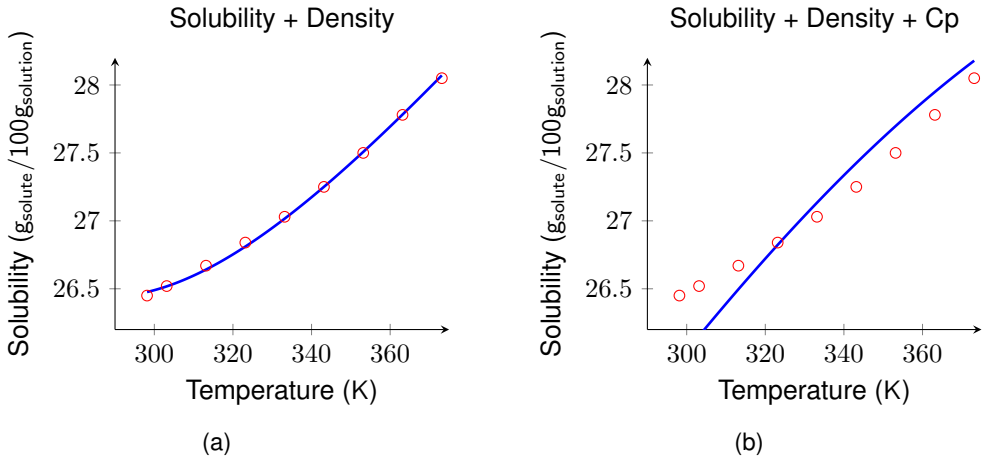

Figure 6.5: Comparison of solubilities results for $NaCl$. (a) Model-Fitting to Solubility + Liquid Phase Density, (b) Model-Fitting to Solubility + Liquid Phase Density + Liquid phase heat capacities(First Attempt)

Approach 6.3.2

In order to get a sufficiently low objective function, it was necessary to add a new parameter: epsilon expansion coefficient between ions and water, $B_{i-water}$. Regarding the results, as was expected, solubilities, liquid phase densities, mean activity coefficients and osmotic coefficients could be obtained with accuracy once again.

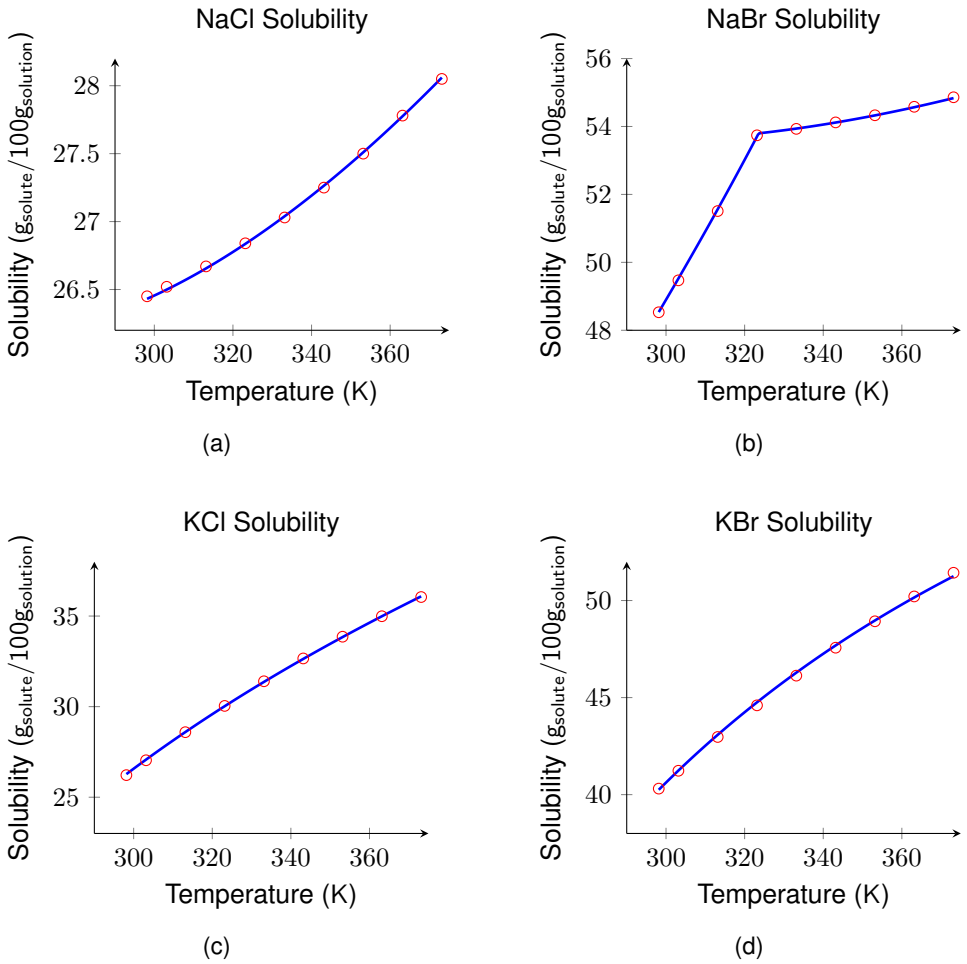

Figure 6.6: Solubility of a salt depending on the temperature, taking into account experimental data on solubility, liquid phase densities and liquid phase heat capacities. The different plots have both experimental ($\circ$) and SAFT predictions data ($-$).

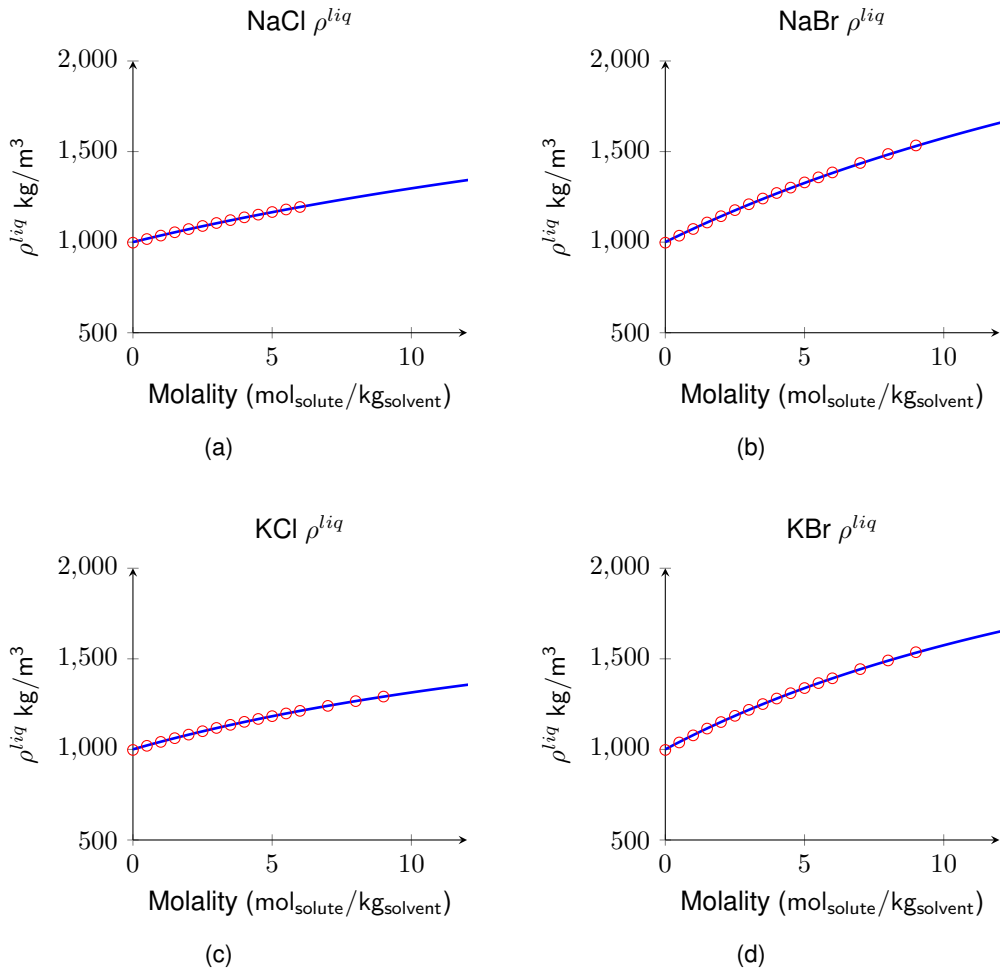

Figure 6.7: Liquid phase density depending on the molality, taking into account experimental data on solubility, liquid phase densities and liquid phase heat capacities. The different plots have both experimental (○) and SAFT predictions data (–).

Mean activity coefficients and osmotic coefficients could be obtained once again, without it being necessary to use experimental data on them. The obtained results can be seen in the Appendix C.3.

Regarding the liquid phase heat capacities, in the literature[22] it is not possible to find them directly published. Instead, apparent molar heat capacity of the solutes is given as a function of the molality. In order to obtain the desired values the Equation 6.1[22] was applied:

$$\Phi_c = \frac{[(1000 + MW)C_p - 1000.C_p^{solvent}]}{m} \tag{6.1}$$

where Φ_c is the apparent molal heat capacity of the solute in cal/mol^oC, m is the molality in $mol/kg_{solvent}$, MW is the molecular weight of the solute in g/mol and $C_p^{solvent}$ is the specific heat of the solvent in cal/g^oC. The result of the heat capacity, C_p will be obtained in units of cal/g^oC and will be subsequently converted to units of J/mol^oC.

The results presented in Figure 6.8 show that the goal was accomplished and that it was possible to obtain a model capable of giving liquid phase heat capacities. Moreover, to obtain these results it was only needed to set two heat capacity values for each compound. This means that the model does not need to make use of a lot of experimental data to provide good results.

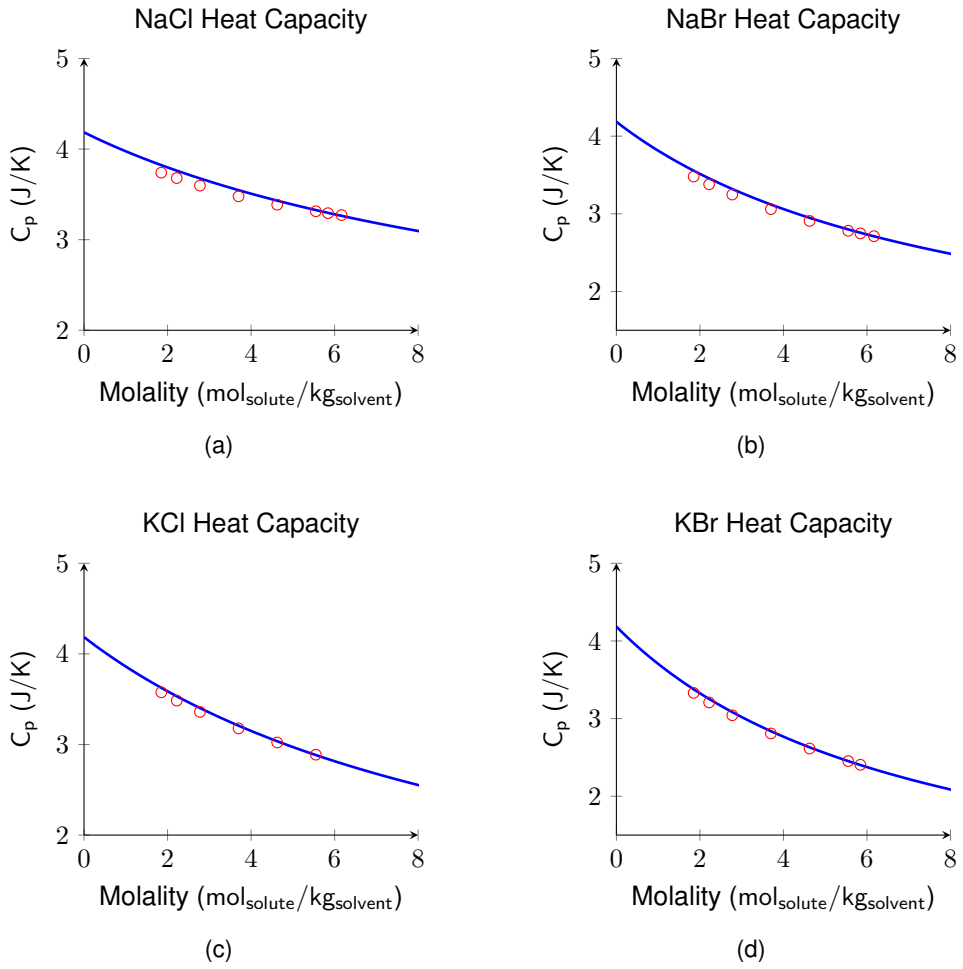

Figure 6.8: Liquid phase heat capacity of a salt depending on the molality, taking into account experimental data on solubility, liquid phase density and liquid phase heat capacities. The different plots have both experimental (○) and SAFT predictions data (−).

At this point the only missing prediction is the dilution enthalpy. With those parameters it is not possible to predict those values, as can be seen in Appendix C.3. Nevertheless, all the regressed parameters are presented in Tables C.5 and C.6 of Appendix C.3.

6.4 Estimation using solubility, liquid phase density and heat capacity and Dilution enthalpy

The last property to be added to the model is the dilution enthalpy or as it is also known, the heat of solution. The dilution enthalpy is the enthalpy change associated with the dissolution of a solute in a solvent at constant pressure, resulting in infinite dilution.[24] As an example we can consider the dissolution of $NaCl$ in water: dissolution of $NaCl$ in water is an endothermic process. The amount of energy used to break apart the hydrogen bounding interactions between water molecules, as well as the energy used to break apart the electrostatic attractions between sodium and chloride ions, is greater than the amount of energy released when new solute-solvent attractions are formed between water molecules and aqueous ions that are in solution.

As is expected, the greater the complexity of the model, the more parameters have to be adjusted. As we are using data on four different properties (solubility, liquid phase density, liquid phase heat capacity

and dilution enthalpy) the model starts to have a considerable complexity. Fitting the parameters in such a way that it is possible to get a relatively good objective function and reliable results demands the fitting of:

- σ_i
- ϵ_{ii}, ϵ_{ij}, $\epsilon_{i-water}$
- $B_{i-water}$, B_{ii}, B_{ij}
- $\Delta\sigma_i$

Good estimates were attempted to be obtained without having to use such a large number of parameters. However, the fewer the parameters that were considered, the worse the results were.

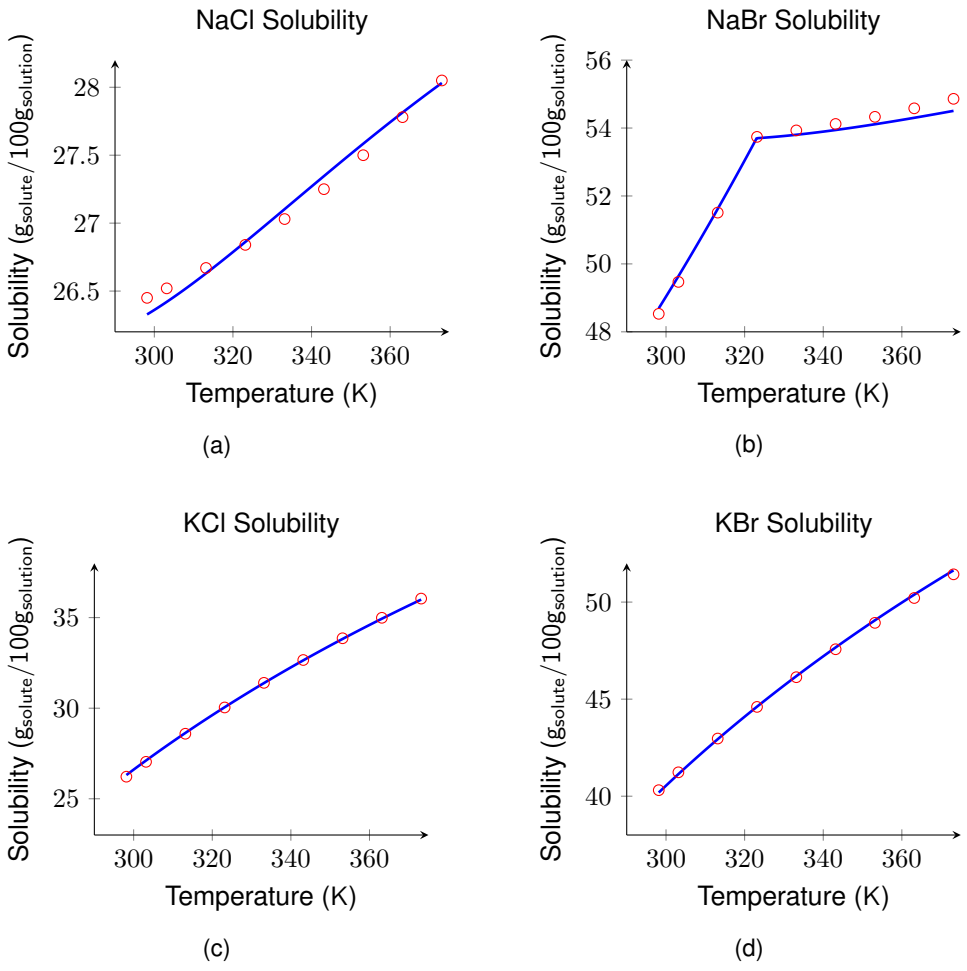

Figure 6.9: Solubility of a salt depending on the temperature, taking into account experimental data on solubility, liquid phase densities, liquid phase heat capacities and dilution enthalpies. The different plots have both experimental (○) and SAFT predictions data (–).

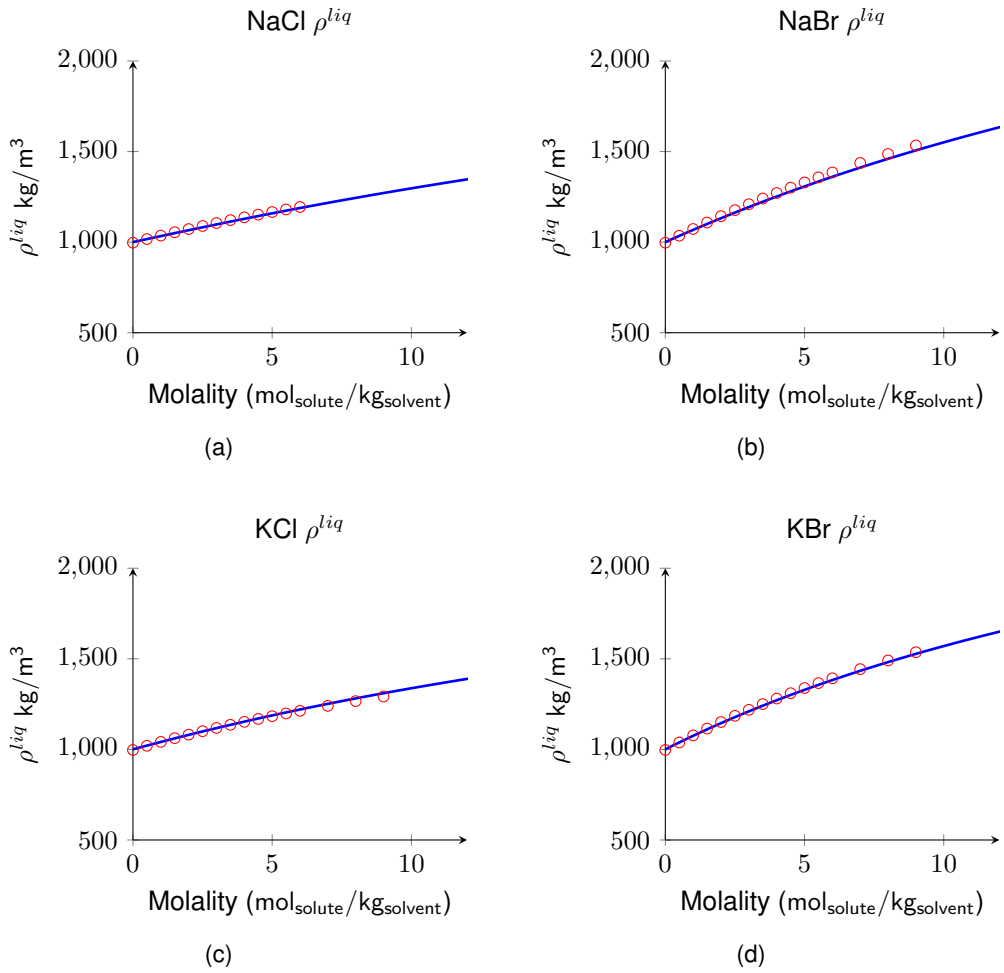

Figure 6.10: Liquid Phase Densities depending on molality, taking into account experimental data on solubility, liquid phase densities, liquid phase heat capacities and dilution enthalpies. The different plots have both experimental (○) and SAFT predictions data (−).

Both mean activity coefficients and osmotic coefficients can be predicted accurately (see Appendix C.4).

With respect to the liquid phase heat capacities, it was also possible to obtain the results in an accurate way. As can be seen in Figure 6.11 all the experimental points are coincident with the ones provided by the model. With only two values of liquid phase heat capacities, at two different molalities, the software is able to predict all the results for the remaining molality values.

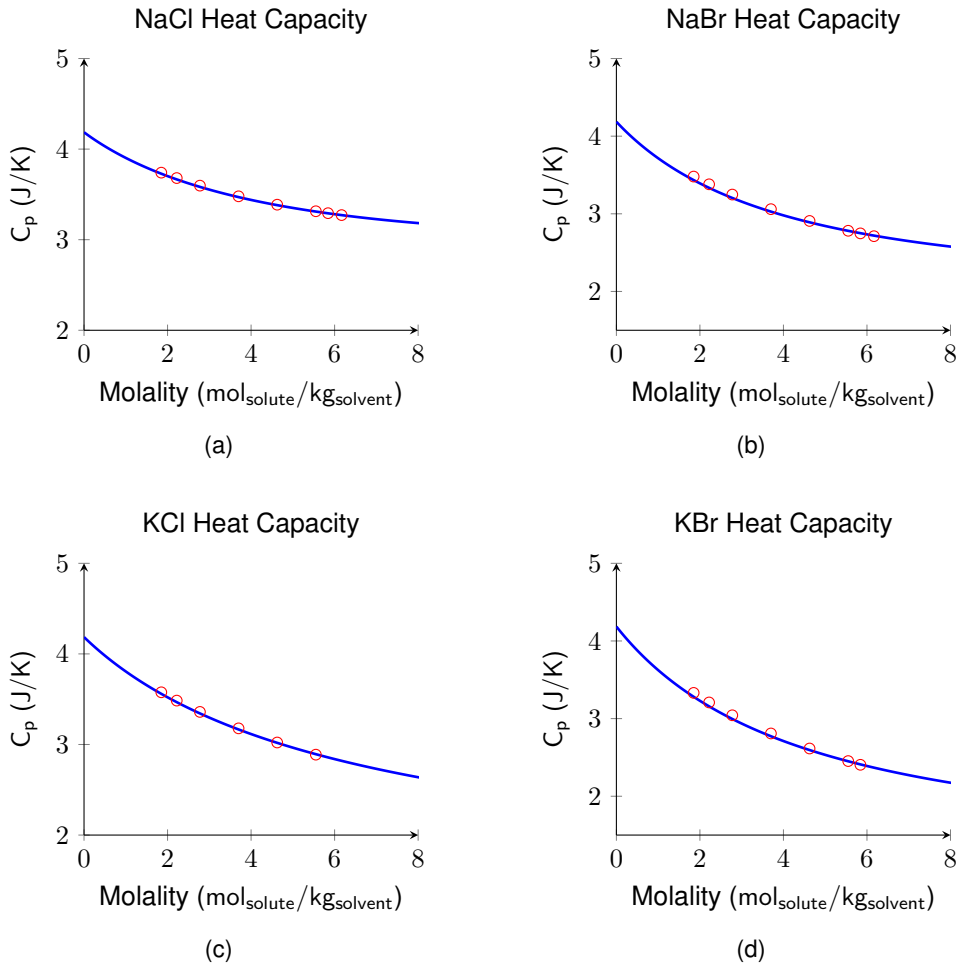

Figure 6.11: Liquid phase heat capacity of a salt depending on the molality, taking into account experimental data on solubility, liquid phase density, liquid phase heat capacities and dilution enthalpy. The different plots have both experimental (○) and SAFT predictions data (–).

Last but not least, in Figure 6.12 it is possible to analyse the obtained results for the dilution enthalpy. While fitting the parameters with all the four properties, different weights were given to the different properties, which ends up by giving different importances to the different considered properties. The data regarding the dilution enthalpy was the one with the lower weight in this parameter estimation. By giving a lower percentage to it, it is expected that its results are further from the experimental results when compared with the other properties. Indeed, analysing the results it is possible to see that the experimental points are not completely coincident with the model. Yet, for a given salt, the change in the dilution enthalpy with the molality presents the same behaviour and tendency both in experimental data and SAFT model.

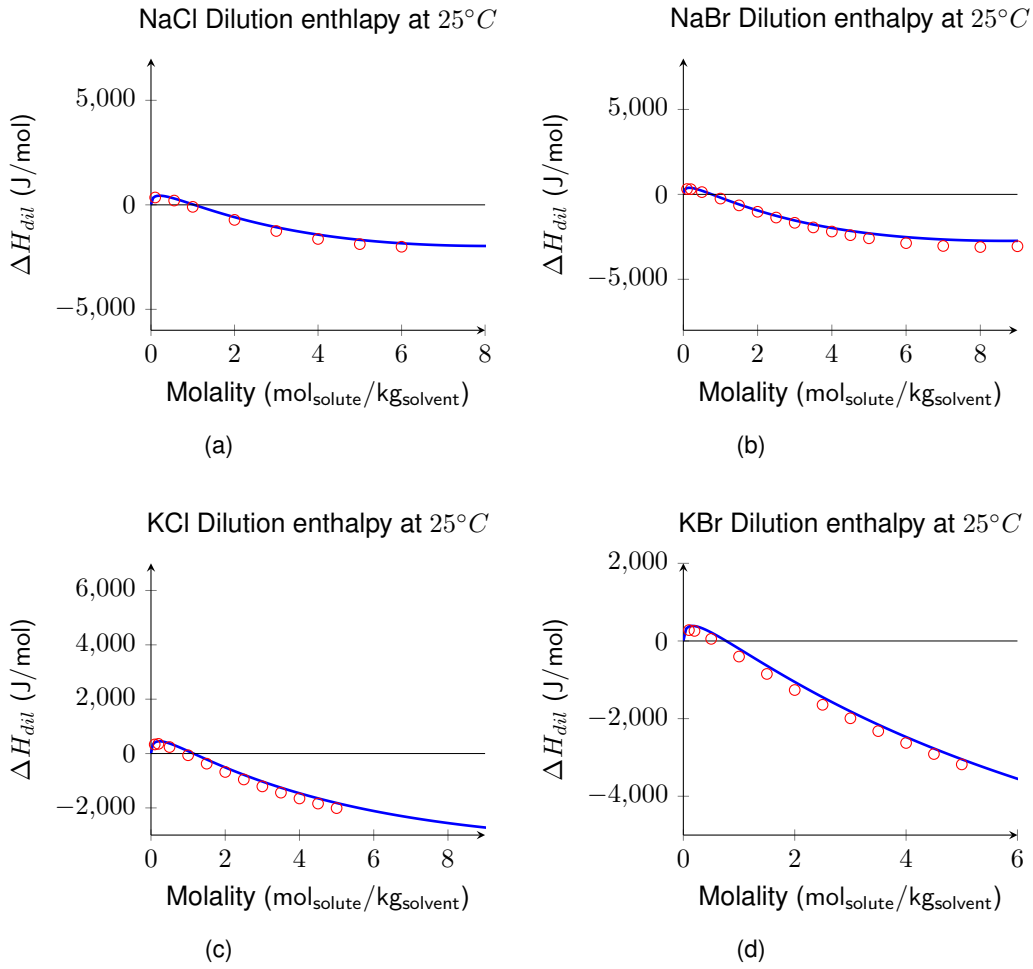

Figure 6.12: Dilution enthalpy of a salt depending on the molality, taking into account experimental data on solubility, liquid phase density, liquid phase heat capacity and dilution enthalpy. The different plots have both experimental (○) and SAFT predictions data (−).

6.5 Remarks

Model with Solubility, Liquid Phase Density, Heat Capacity and Dilution Enthalpy

The obtained parameters for the model that fits all the properties at the same time are presented in Table 6.2 .

Table 6.2: Sigma values for the model with solubilities, liquid phase densities, liquid phase heat capacities and dilution enthalpies. Values of ionic σ for the different ions.

	σ_i	$\Delta\sigma_i$	σ_i^{Born}
$Na^+ - Na^+$	$2.2698E-10$	$1.8103E-10$	$4.0801E-10$
$Cl^- - Cl^-$	$3.0289E-10$	$1.3000E-10$	$4.3289E-10$
$K^+ - K^+$	$2.8989E-10$	$1.8436E-12$	$2.9173E-10$
$Br^- - Br^-$	$3.5832E-10$	$1.5272E-10$	$5.1103E-10$

Considering the periodic table, it is expected that: $\sigma_{Na^+}^{Born} < \sigma_{K^+}^{Born}$ and that $\sigma_{Cl^-}^{Born} < \sigma_{Br^-}^{Born}$. Yet, by analysing the obtained results, it is possible to see that the expected results are not obtained for the cations. The ionic sigma increments for Na^+ and K^+ have different orders of magnitude, and because

of that the size of bromide is much smaller when compared with all the other ions. However, the σ_i values are obtained in the right order, which is already a good accomplishment.

Furthermore, by taking a look at the obtained results for the final epsilons, at 298.15K, it is possible to see that for the interactions between sodium and water, and potassium and water, negative values are obtained. Once again, this is not physically reasonable and it ends up by being a problem that needs to be further studied.

Table 6.3: Parameter Estimation Values for the model with solubilities, liquid phase densities, liquid phase heat capacities and dilution enthalpies. Values of ϵ for the different ions interactions.

	ϵ_0	B	ϵ_{final}^{298K}
$Na^+ - Na^+$	1123.45	-311.75	1122.41
$Cl^- - Cl^-$	15.17	-2032.92	8.35
$K^+ - K^+$	1119.98	-9112.48	1089.41
$Br^- - Br^-$	17.22	-2432.64	9.06
$Na^+ - Cl^-$	973.62	-168474.92	408.55
$Na^+ - Br^-$	1457.90	-159886.49	921.63
$K^+ - Cl^-$	1177.56	-62843.49	966.78
$K^+ - Br^-$	1532.85	-54745.33	1349.24
$Na^+ - H_2O$	50.05	-255972.37	-808.48
$Cl^- - H_2O$	1677.70	23052.37	1755.02
$K^+ - H_2O$	9.73	-109398.41	-357.20
$Br^- - H_2O$	1465.06	32677.75	1574.67

In Table 6.4 all the obtained results are summed up for every approach that was made.

Table 6.4: Fitted properties and obtained results for Solubilities, Liquid phase densities, Mean Activity Coefficients, Liquid phase heat capacities, dilution enthalpies and osmotic coefficients. The ✓ is for the correct values, the × for incorrect values and the ± for results that are not completely correct.

Fitted properties \Results	Solubility	Liquid Phase Densities	Activity	Liquid phase C_p	ΔH^{dil}	Osmotics
Solubility	✓	×	±	×	×	KCl and $NaBr$ ± $NaCl$ and KBr ×
Solubility+Liquid Phase Densities	✓	✓	✓	×	×	✓
Solubility+Liquid Phase Densities + Liquid Phase C_p	✓	✓	✓	✓	×	✓
Solubility+Liquid Phase Densities + Liquid Phase C_p + ΔH^{dil}	✓	✓	✓	✓	✓	✓

A summary of the estimated parameters for each approach is presented below.

Table 6.5: Adjustable parameters that were fitted in each approach.

Approach	σ_i	ϵ_{ii}	ϵ_{ij}	$\epsilon_{i-water}$	$\Delta\sigma_i$	$B_{i-water}$	B_{ii}	B_{ij}
6.1	✓	✓	✓	✓				
6.2.1	✓	✓	✓	✓				
6.2.2	✓	✓	✓	✓	✓			
6.3.1	✓	✓	✓	✓	✓			
6.3.2	✓	✓	✓	✓	✓	✓		
6.4	✓	✓	✓	✓	✓	✓	✓	✓

6.6 Extension to other salts

As was seen in the previous chapter, an optimized model has been developed for a small group of salts, so the results obtained above can now be used to extend the model. In this first group, the salts considered were: $NaCl$, KCl, $NaBr$ and KBr, which means that the parameter estimation was applied to the Na^+, Cl^-, K^+ and Br^- ions. After achieving the best possible model in a small "sample" of salts, the goal was to enhance the amount of salts to which the model could be applied.

The adopted strategy consisted of setting the obtained parameters for the first ions and then do a new parameter estimation for the missing ones. This means that the first model parameters were fixed in the Databank and then the new ion parameters were estimated and optimized. By using this strategy we can guarantee the decrease in the number of parameters being estimated simultaneously, and, at the same time, have reliable results.

The model was extended to the use of iodine, caesium, rubidium, ammonia and nitrate based salts. In view of this addition, experimental data of new salts has been considered, which includes data on NaI, KI, $RbCl$, $RbBr$, $CsCl$, $CsBr$, NH_4Cl, NH_4Br, $NaNO_3$ and KNO_3.

The ions corresponding to all these salts were not studied all at the same time as had been done before, but, instead, they were studied in groups. All the obtained results are presented in the following section.

The order of studies is presented in the Table 6.6.

Table 6.6: Summary and the order in which the salts were studied.

	Cl^-	Br^-	I^-	NO_3^-
Na^+	1		4	6
K^+				
Rb^+	2			
Cs^+	3			
NH_4^+	5			

Earlier in this work, it was concluded that to be able to catch all the properties, it is necessary to use data on all of them. In this section of the work only the final results will be shown. Even though the used methodology was applied in the same way as before, the results do not need to be shown due to the fact that they were only used to make the fitting process smoother. By using a step-by-step approach, it is easier to obtain good initial estimatives and a good objective function with accurate theoretical predictions. So, to obtain these results it was used the same strategy as before: using just solubility first and then adding one property at a time.

The solubility predictions show that SAFT is capable of providing almost all the data accurately. By analysing Figure 6.13, it is possible to see that the model is able to follow all the experimental data tendencies and give accurate results.

Regarding the $CsBr$ predictions, there are no certainties in terms of the predicted results. Besides the fact that, in the literature, it is only possible to find solubility data at 25°C, it was not possible either to find the solid phase heat capacity dependence with temperature. SAFT, as expected, was able to catch the point at this temperature, however there is not a way to know if all the other values are correct, since they are only based on a solubility value and calculated with a wrong solid heat capacity Vs Temperature dependence.

Another point that is worth being analysed is the NaI solubility predictions. NaI is in a hydrate form, from 0°C to 65°C. However, the model is not able to catch its solubility in this range of temperatures. There was an attempt to provide the solubility value of $NaI.2H_2O$ at 25°C in the parameter estimation, because this strategy has worked before for $NaBr$. Yet, it was not possible to get good results in this attempt. On the other hand, results for the anhydrous salt are accurate and trustworthy.

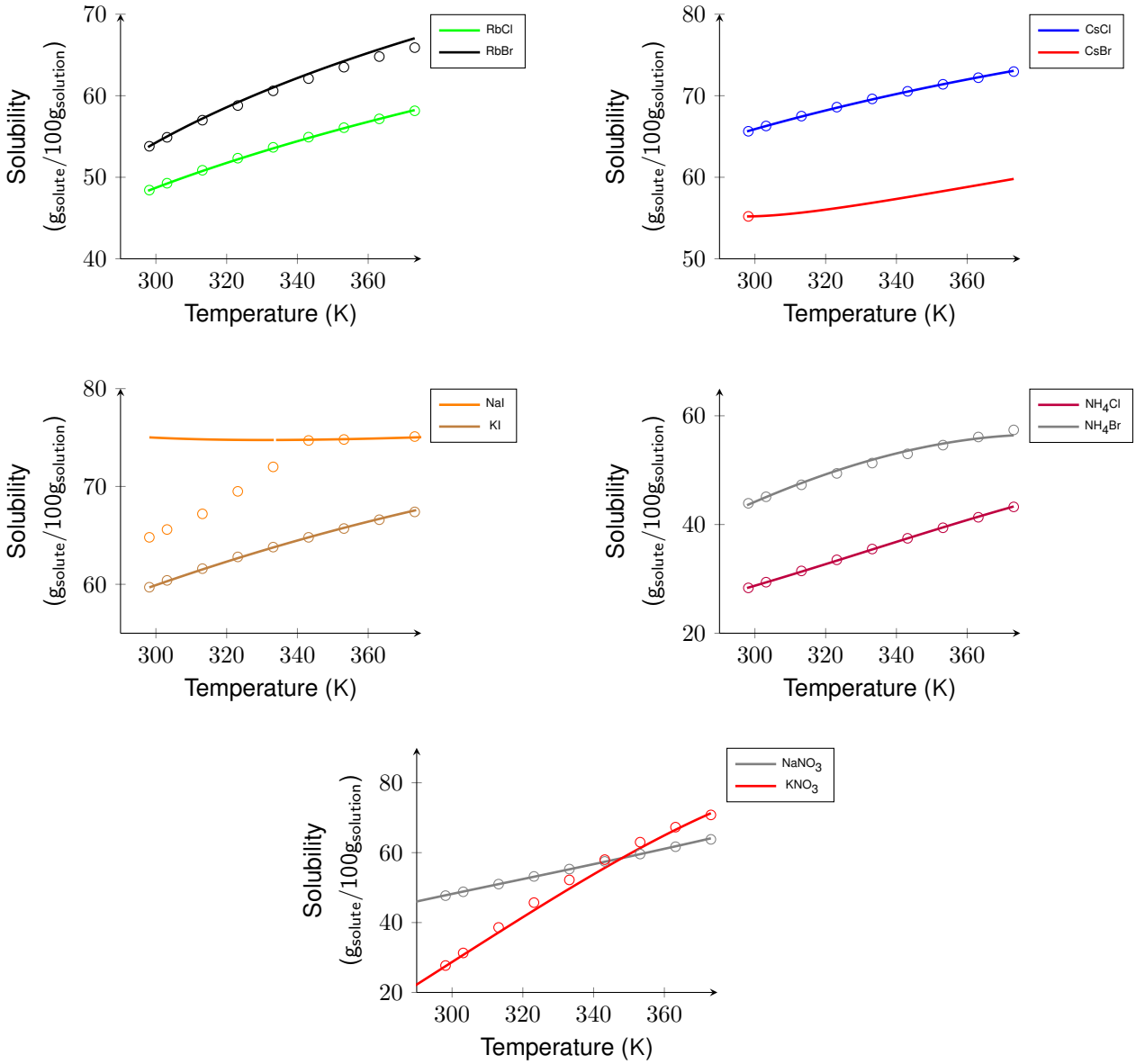

Figure 6.13: Solubility predictions for other compounds with an extension of the previous model. The model results are represented by the continuous line and the experimental points by the circular marks.

Liquid phase densities were also obtained accurately. This result was already expected since the parameters are being fitted to all the properties at the same time. The results are presented below.

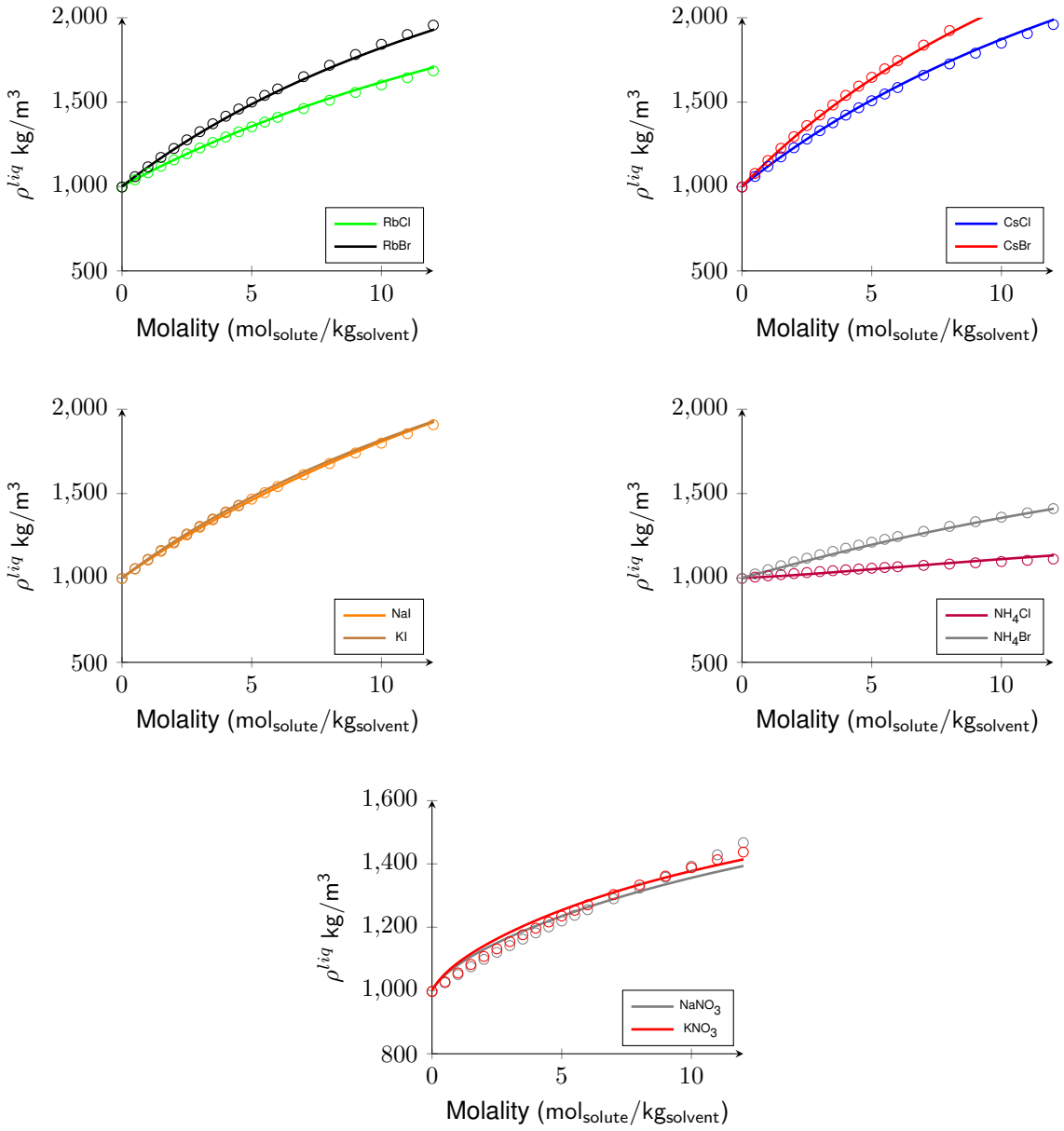

Figure 6.14: Liquid phase densities predictions for other compounds with an extension of the previous model. The model results are represented by the continuous line and the experimental points by the circular marks.

Liquid phase heat capacities were also fitted for all the compounds. Even though it was not possible to find a lot of data for some of the compounds, it is possible to see that the results were obtained with accuracy.

Almost all the existent experimental data is at low molality values. Nonetheless, the model predicts the heat capacity values for higher molalities. Once again, to obtain good predictions it was not necessary to provide a lot of experimental data. When only using two experimental values it is possible to obtain a model that fits well to the experimental results. The obtained results can be observed in Figure 6.15.

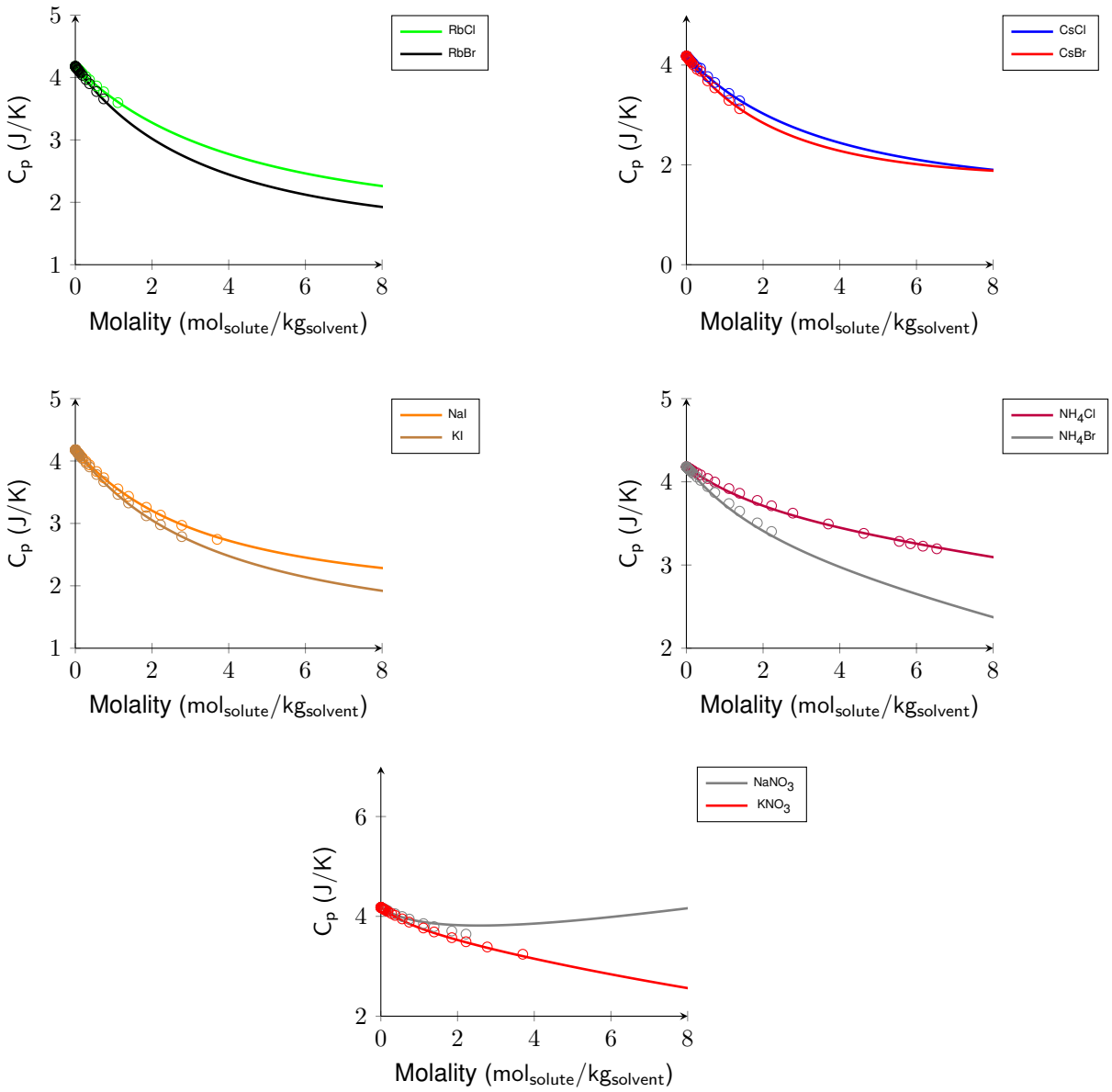

Figure 6.15: Liquid phase heat capacities predictions for other compounds with an extension of the previous model. The model results are represented by the continuous line and the experimental points by the circular marks.

In the absence of experimental data, it was not possible to build a model that is capable of predicting dilution enthalpies for most of the compounds. Either it was not possible to find the needed data, or the existing one was only based on predictions, instead of referring to real experiments.

In view of the above, it was only possible to obtain the dilution enthalpies plot for NaI and KI. The results, presented in Figure 6.16, show that the results were obtained correctly.

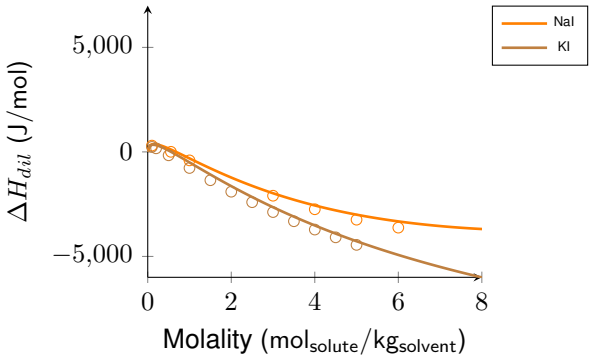

Figure 6.16: Dilution Enthalpies predictions for other compounds with an extension of the previous model. The model results are represented by the continuous line and the experimental points by the circular marks.

The scope of this work was, mainly, to understand if it would be possible to obtain models that were able to predict solubilities, heat capacities and heats of dilution. Throughout the studies mean activity coefficients and osmotic coefficients were also analysed in order to understand if it would be possible to obtain the right predictions without needing to provide experimental data. As was seen before, for the first obtained model all the results converged across the experimental data. However, for the model extension it was not possible to obtain good predictions for all of the compounds. Regarding the mean activity coefficients, good results were only accomplished for $RbCl$, $RbBr$, NaI and KI.

One important feature when going from the ideal gas conception to the infinite dilution state is the Gibbs enthalpy of solvation. One of the reasons why it is impossible to obtain good predictions for mean activity coefficients may be the fact that these predictions are based on Gibbs solvation enthalpies values that are not well predicted by the model. (See model solvation enthalpy predictions against experimental values in the Appendix C.5. This values were obtained by using a gProms model prepared to calculate them.).

Furthermore, osmotic coefficients were not predicted accurately either. The model itself is not robust enough to provide good predictions for these two properties in this range of compounds.

All the results on mean activity coefficients and osmotic coefficients can be seen in the Appendix C.5.

Chapter 7

Conclusions

The conventional strategy to determine SAFT parameters for electrolyte systems is usually based on regressing a combination of properties including activity coefficients, osmotic coefficients, vapour pressures and liquid phase densities. This study demonstrates that this methodology does not guarantee that the obtained parameters can be used to predict calorific properties, such as heat capacities and heats of dilution. We propose that calorific properties should always be included in the regression of parameters when they are available. The main conclusions of this study are:

- It is possible to fit the parameters to solubilities and to obtain accurate theoretical predictions for it;
- If one wants to obtain accurate computations on solubilities, liquid phase heat capacities and dilution enthalpies it is necessary to fit to every property;
- In order to obtain accurate predictions, it is not necessary to use a lot of experimental data. With only two points at different molalities, it is possible to obtain good results for liquid phase heat capacities, liquid phase densities and dilution enthalpies;
- The first developed model for $NaCl$, $NaBr$, KCl and KBr is able to provide accurate results for mean activity coefficients and osmotic coefficients without them being included in the fit;
- The negative values of the cross ion-water dispersion energy might be due to some shortcomings of the Born contribution which need to be compensated ;
- A sequential fit of different salts is a suitable approach to develop parameters from ionic groups;
- NO_3^- and NH_4^+ are not easy to model, mainly for two reasons:

  - Both ions are not spherical, especially the nitrate. Their shape factor was considered and set as 1 and this may lead to difficulties with its fitting;

  - One of the data needed for the parameters fitting is the ideal gas heat capacity. For monoatomic species this value is known and set as 20.8. However, neither of these two species is monoatomic, and, because of that, their ideal gas heat capacity has a different value (which was not considered in the fitting.);

Bibliography

[1] J. Pàmies Corominas, "Bulk and interfacial properties of chain fluids: a molecular modelling approach," Ph.D. dissertation, 2004.

[2] V. Papaioannou, "A molecular-based group contribution equation of state for the description of fluid phase behaviour and thermodynamic derivative properties of mixtures (SAFT- γ Mie)," no. December, 2012.

[3] G. M. Kontogeorgis, B. Maribo-Mogensen, and K. Thomsen, "The Debye-Hückel theory and its importance in modeling electrolyte solutions," *Fluid Phase Equilibria*, 2018. [Online]. Available: http://linkinghub.elsevier.com/retrieve/pii/S0378381218300074

[4] J. M. Schreckenberg, S. Dufal, A. J. Haslam, C. S. Adjiman, G. Jackson, and A. Galindo, "Modelling of the thermodynamic and solvation properties of electrolyte solutions with the statistical associating fluid theory for potentials of variable range," *Molecular Physics*, vol. 112, 2014.

[5] D. K. Eriksen, G. Lazarou, A. Galindo, G. Jackson, C. S. Adjiman, and A. J. Haslam, "Development of intermolecular potential models for electrolyte solutions using an electrolyte SAFT-VR Mie equation of state," *Molecular Physics*, vol. 114, no. 18, 2016.

[6] B. Maribo-mogensen, *Development of an Electrolyte CPA Equation of state for Applications in the Petroleum and Chemical Industries Equation of State for Applications in the*, 2014, no. June. [Online]. Available: http://orbit.dtu.dk/en/persons/bjoern-maribomogensen(597d1611-cf48-444c-a982-52766587bce5)/publications.html

[7] S. Dufal, "Development and application of advanced thermodynamic molecular description for complex reservoir fluids containing carbon dioxide and brines," 2013.

[8] M. A. Selam, I. G. Economou, and M. Castier, "A thermodynamic model for strong aqueous electrolytes based on the eSAFT-VR Mie equation of state," *Fluid Phase Equilibria*, vol. 464, pp. 47–63, 2018.

[9] T. Lafitte, V. Papaioannou, S. Dufal, and C. C. Pantelides, "A general framework for solid-liquid equilibria in pharmaceutical systems."

[10] D. D. Wagman, W. H. Evans, V. B. Parker, R. H. Schumm, I. Halow, S. M. Bailey, K. L. Churney, and R. L. Nuttall, "The NBS Tables of Chemical Thermodynamic Properties," 1982.

[11] T. Lafitte, "Technical Training – gSAFT Session," pp. 1–24, 2017.

[12] V. Papaioannou, T. Lafitte, C. Avendaño, C. S. Adjiman, G. Jackson, E. A. Müller, and A. Galindo, "Group contribution methodology based on the statistical associating fluid theory for heteronuclear molecules formed from Mie segments," *Journal of Chemical Physics*, vol. 140, no. 5, 2014.

[13] T. Lafitte, A. Apostolakou, C. Avendaño, A. Galindo, C. S. Adjiman, E. A. Müller, and G. Jackson, “Accurate statistical associating fluid theory for chain molecules formed from Mie segments,” *Journal of Chemical Physics*, vol. 139, no. 15, 2013.

[14] “NIST Chemistry WebBook.” [Online]. Available: https://webbook.nist.gov/chemistry/

[15] R. H. Perry and D. W. Green, *Perry’s Chemical Engineers’ Handbook*, 2008, vol. 1.

[16] A. Seidell, *Solubilities of Inorganic and Organic Compounds: A compilation of quantitative solubilty data from the periodical literature*, 2nd ed., New York, 1919.

[17] B. S. Krumgalz, “Temperature dependence of mineral solubility in water. Part I. Alkaline and Alkaline earth chlorides,” *Journal of Physical and Chemical Reference Data*, vol. 46, 2017. [Online]. Available: http://dx.doi.org/10.1063/1.5010290

[18] S. P. Pinho and E. A. Macedo, “Solubility of NaCl, NaBr, and KCl in water, methanol, ethanol, and their mixed solvents,” *Journal of Chemical and Engineering Data*, vol. 50, no. 1, pp. 29–32, 2005.

[19] D. Lide, “Aqueous Solubility of Inorganic Compounds at Various Temperatures,” *CRC Handbook of Chemistry and Physics*, 2005. [Online]. Available: papers2://publication/uuid/55E853FE-9E62-4EEC-97D7-AFAB12AA3361

[20] J. W. Lorimer, M. Salomon, and C. L. Young, *Solubility data series: Alkali metal and ammonium chlorides in water and heavy water (binary systems)*, 1991, vol. 47.

[21] B. S. Krumgalz, R. Pogorelsky, and K. S. Pitzer, “Volumetric Properties of Single Aqueous Electrolytes from Zero to Saturation Concentration at 298.15K Represented by Pitzer’s Ion-Interaction Equations,” *J.Phys.Chem*, vol. 25, no. 2, p. 663, 1995.

[22] V. B. Parker, “Thermal Properties of Aqueoues Uni-univalent Electrolytes,” pp. 1–66, 1965.

[23] W. J.Hammer and Y.-C. Wu, “Osmotic Coefficients and Mean Activity Coefficients of Uni-Valent Electrolytes in water at 25 Degrees,” *J. Phys. Chem.*, vol. 1, no. 4, p. 1047, 1972.

[24] “Heat of Solution.” [Online]. Available: https://courses.lumenlearning.com/introchem/chapter/heat-of-solution/

[25] W. R. Fawcett, “Thermodynamic Parameters for the Solvation of Monatomic Ions in Water,” *The Journal of Physical Chemistry B*, vol. 103, no. 50, pp. 11 181–11 185, 1999. [Online]. Available: http://dx.doi.org/10.1021/jp991802n{%}5Cnhttp://pubs.acs.org/doi/abs/10.1021/jp991802n

Appendix A

Fitting solid phase properties

One of the most pressing challenges whilst modelling electrolyte solutions is the lack of data in terms of solid phase properties. One of the possible constraints is the missing information on hydrated forms, which unfortunately, is hard to find in the literature. Apart from the formation properties, such as enthalpy and entropy of formation, others are needed in order to proceed to the parameter fitting.

By taking a look at the previous chapters, it is easy to understand that one of the reasons why hydrates could not be fitted was because of the absence of data on solid phase heat capacities as a function of temperature. At this point, it was of interest to understand if it would be possible to find the dependency of the solid phase heat capacities with temperature, while considering only solubility data.

A.1 Predicting Solid Heat Capacities with solubility data

The solid heat capacity dependence with temperature is used as a third degree polynomial, as presented in Equation A.1:

$$C_p^{solid} = a + b.T + c.T^2 + d.T^3 \tag{A.1}$$

This attempt to fit solid heat capacities was carried out with the $MgCl_2.6H_2O$ hydrate. The reason for its choice was based both on the existence of experimental data on its solubility and the existence of the heat capacity value of its solid phase at 25℃ in the literature.[10] Having the value of the wanted property at 25℃ is an advantage in a way that it can help in the understanding of which coefficient values should be expected.

After the decision of trying to discover only the a and b coefficients, it was seen that it was possible to fit the heat capacity values to solubility values. This means that it was possible to obtain accurate predictions for the solubility with the obtained fitted parameters. (see Figure A.1)

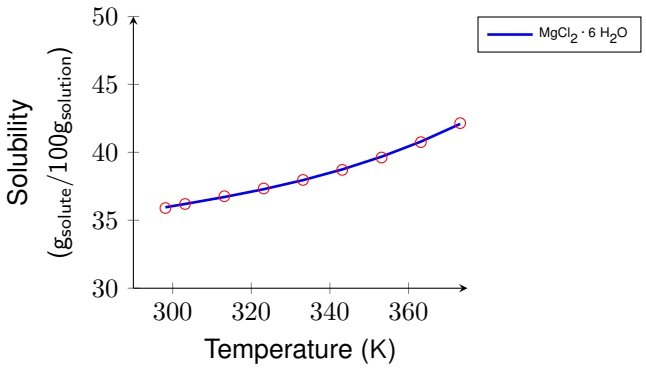

Figure A.1: Solubility predictions for $MgCl_2 \cdot 6\,H_2O$ when fitting the solid heat capacity coefficients. The experimental data is represented by ($\circ$) and SAFT predictions by ($-$)

However, when analysing the results it was concluded that the solid heat capacities were not that reliable. The dependence shown in Figure A.2 show that with the temperature increase, the value of the C_p^{solid} decreases. In some kinds of compounds this can happen. However, this sharp drop in the obtained values causes a lack of confidence in the accuracy of the values.

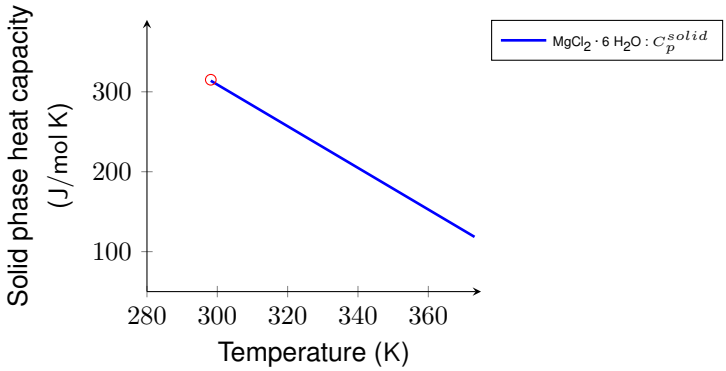

Figure A.2: Solid phase heat capacity predictions for $MgCl_2 \cdot 6\,H_2O$ when fitting the solid heat capacity coefficients to solubility values. The experimental data is represented by ($\circ$) and SAFT predictions by ($-$)

As it is not possible to know if the obtained results are trustworthy, these predictions were chosen not to be used.

In addition to the study showed before, the $NaCl$ case was also studied. For $NaCl$ it was possible to obtain accurate results for solubilities when fitting to the a and b coefficients of the solid heat capacity equation as a function of temperature. However, the obtained coefficients were not in line with the ones presented in the literature. (NIST databank)

Appendix B

Gibbs Energy of Solvation

The calculated free energies of solvation are compared with the experimental data measured by Fawcett[25] in the following table. As can be seen, the average of error is rather large, showing that there is not a good agreement between experimental and calculated data.

Table B.1: Gibbs energy of solvation ΔG^s of the ions studied: experimental values of Fawcett[25] and SAFT calculations.

Ion	ΔG^s_{exp} (kJ/mol)	ΔG^s_{SAFT} (kJ/mol)	%Δ
Na^+	-424	-268.91	36.58
K^+	-352	-410.09	16.50
Rb^+	-329	-376.07	14.31
Cs^+	-	-338.16	-
NH_4^+	-	-301.69	-
Br^-	-278	-425.53	53.07
Cl^-	-304	-457.65	50.54
I^-	-243	-374.53	54.13
NO_3^-	-	-983.43	-

Appendix C

Parameter Estimation Results

C.1 Estimation using solubility

C.1.1 Liquid Phase Density results

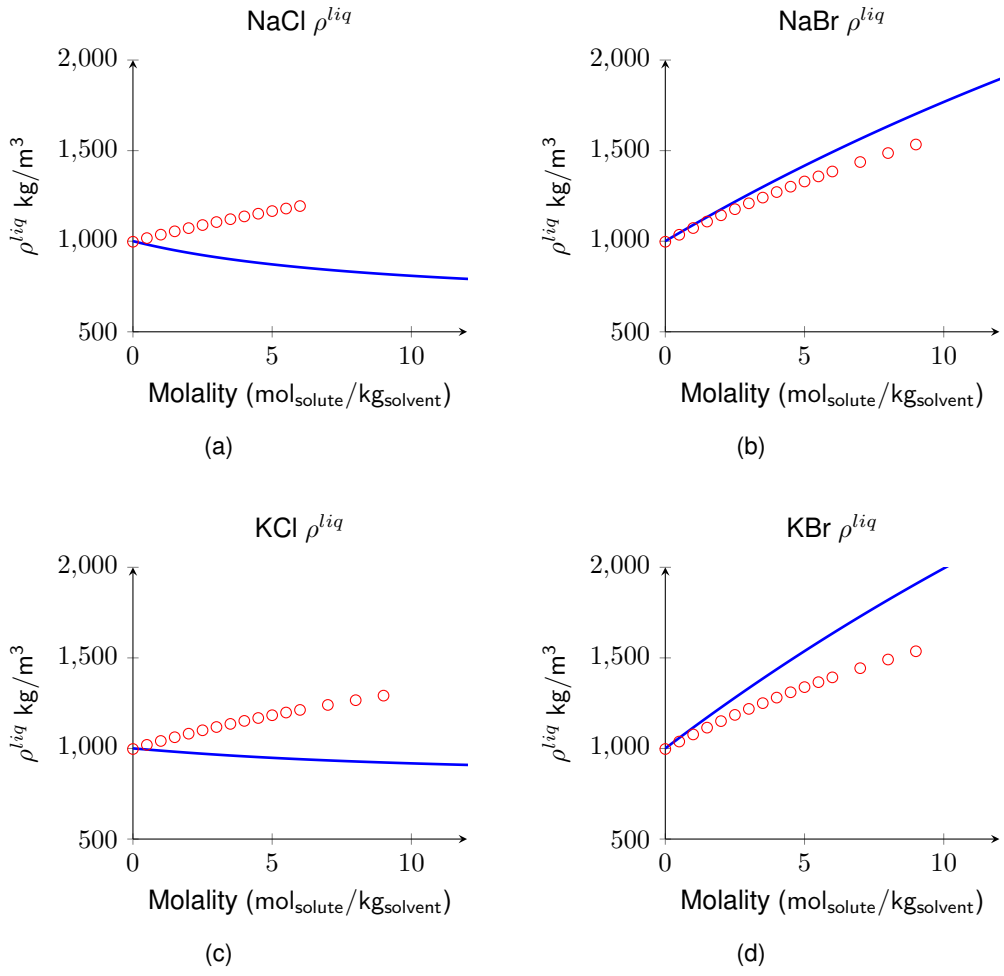

Figure C.1: Liquid phase density depending on the molality, taking into account only experimental data on solubility. The different plots have both experimental (○) and SAFT predictions data (−).

C.1.2 Liquid Phase Heat Capacity results

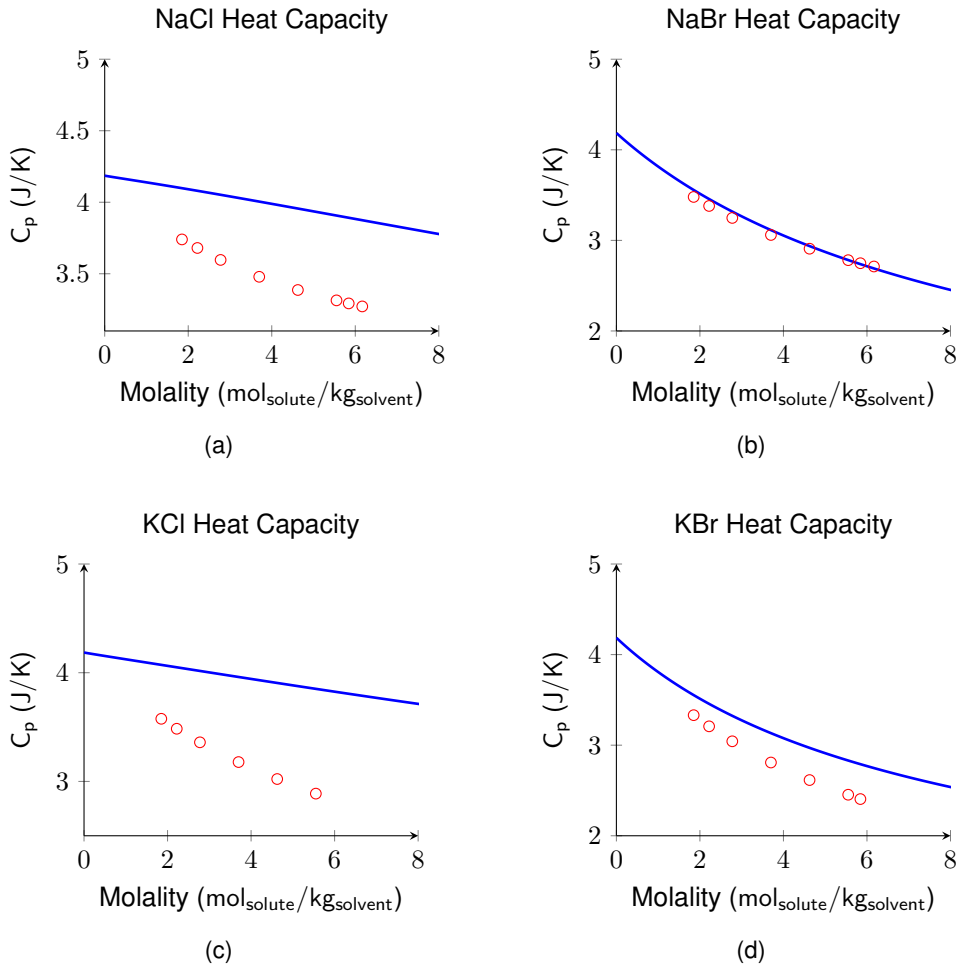

Figure C.2: Liquid phase heat capacity of a salt depending on the molality, taking into account only experimental data on solubility. The different plots have both experimental (○) and SAFT predictions data (−).

C.1.3 Dilution Enthalpy results

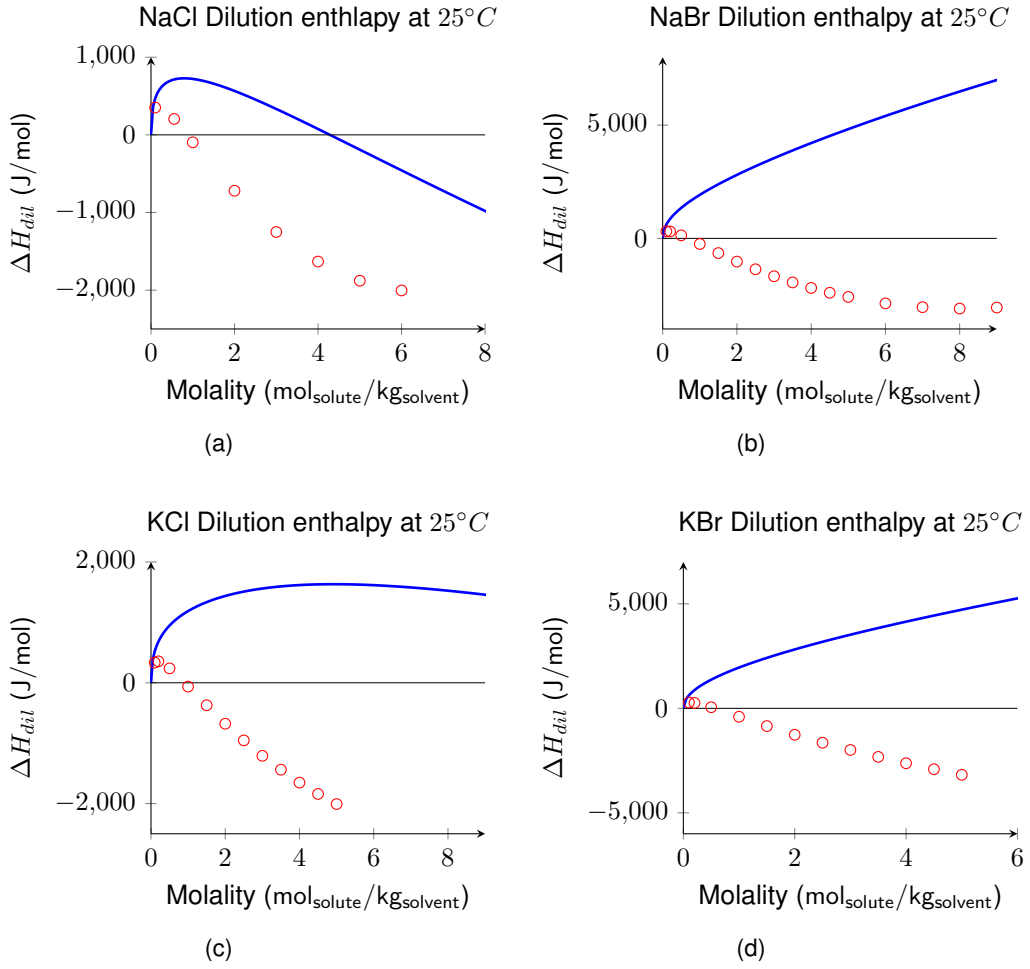

Figure C.3: Dilution enthalpy of a salt depending on the molality, taking into account only experimental data on solubility. The different plots have both experimental (○) and SAFT predictions data (−).

C.1.4 Mean activity coefficient results

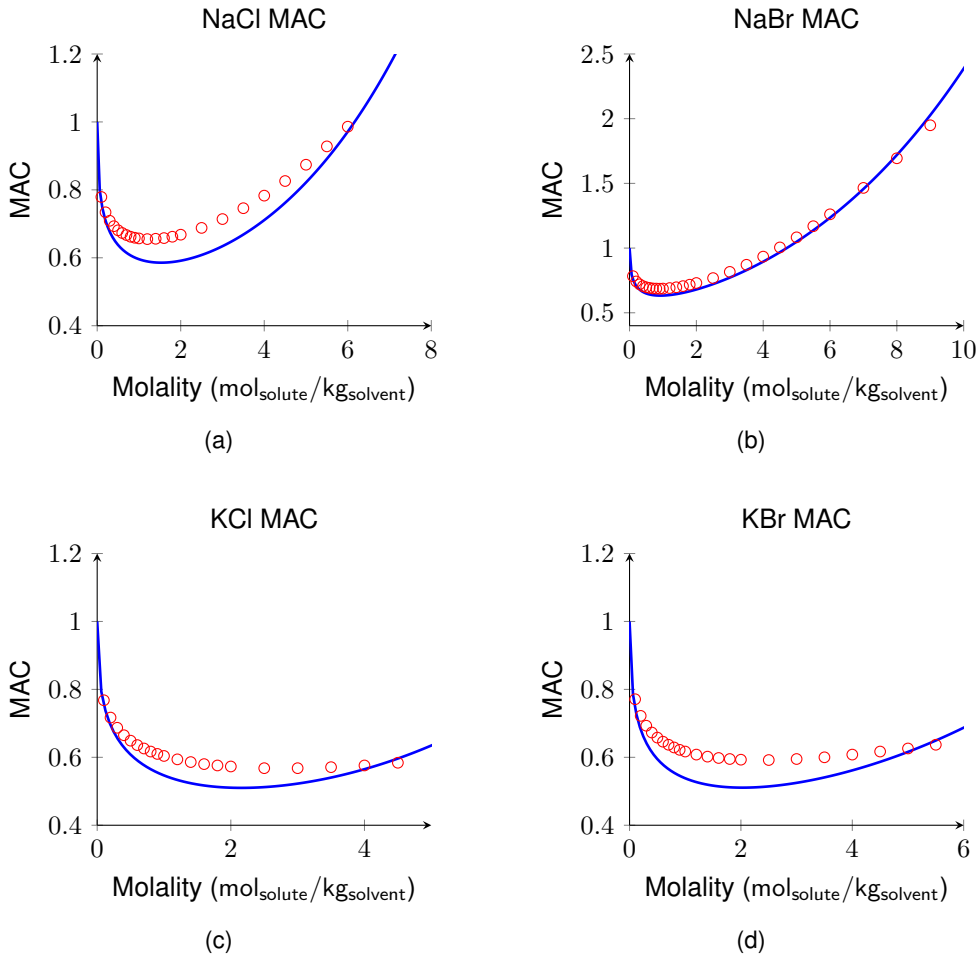

Figure C.4: Mean activity coefficient of a salt depending on the molality, taking into account only experimental data on solubility. The different plots have both experimental (○) and SAFT predictions data (–).

C.1.5 Osmotic Coefficient results

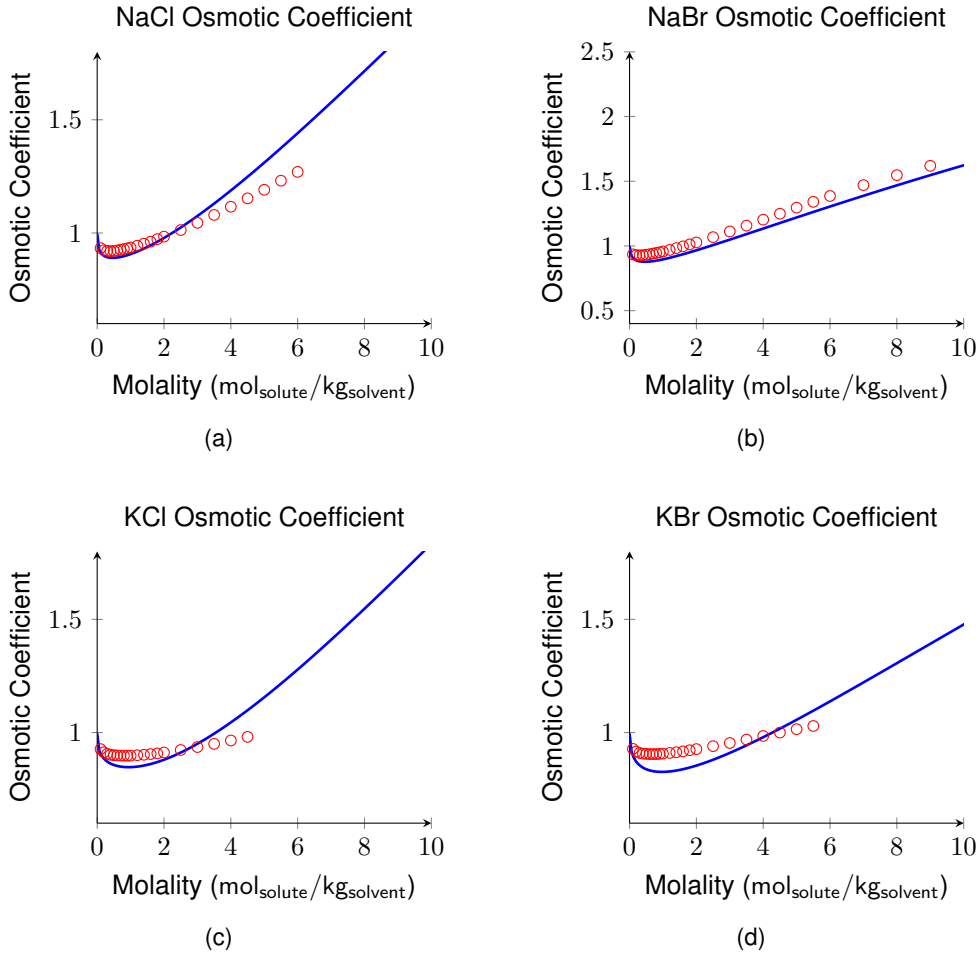

Figure C.5: Osmotic coefficients of a salt depending on the molality, taking into account only experimental data on solubility. The different plots have both experimental (○) and SAFT predictions data (–).

Table C.1: Obtained parameters when only fitting to solubilities. Values of ionic σ for the different ions.

	σ	$\Delta\sigma_i$	σ_i^{Born}
$Na^+ - Na^+$	$1.3365E-10$	-	$1.3365E-10$
$Cl^- - Cl^-$	$5.7843E-10$	-	$5.7843E-10$
$K^+ - K^+$	$1.2796E-10$	-	$1.2796E-10$
$Br^- - Br^-$	$3.5422E-10$	-	$3.5422E-10$

Table C.2: Obtained parameters when only fitting to solubilities. Values of ϵ for the different ions interactions.

	ϵ_0	B	ϵ_{final}^{298K}
$Na^+ - Na^+$	653.23	-	653.23
$Cl^- - Cl^-$	1304.17	-	1304.17
$K^+ - K^+$	1999.87	-	1999.87
$Br^- - Br^-$	3.59	-	3.59
$Na^+ - Cl^-$	2.97	-	2.97
$Na^+ - Br^-$	311.51	-	311.51
$K^+ - Cl^-$	1105.47	-	1105.47
$K^+ - Br^-$	495.64	-	495.64
$Na^+ - H_2O$	1037.49	-	1037.49
$Cl^- - H_2O$	428.13	-	428.13
$K^+ - H_2O$	1858.20	-	1858.20
$Br^- - H_2O$	243.66	-	243.66

C.2 Estimation using Solubility and Liquid Phase Density

C.2.1 First Attempt

Solubility

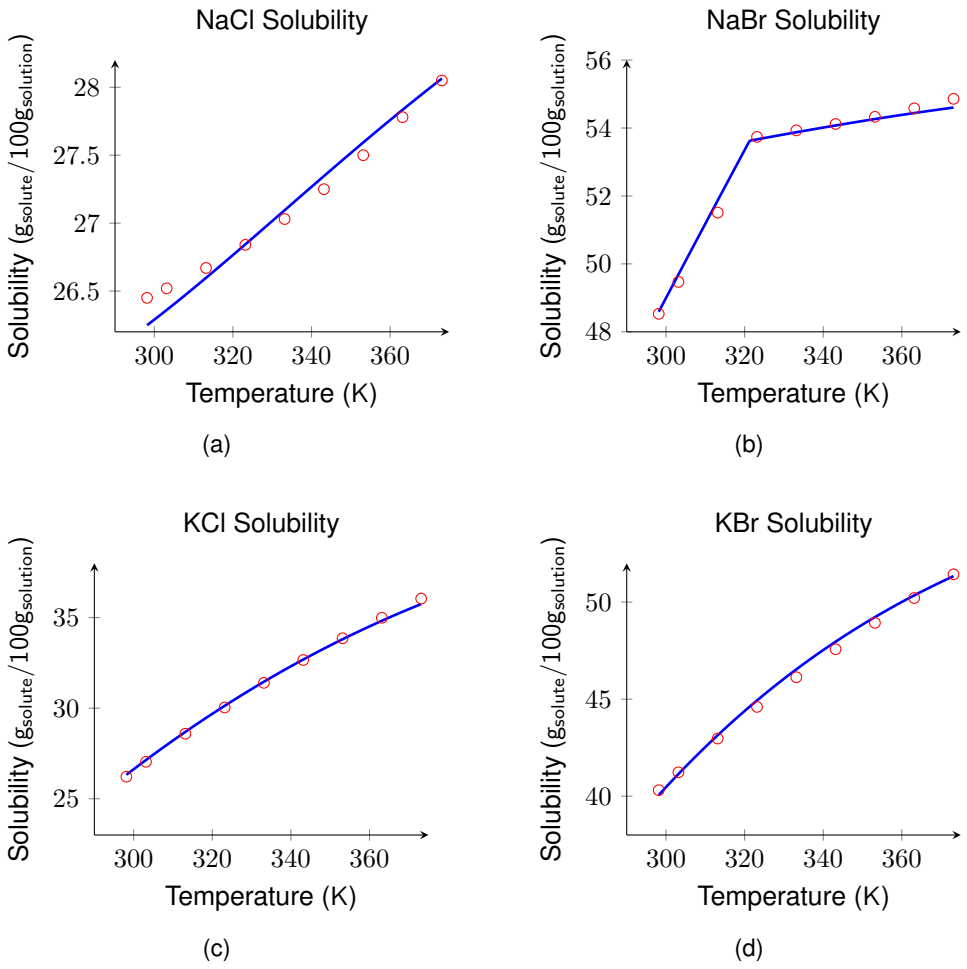

Figure C.6: Solubility of a salt depending on the temperature, taking into account only experimental data on solubility and liquid phase densities. The different plots have both experimental (○) and SAFT predictions data (−).

Liquid Phase Density results

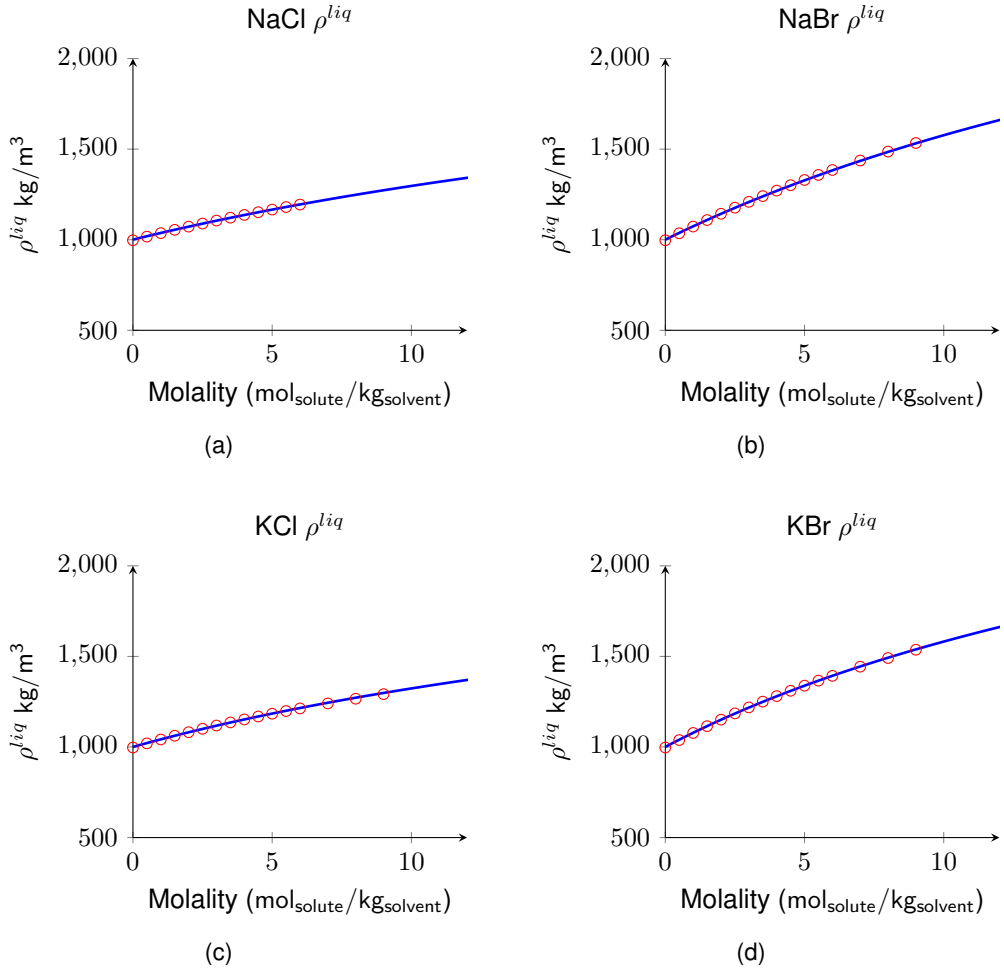

Figure C.7: Liquid phase density depending on the molality, taking into account only experimental data on solubility and liquid phase densities. The different plots have both experimental (○) and SAFT predictions data (–).

Liquid Phase Heat Capacity results

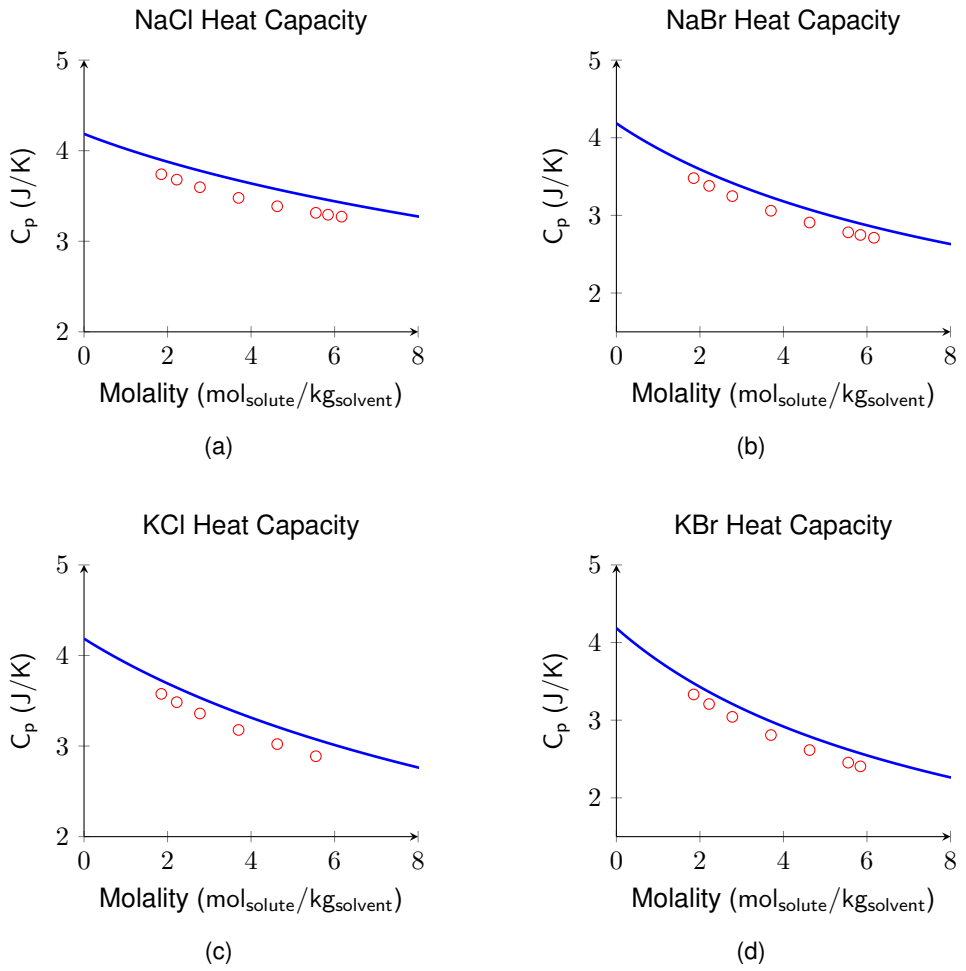

Figure C.8: Liquid phase heat capacity of a salt depending on the molality, taking into account experimental data on solubility and liquid phase density. The different plots have both experimental (○) and SAFT predictions data (−).

Dilution Enthalpy results

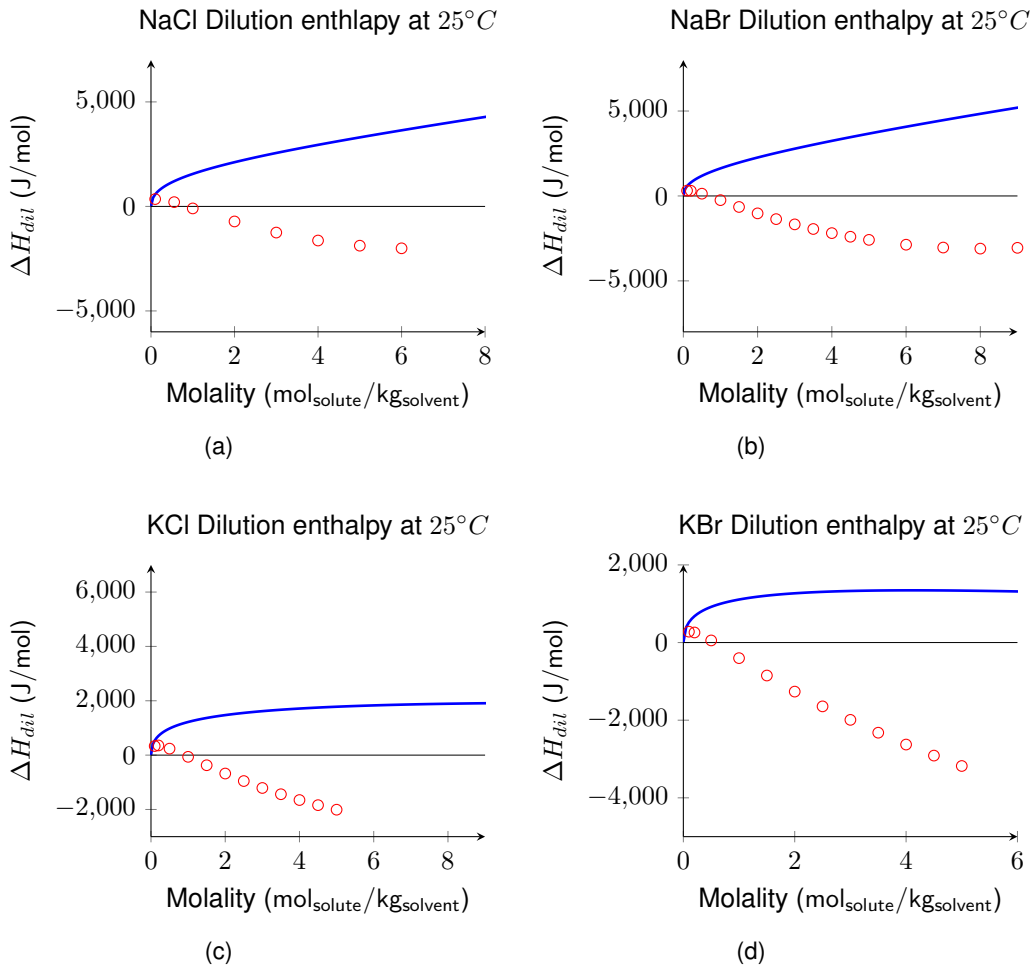

Figure C.9: Dilution enthalpy of a salt depending on the molality, taking into account experimental data on solubility and liquid phase density. The different plots have both experimental (○) and SAFT predictions data (−).

Mean Activity Coefficient results

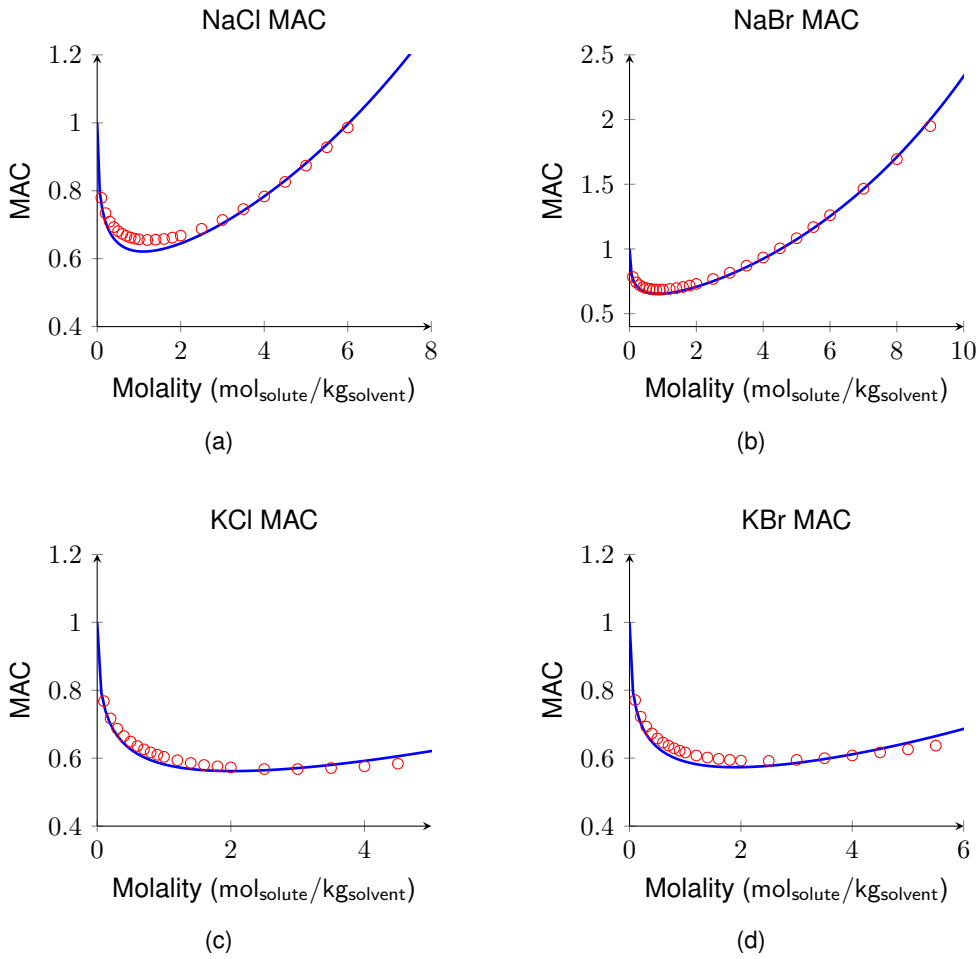

Figure C.10: Mean activity coefficient of a salt depending on the molality, taking only into account experimental data on solubility and liquid phase densities. The different plots have both experimental (○) and SAFT predictions data (−).

Osmotic Coefficients results

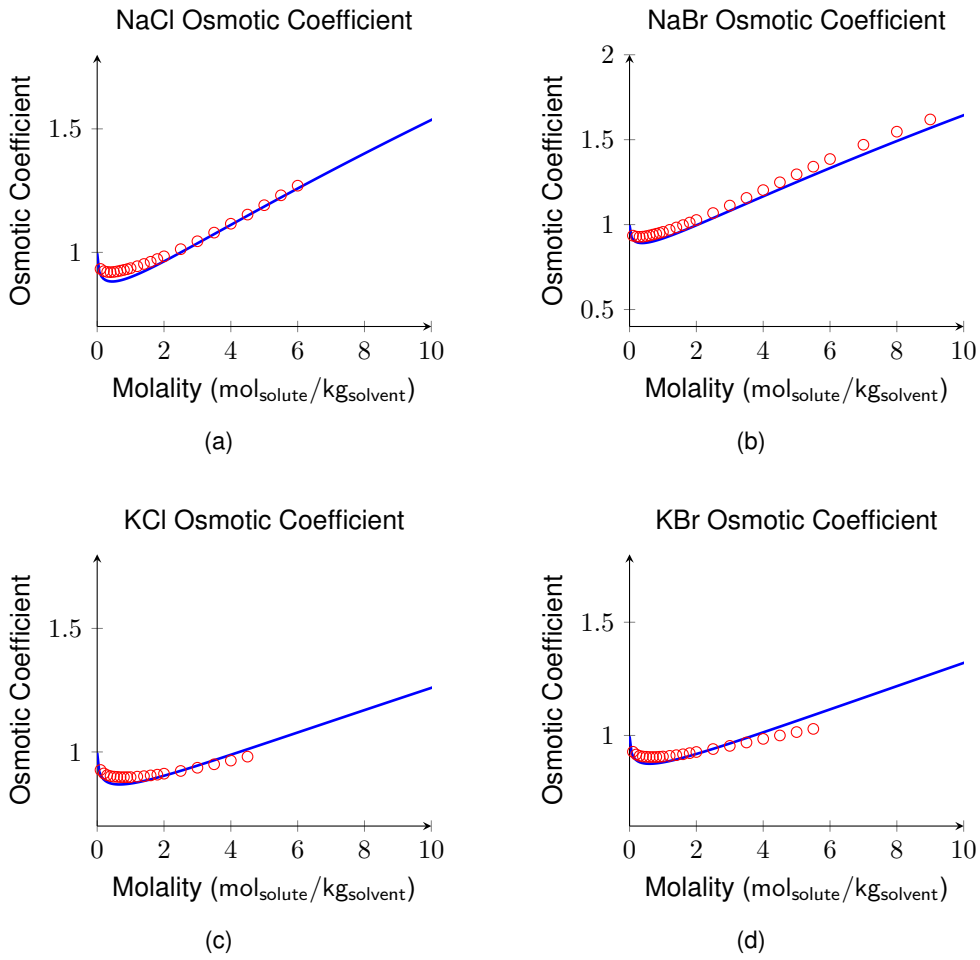

Figure C.11: Osmotic coefficients of a salt depending on the molality, taking only into account experimental data on solubility and liquid phase densities. The different plots have both experimental (∘) and SAFT predictions data (−).

C.2.2 Second Attempt

Liquid Phase Heat Capacity results

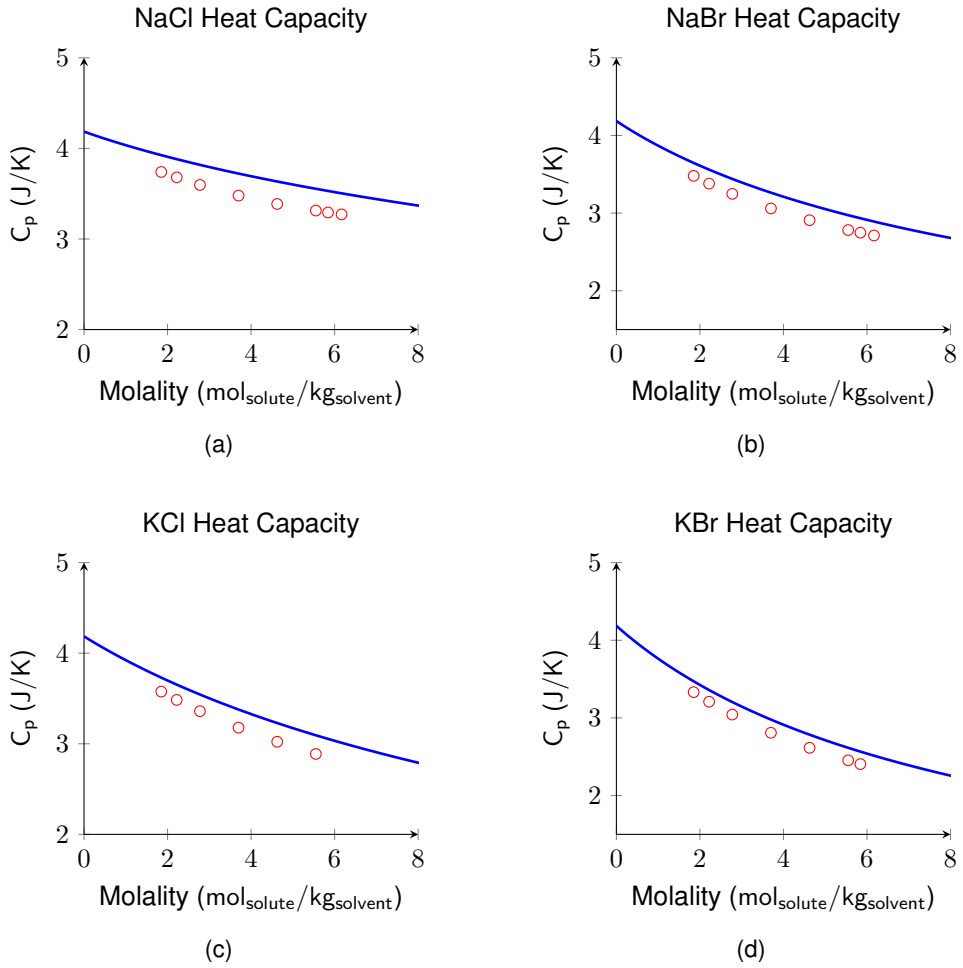

Figure C.12: Liquid phase heat capacity of a salt depending on the molality, taking into account only experimental data on solubility and liquid phase density. The different plots have both experimental (○) and SAFT predictions data (–).

Dilution Enthalpy results

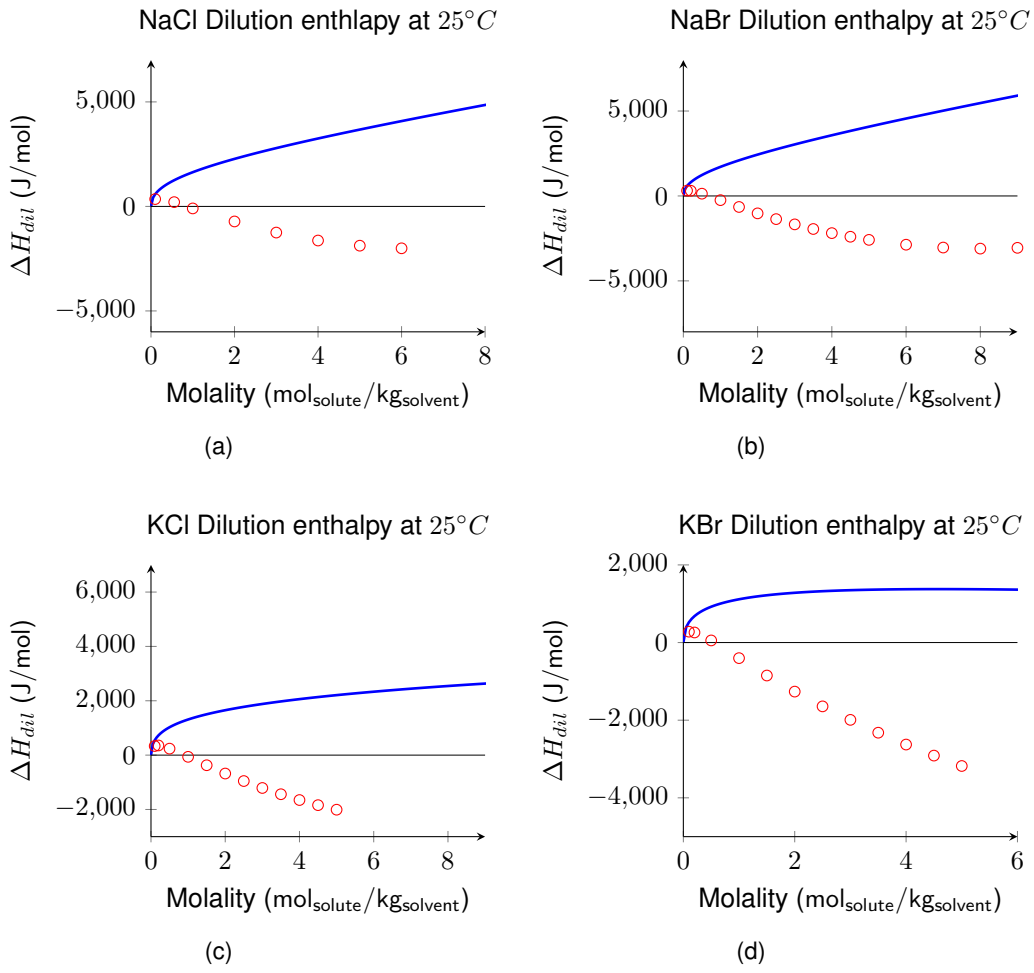

Figure C.13: Dilution enthalpy of a salt depending on the molality, taking into account experimental data on solubility and liquid phase density. The different plots have both experimental (○) and SAFT predictions data (−).

Mean Activity Coefficients

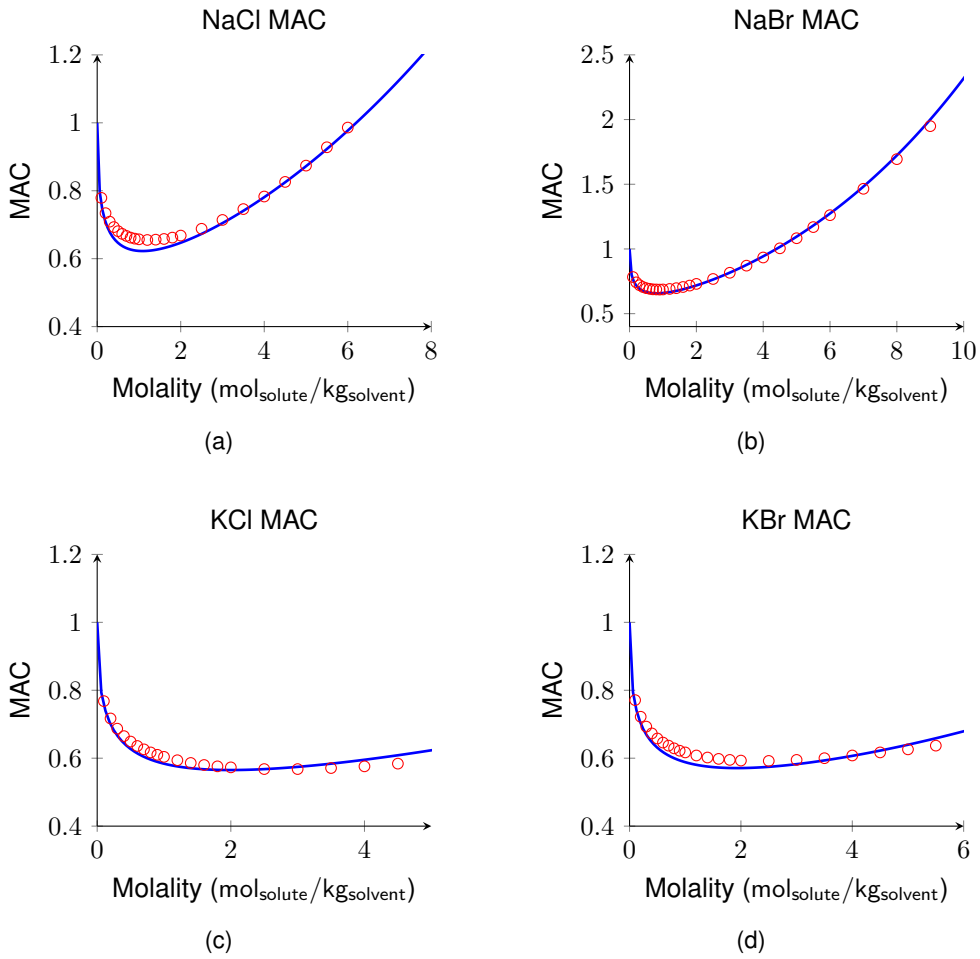

Figure C.14: Mean activity coefficient of a salt depending on the molality, taking into account only experimental data on solubility and liquid phase densities. The different plots have both experimental (○) and SAFT predictions data (−).

Osmotic Coefficients results

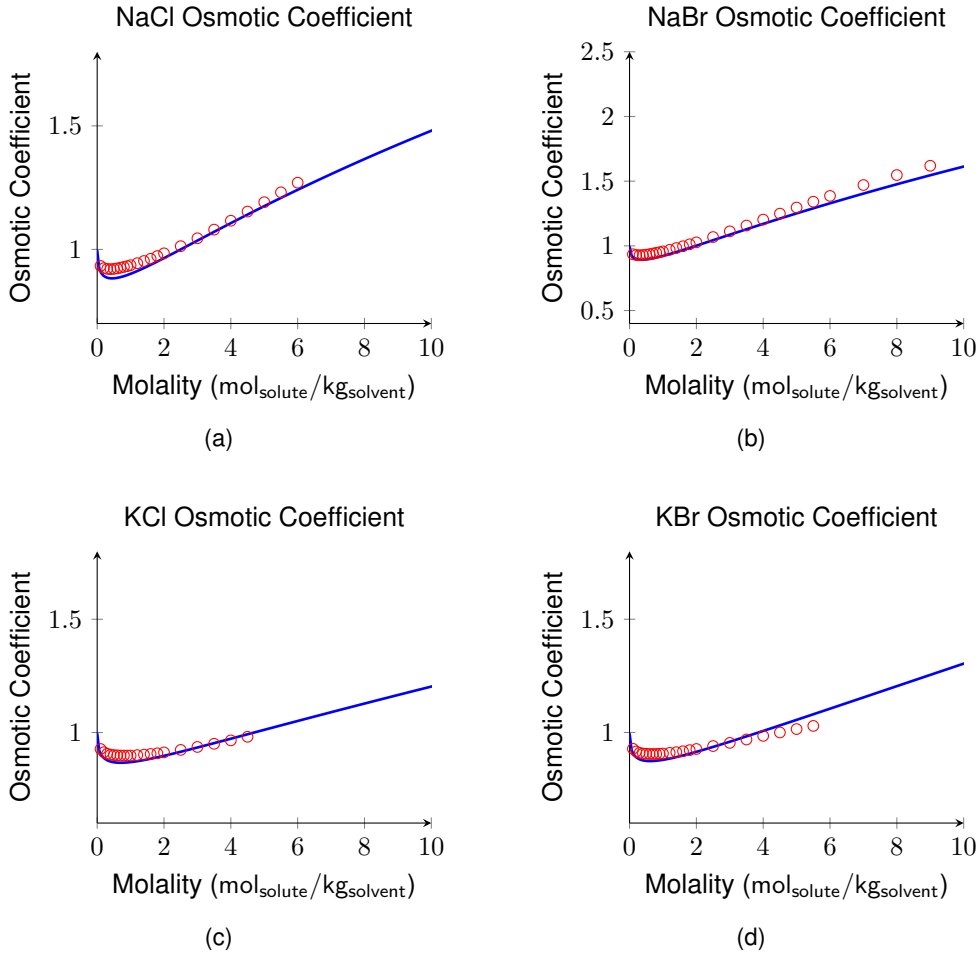

Figure C.15: Osmotic coefficients of a salt depending on the molality, taking into account only experimental data on solubility and liquid phase densities. The different plots have both experimental (∘) and SAFT predictions data (−).

Table C.3: Obtained parameters when fitting to solubilities and liquid phase densities. Values of ionic σ for the different ions.

	σ	$\Delta\sigma_i$	σ_i^{Born}
$Na^+ - Na^+$	$1.2167E-10$	$3.8873E-11$	$1.6055E-10$
$Cl^- - Cl^-$	$4.0519E-10$	$1.8384E-10$	$5.8903E-10$
$K^+ - K^+$	$1.3830E-10$	$8.2390E-12$	$1.4653E-10$
$Br^- - Br^-$	$4.3378E-10$	$1.5095E-13$	$4.3393E-10$

Table C.4: Obtained parameters when fitting to solubilities and liquid phase densities. Values of ϵ for the different ions interactions.

	ϵ_0	B	ϵ_{final}^{298K}
$Na^+ - Na^+$	2914.94	-	2914.94
$Cl^- - Cl^-$	5.00	-	5.00
$K^+ - K^+$	690.32	-	690.32
$Br^- - Br^-$	9.17	-	9.17
$Na^+ - Cl^-$	50.19	-	50.19
$Na^+ - Br^-$	299.17	-	299.17
$K^+ - Cl^-$	5.01	-	5.01
$K^+ - Br^-$	176.72	-	176.72
$Na^+ - H_2O$	1706.05	-	1706.05
$Cl^- - H_2O$	9.06	-	9.06
$K^+ - H_2O$	704.24	-	704.24
$Br^- - H_2O$	51.19	-	51.19

C.3 Estimation using solubility, liquid phase density and heat capacity

C.3.1 First Attempt

Solubility

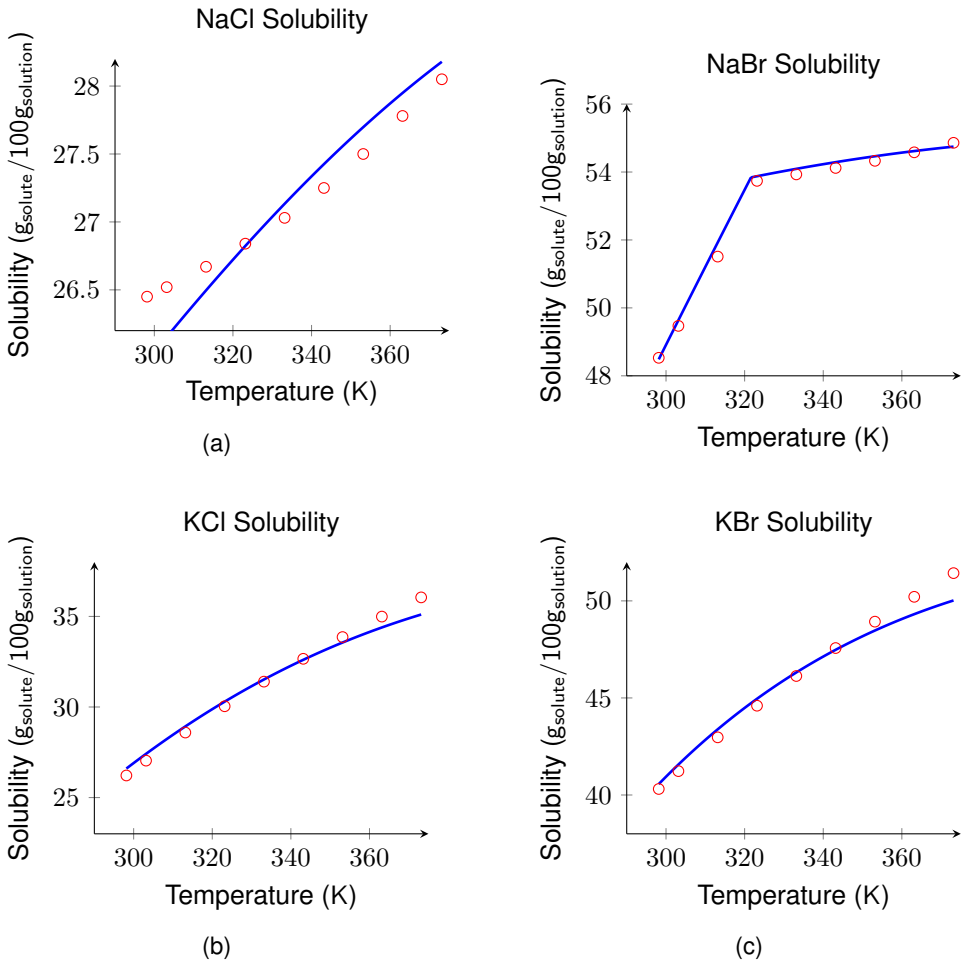

Figure C.16: Solubility of a salt depending on the molality, taking into account experimental data on solubility, liquid phase densities and liquid phase heat capacities. The different plots have both experimental (○) and SAFT predictions data (–).

Liquid Phase Density results

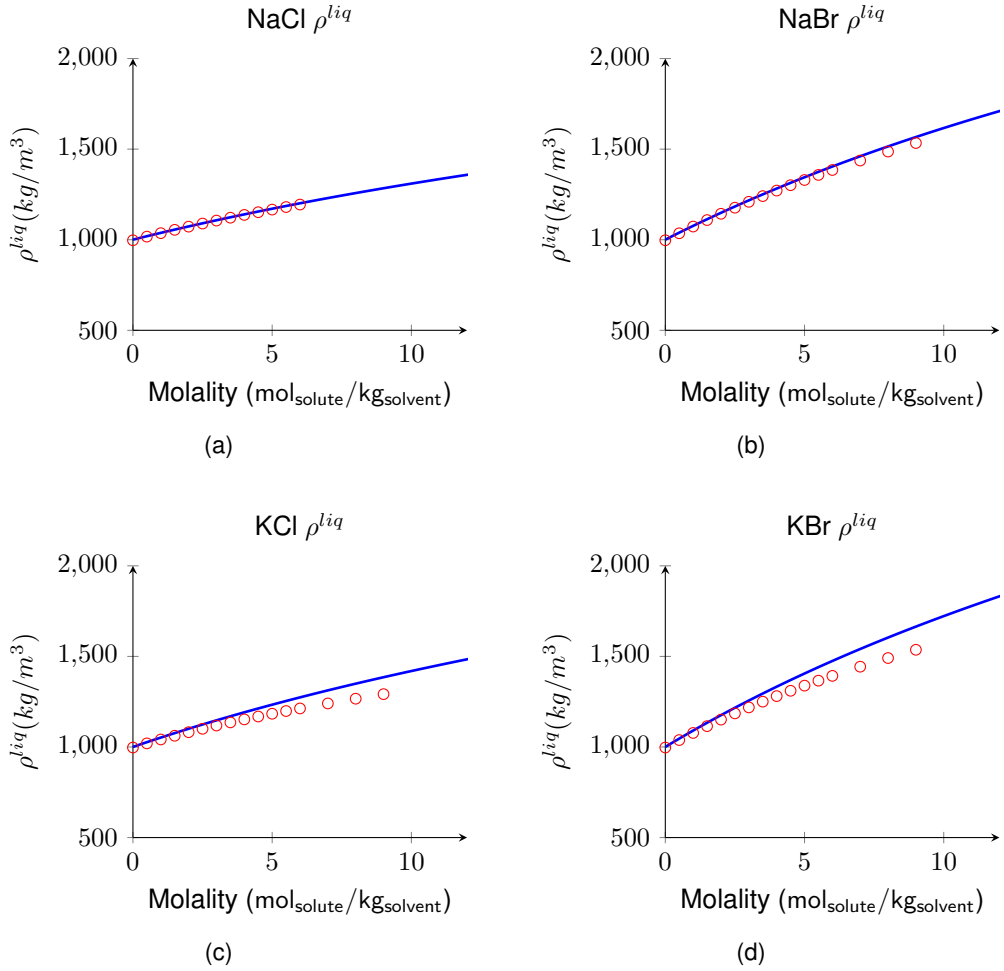

Figure C.17: Liquid phase density depending on the molality, taking into account experimental data on solubility, liquid phase densities and liquid phase heat capacities. The different plots have both experimental (○) and SAFT predictions data (−).

Liquid Phase Heat Capacity results

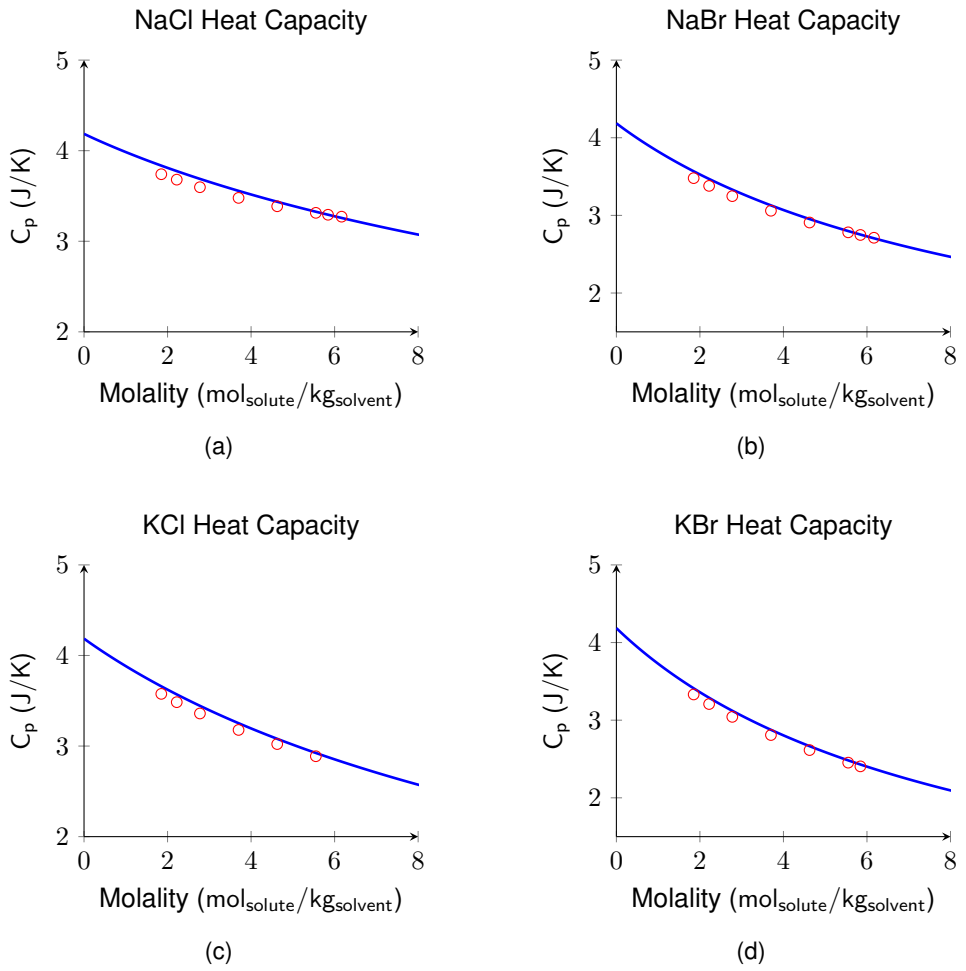

Figure C.18: Liquid phase heat capacity depending on the molality, taking into account experimental data on solubility, liquid phase densities and liquid phase heat capacities. The different plots have both experimental (○) and SAFT predictions data (−).

Dilution Enthalpy results

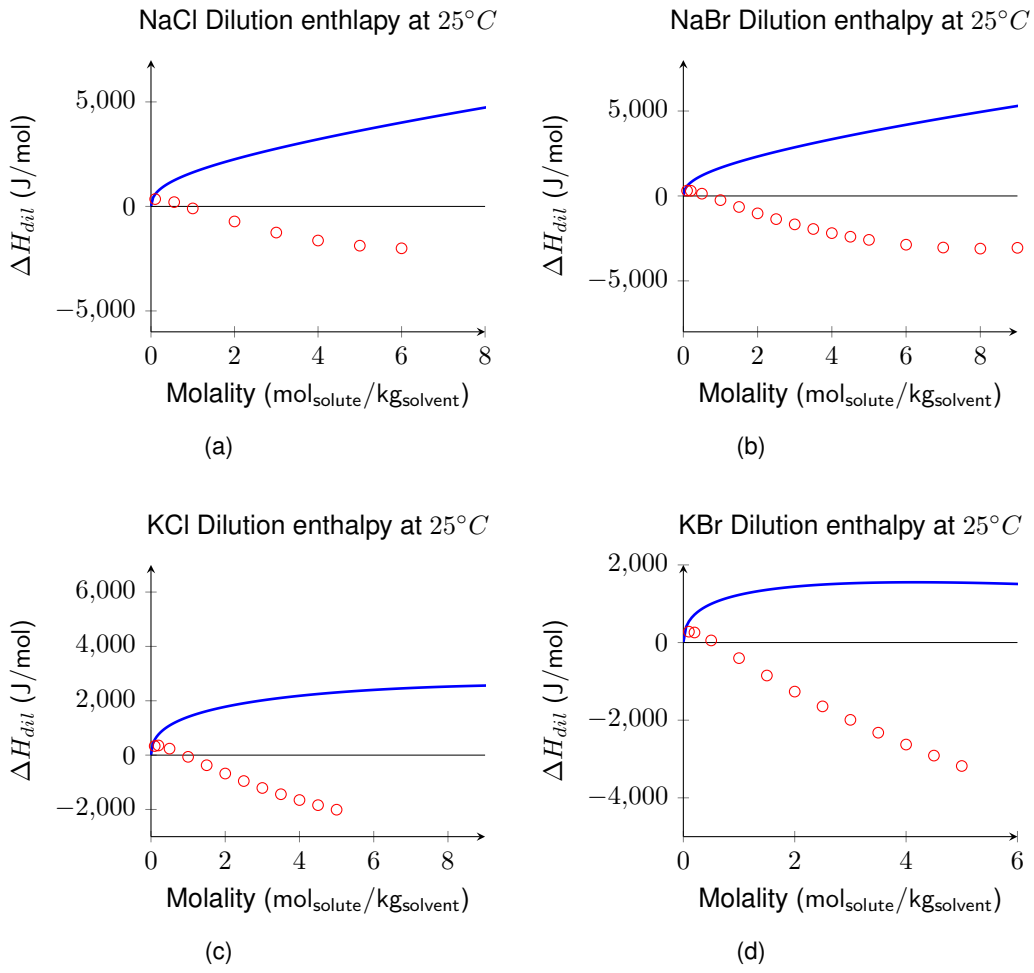

Figure C.19: Dilution enthalpy depending on the molality, taking into account experimental data on solubility, liquid phase densities and liquid phase heat capacities. The different plots have both experimental (○) and SAFT predictions data (−).

Mean Activity Coefficient results

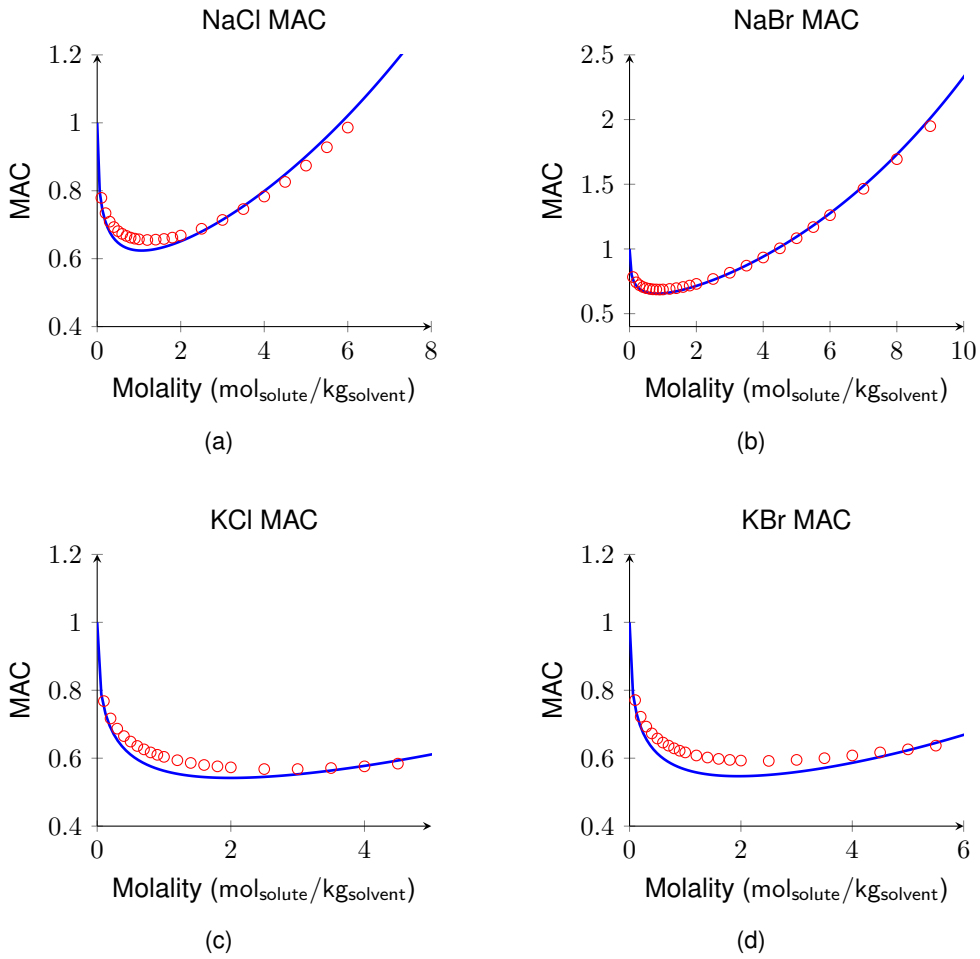

Figure C.20: Mean activity coefficients depending on the molality, taking into account experimental data on solubility, liquid phase densities and liquid phase heat capacities. The different plots have both experimental (∘) and SAFT predictions data (−).

Osmotic Coefficient results

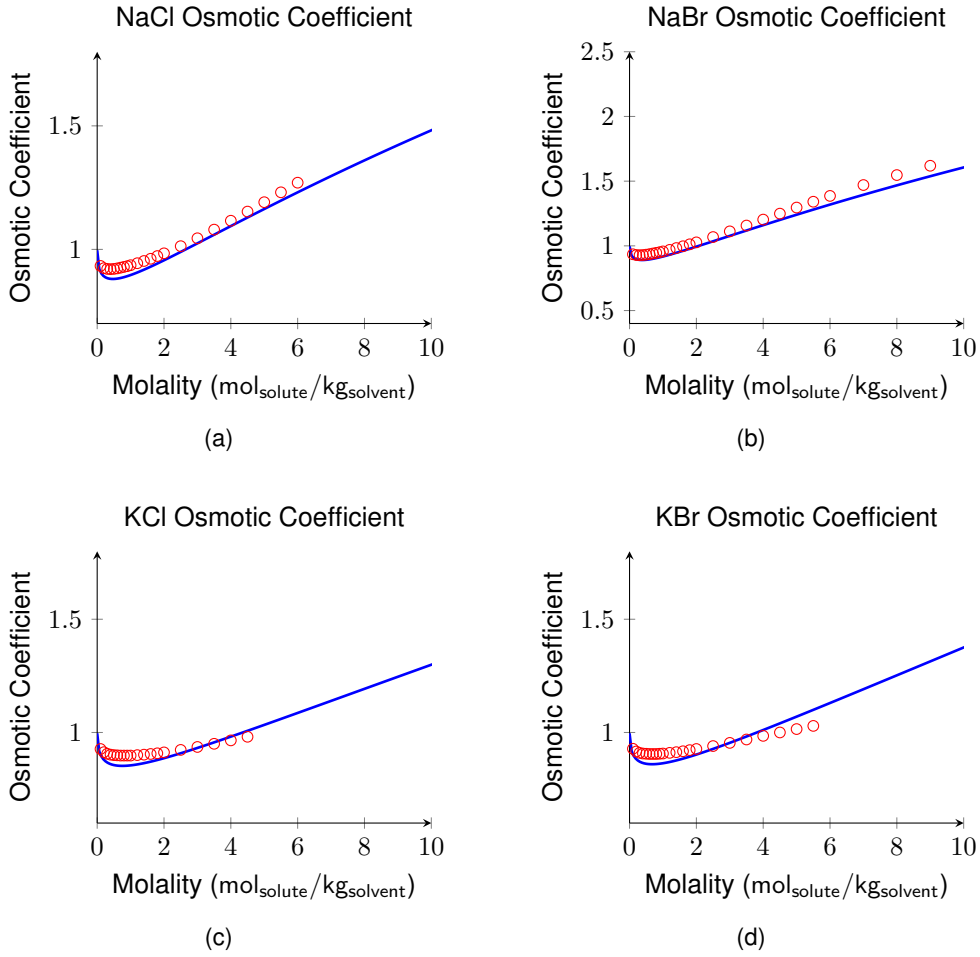

Figure C.21: Osmotic coefficients depending on the molality, taking into account experimental data on solubility, liquid phase densities and liquid phase heat capacities. The different plots have both experimental (○) and SAFT predictions data (−).

C.3.2 Second Attempt

Dilution enthalpy results

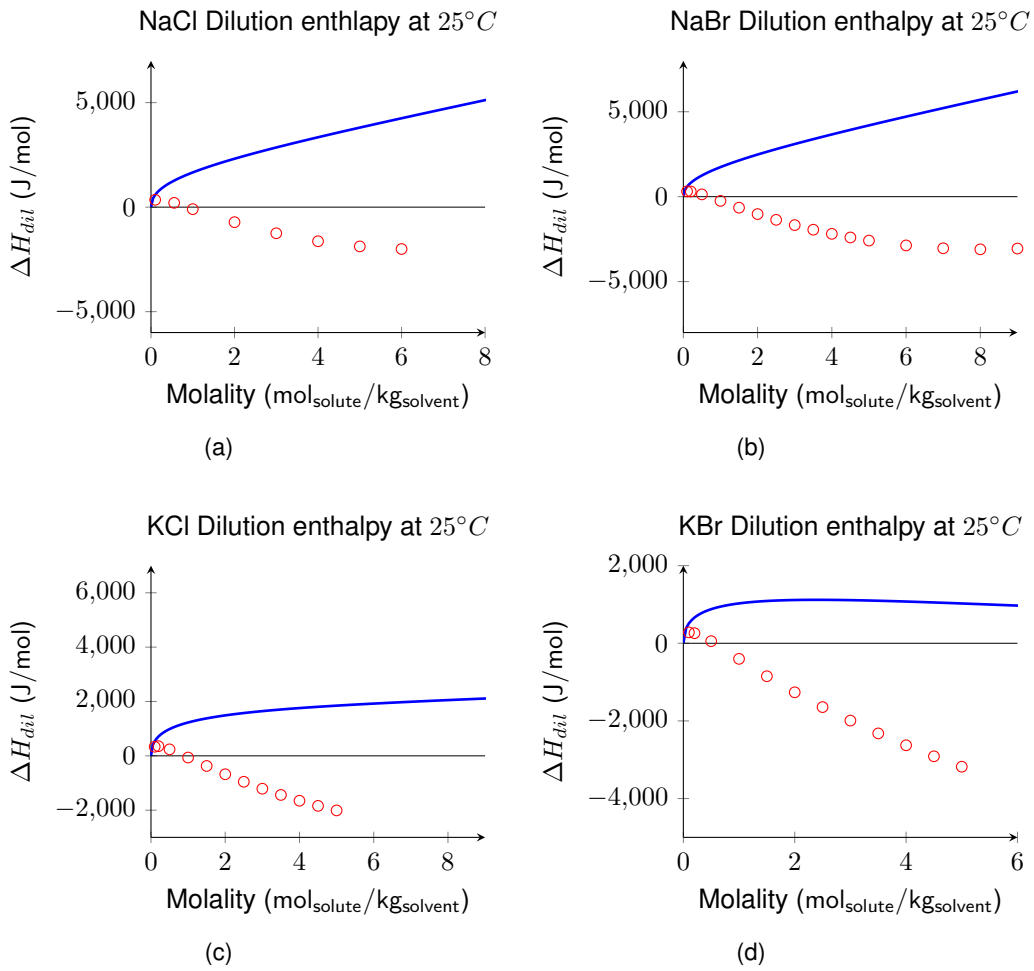

Figure C.22: Dilution enthalpy depending on the molality, taking into account experimental data on solubility, liquid phase densities and liquid phase heat capacities. The different plots have both experimental (○) and SAFT predictions data (−).

Mean Activity Coefficients

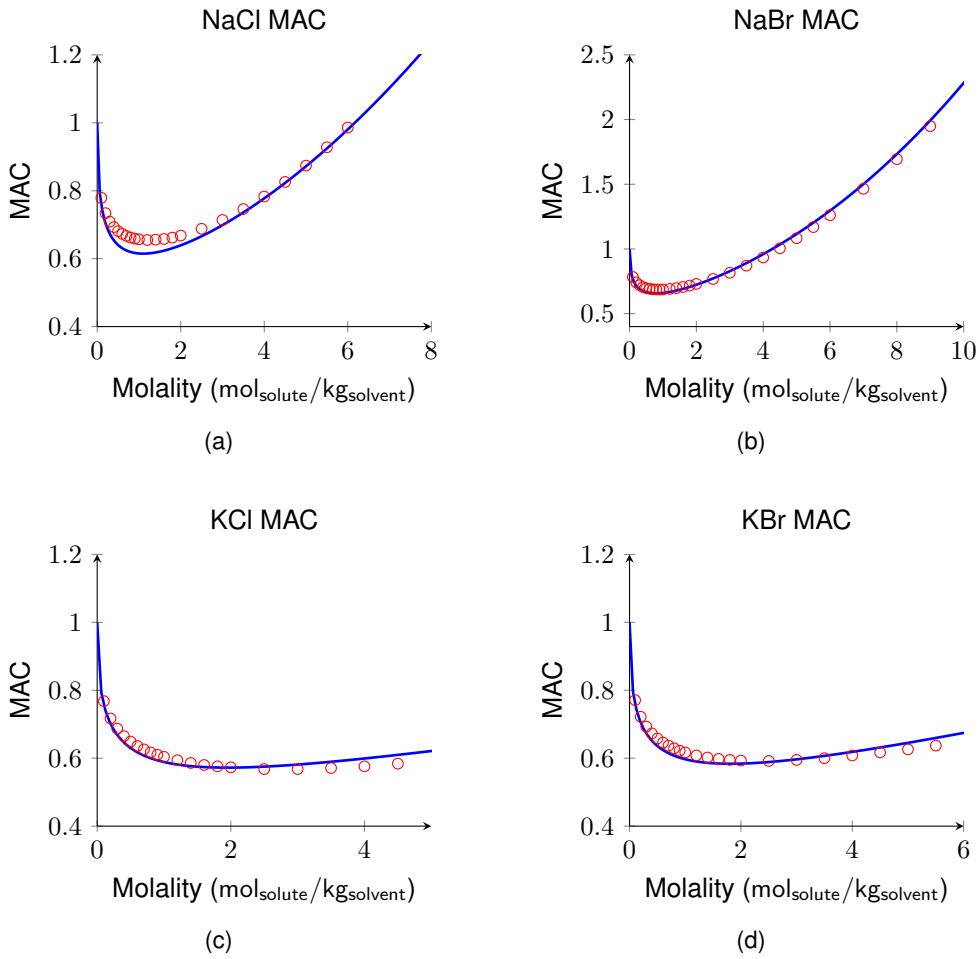

Figure C.23: Mean activity coefficients depending on the molality, taking into account experimental data on solubility, liquid phase densities and liquid phase heat capacities. The different plots have both experimental (∘) and SAFT predictions data (−).

Osmotic Coefficient results

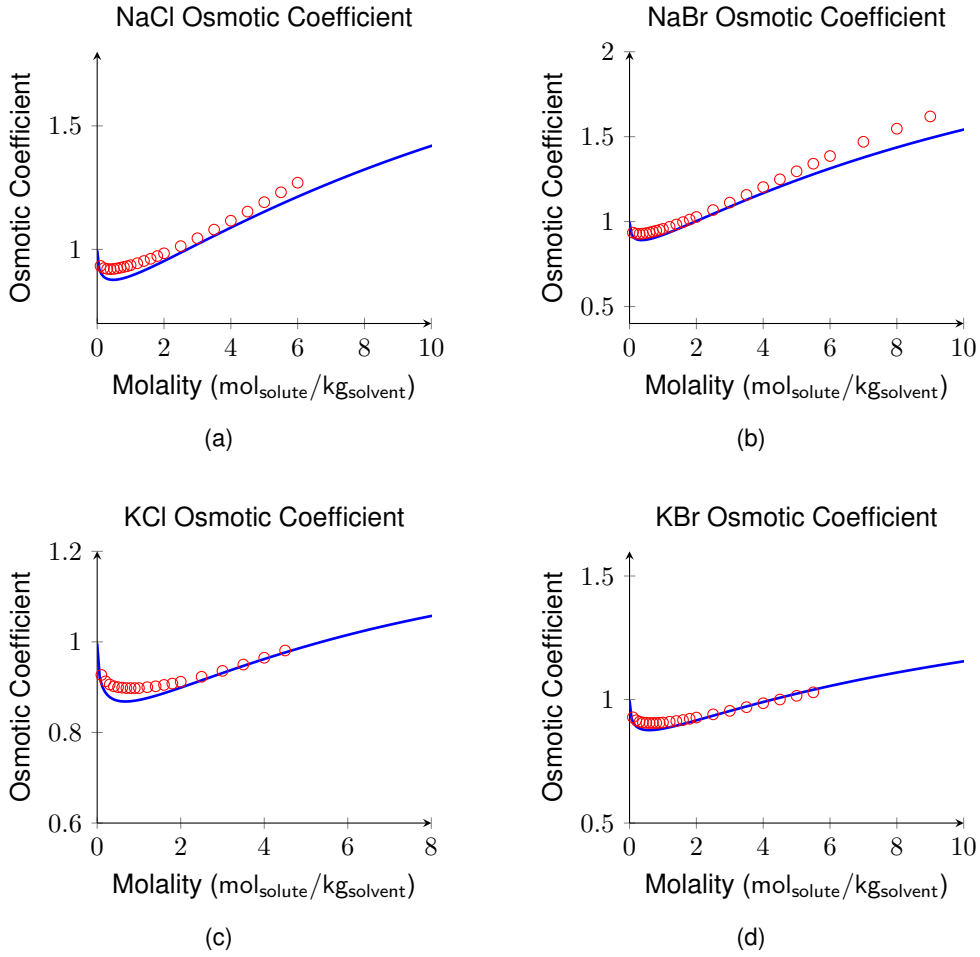

Figure C.24: Osmotic coefficients depending on the molality, taking into account experimental data on solubility, liquid phase densities and liquid phase heat capacities. The different plots have both experimental (○) and SAFT predictions data (–).

Model with Solubility, Liquid Phase Density and Heat Capacity

Table C.5: Obtained parameters when fitting to solubilities, liquid phase densities and liquid phase heat capacities. Values of ionic σ for the different ions.

	σ	$\Delta\sigma_i$	σ_i^{Born}
$Na^+ - Na^+$	$8.3282E-11$	$1.9271E-10$	$2.7599E-10$
$Cl^- - Cl^-$	$4.0633E-10$	$2.1980E-10$	$6.2614E-10$
$K^+ - K^+$	$1.3147E-10$	$1.0712E-10$	$2.3859E-10$
$Br^- - Br^-$	$4.4278E-10$	$4.6690E-11$	$4.8947E-10$

Table C.6: Obtained parameters when fitting to solubilities, liquid phase densities and liquid phase heat capacities. Values of ϵ for the different ions interactions.

	ϵ_0	B	ϵ_{final}^{298K}
$Na^+ - Na^+$	326.98	-	326.98
$Cl^- - Cl^-$	4.73	-	4.73
$K^+ - K^+$	2.01	-	2.01
$Br^- - Br^-$	5.47	-	5.47
$Na^+ - Cl^-$	20.02	-	20.02
$Na^+ - Br^-$	290.68	-	290.68
$K^+ - Cl^-$	3.61	-	3.61
$K^+ - Br^-$	258.84	-	258.84
$Na^+ - H_2O$	1959.42	-7191.17	1935.30
$Cl^- - H_2O$	135.98	-22969.98	58.94
$K^+ - H_2O$	778.27	-4393.60	763.53
$Br^- - H_2O$	170.80	-17711.14	111.39

C.4 Estimation using solubility, liquid phase density, liquid phase heat capacity and dilution enthalpy

C.4.1 Mean Activity Coefficients results

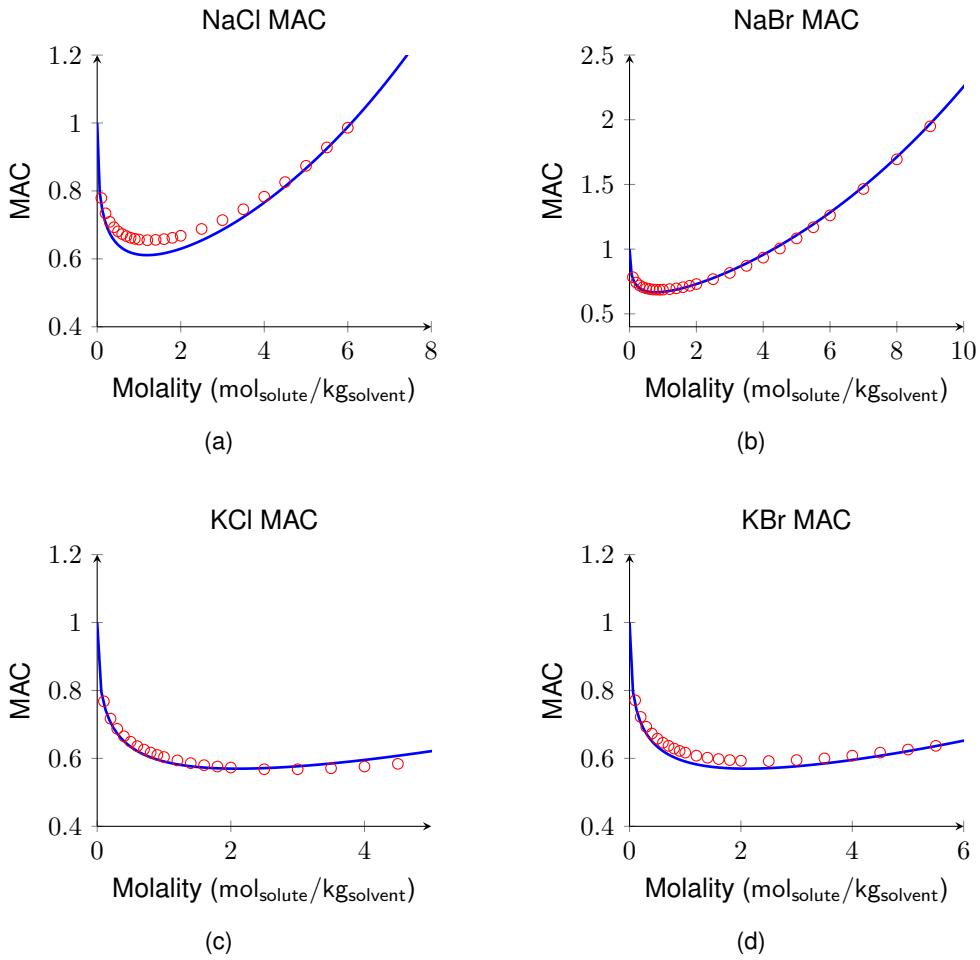

Figure C.25: Mean activity coefficients depending on the molality, taking into account experimental data on solubility, liquid phase densities, liquid phase heat capacities and dilution enthalpies. The different plots have both experimental (○) and SAFT predictions data (−).

C.4.2 Osmotic Coefficient results

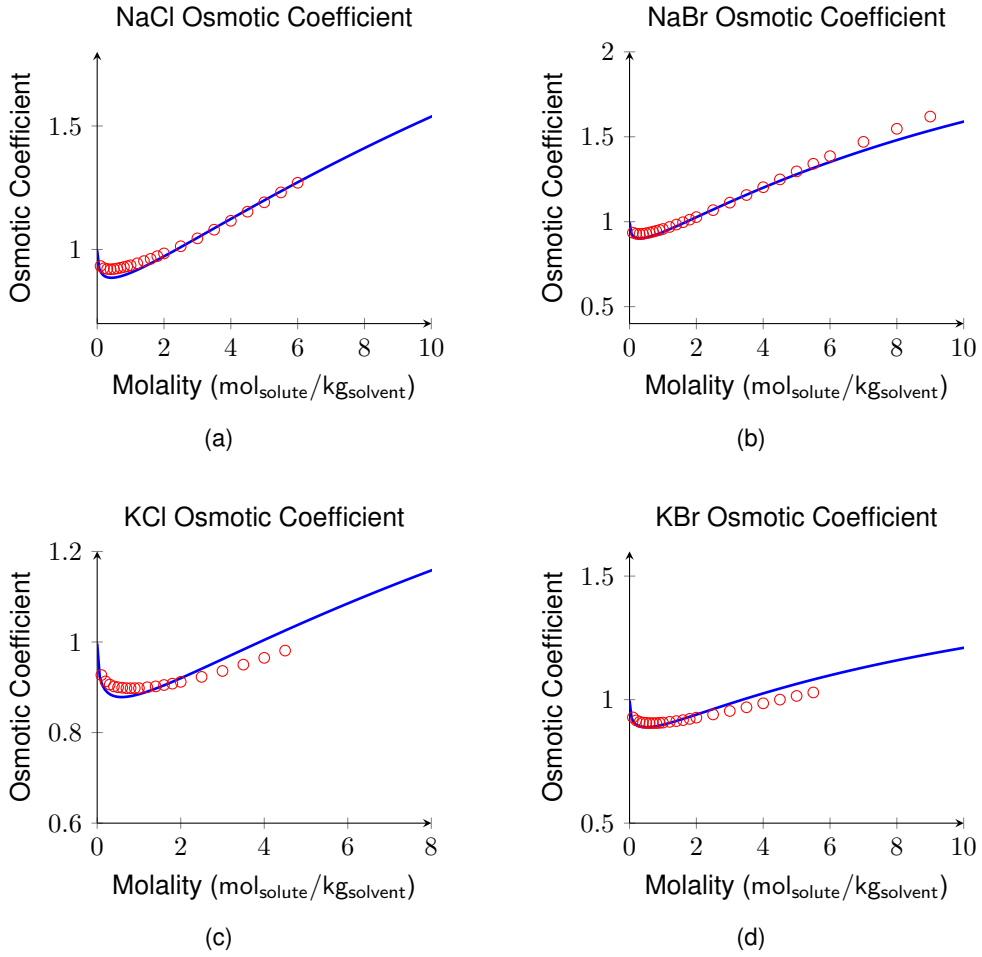

Figure C.26: Osmotic coefficients depending on the molality, taking into account experimental data on solubility, liquid phase densities, liquid phase heat capacities and dilution enthalpies. The different plots have both experimental (○) and SAFT predictions data (−).

C.5 Model Extension

C.5.1 Mean Activity Coefficients results

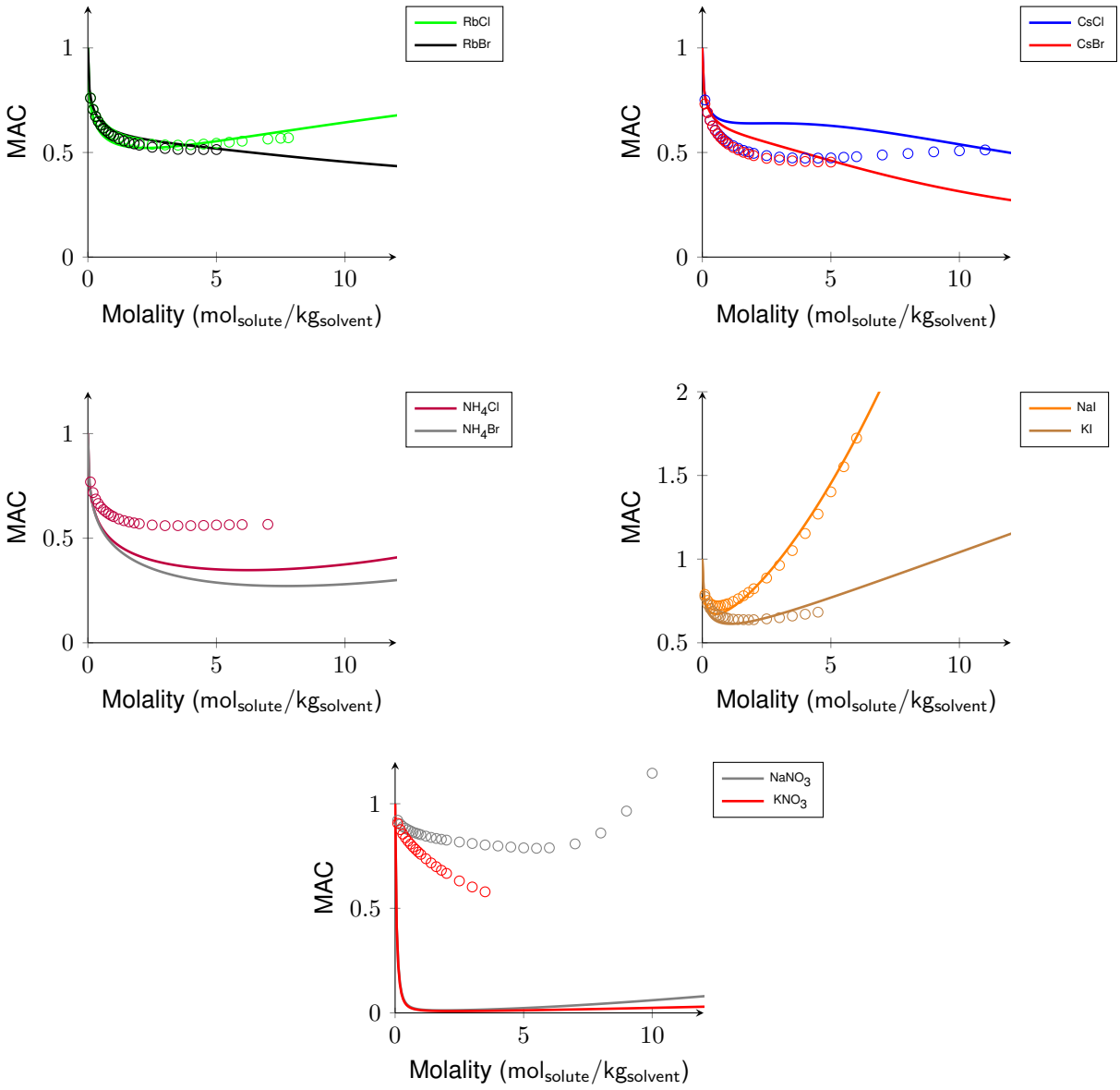

Figure C.27: Mean activity coefficients for the final model extension

C.5.2 Osmotic Coefficients results

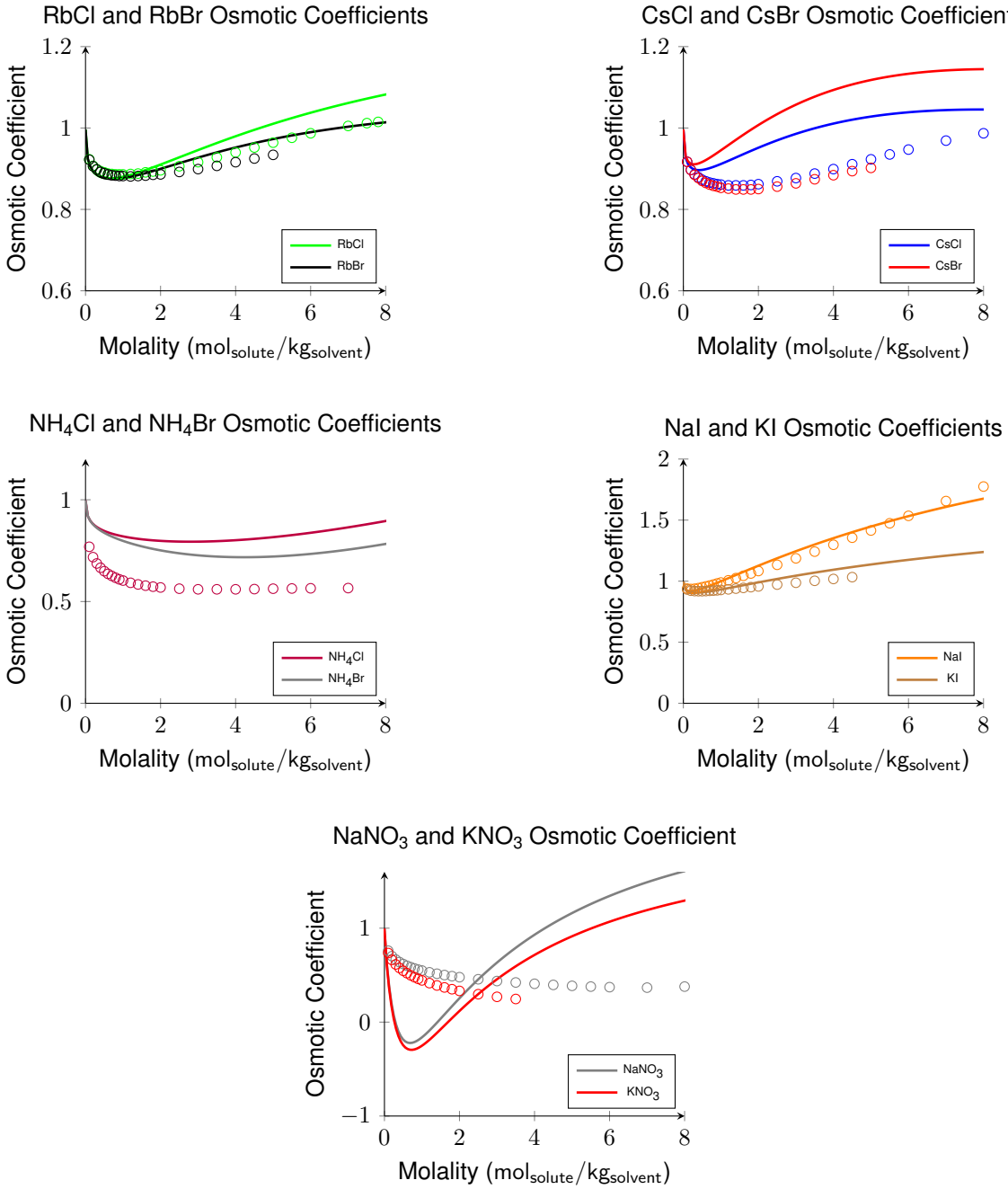

Figure C.28: Osmotic coefficients for the final model extension

Table C.7: Obtained parameters for the final models. Values of ionic σ for the different ions.

	σ	$\Delta\sigma_i$	σ_i^{Born}
$Rb^+ - Rb^+$	$3.3510E-10$	$2.0381E-14$	$3.3512E-10$
$Cs^+ - Cs^+$	$3.6837E-10$	$2.1980E-12$	$3.7057E-10$
$NH_4^+ - NH_4^+$	$3.2112E-10$	$4.2126E-16$	$3.2112E-10$
$I^- - I^-$	$3.8249E-10$	$1.3610E-10$	$5.1859E-10$
$NO_3^- - NO_3^-$	$4.1769E-10$	$2.5000E-10$	$6.6769E-10$

Table C.8: Obtained parameters for the $RbCl$ and $RbBr$ final model. Values of ϵ for the different ions interactions.

	ϵ_0	B	ϵ_{final}^{298K}
$Rb^+ - Rb^+$	1823.56	-	1823.56
$Rb^+ - Cl^-$	880.05	-	880.05
$Rb^+ - Br^-$	1339.29	-	1339.29
$Rb^+ - H_2O$	241.59	-59123.40	43.29

Table C.9: Obtained parameters for the $CsCl$ and $CsBr$ final model. Values of ϵ for the different ions interactions.

	ϵ_0	B	ϵ_{final}^{298K}
$Cs^+ - Cs^+$	2819.42	-	2819.42
$Cs^+ - Cl^-$	102.08	-184919.42	-518.14
$Cs^+ - Br^-$	13.44	108926.66	378.78
$Cs^+ - H_2O$	283.77	-55927.60	96.18

Table C.10: Obtained parameters for the NH_4Cl and NH_4Br final model. Values of ϵ for the different ions interactions.

	ϵ_0	B	ϵ_{final}^{298K}
$NH_4^+ - NH_4^+$	50.87	-7625.57	25.29
$NH_4^+ - Cl^-$	3377.14	-1120732.74	-381.81
$NH_4^+ - Br^-$	3784.60	-1103343.88	83.97
$NH_4^+ - H_2O$	0.10	-385599.78	-1293.21

Table C.11: Obtained parameters for the NaI and KI final model. Values of ϵ for the different ions interactions.

	ϵ_0	B	ϵ_{final}^{298K}
$I^- - I^-$	5.35	-761.23	2.80
$Na^+ - I^-$	620.54	-117434.26	226.66
$K^+ - I^-$	798.12	-9079.34	767.66
$I^- - H_2O$	953.10	56042.59	1141.07

Table C.12: Obtained parameters for the $NaNO_3$ and KNO_3 final model. Values of ϵ for the different ions interactions.

	ϵ_0	B	ϵ_{final}^{298K}
$NO_3^- - NO_3^-$	45.23	-	45.23
$Na^+ - NO_3^-$	7144.44	-160833.42	6605.00
$K^+ - NO_3^-$	7662.99	-357970.76	6462.35
$NO_3^- - H_2O$	4427.90	-168810.66	3861.70